KINESIN MOTOR PROTEIN INHIBITORS: TOWARD THE SYNTHESIS OF ADOCIASULFATE ANALOGS

by

CHETAN PADMAKAR DARNE

(Under the Direction of TIMOTHY M. DORE)

ABSTRACT

Cell division and intracellular functions are dependent on kinesin motor proteins. These proteins convey their cellular cargos by “walking” along the microtubule tracks. Specific inhibitors of kinesin would selectively abolish its activity *in vivo*, and knowledge regarding this inhibition pathway would aid our understanding regarding the enzyme mechanism. Currently, few inhibitors of kinesins exist. The marine natural products adociasulfates (AS) might act as lead compounds toward designing analogous inhibitors. Only AS-1 has been synthesized, requiring twenty-eight steps; therefore, we envisioned the synthesis of simpler analogs via shorter routes. We attempted functionalizing commercial steroids at one end, while the other end was transformed into an anionic moiety pivotal for binding with the kinesin motor domain. Though our AS analog does not inhibit the ATPase activity of human kinesin, this synthetic approach is practical and with some modifications, offers the potential to generate bioactive analogs of therapeutic importance.

INDEX WORDS: kinesin, motor protein inhibitors, adociasulfate, AS analog

KINESIN MOTOR PROTEIN INHIBITORS: TOWARD THE SYNTHESIS OF ADOCIASULFATE ANALOGS

by

CHETAN PADMAKAR DARNE

B.Sc., University of Bombay, India, 1994

M.Sc., University of Mumbai, India, 1998

A Thesis Submitted to the Graduate Faculty of The University of Georgia in Partial Fulfillment of the Requirements for the Degree

MASTER OF SCIENCE

ATHENS, GEORGIA

2005

KINESIN MOTOR PROTEIN INHIBITORS: TOWARD THE SYNTHESIS OF ADOCIASULFATE ANALOGS

by

CHETAN PADMAKAR DARNE

Major Professor: Timothy M. Dore

Committee: George Majetich
Robert Phillips

Electronic Version Approved:

Maureen Grasso
Dean of the Graduate School
The University of Georgia
May 2005

DEDICATION

To my family members- for their unconditional love and encouragement, and for keeping my faith alive.

ACKNOWLEDGEMENTS

I thank my advisor Dr. Timothy Dore for the original idea regarding the adociasulfate project. His comments and suggestions have been very helpful to me. My sincere thanks to Dr. George Majetich and Dr. Robert Phillips for not only serving on my thesis committee, but also for allowing me to use numerous chemicals and other resources from their respective laboratories. Joel Shimkus and Yang Lee are gratefully acknowledged for helping me procure various reagents from the Majetich Lab., as and when needed. The IR spectra were recorded in the de Haseth lab., and I am indebted to Dr. James de Haseth and Brian Loudermilk for helping me beyond the call of duty.

I express my gratitude toward my former colleague Dr. Olesya Fedoryak for being a wonderful friend. It has been a pleasure working with Khalilah Reddie. I have had numerous discussions on chemistry with her, and every time I have learned something new. Her ideas and suggestions have been immensely useful to me in my project. I also wish to mention Sameer Kawatkar and Sampat Ingale for having helped me time and again.

Finally, I am beholden to my family members, especially my parents for their affection and support. They were always there when I needed them. Without their encouragement this thesis would not have been possible.

TABLE OF CONTENTS

Page

LIST OF TABLES

Page

LIST OF FIGURES

Page

CHAPTER 1

KINESIN MOTOR PROTEINS

Introduction

Cells need to distribute various kinds of proteins and lipids, after their synthesis, to their respective destinations. Intracellular transport is important for cellular morphogenesis and functioning,[1] wherein the essential materials are transported in membranous organelles and vesicles. This function is conducted effectively by the cytoskeletal motor proteins, which convert chemical energy, by nucleotide hydrolysis (conversion of ATP $\rightarrow$ ADP), into mechanical force necessary for unidirectional movement along cytoskeletal polymers.[2] The motor proteins are most broadly categorized according to the type of cytoskeletal polymer with which they interact. Kinesin, dynein and myosin are the three distinct classes of molecular motors. While myosin uses actin filaments as its tracks, microtubules (MTs, which are long, hollow cylinders of 25 nm diameter, comprising α- and β-tubulins), act as the "rail" on which kinesin and dynein "walk".[3] Kinesin and dynein are mostly used for long distance transportation.

Kinesin-1 (*aka* conventional kinesin, KIF5 or KHC) is the founding member of a large superfamily of MT activated motors, known as the kinesins. KIF5 was discovered twenty years ago in a giant squid fast axoplasmic transport system, and was aptly named 'kinesin' for its force-producing ability.[4,5] The kinesin superfamily now consists of >140 proteins identified in organisms ranging from fungi to plants and animals, including humans.[6] Most kinesins, including KIF5, are MT plus-end directed motors[3,5] that move processively on the MT surface lattice along paths parallel to the protofilaments, interacting with one binding site per tubulin

dimer. The kinesin dimer takes alternate fast and slow steps of ~8 nm, and may take >100 "limping" steps, and travel a distance of more than 1 μm before releasing from the MT surface. Each step is associated with one cycle of ATP hydrolysis.[7,8,9]

Kinesin: a Brief Classification

The mammalian genome contains 45 kinesin genes. Kinesin-1 itself forms a family, wherein KIF5A, KIF5B and KIF5C have been identified in mouse, HsuKHC and HsnKHC in humans and one another member in metazoans like sea urchin and *Drosophila*. KIF5B and HusKHC are expressed ubiquitously in many tissues, while KIF5A, KIF5C, and HsnKHC are specific to nerve tissue.[1,10] Rotary shadowing and biochemical analysis shows that there are five types of kinesins: monomeric, homo- and heterodimeric, heterotrimeric, and heterotetrameric.[11]

Structural Features of Kinesin-1

KIF5 is a heterotetramer of 380 kDa, comprising two 120 kDa kinesin heavy chains (KHCs) and two 64 kDa kinesin light chains (KLCs), forming an 80 nm, asymmetric rod-like molecule (Figure 1). Electron microscopy and biochemical analyses reveal that the kinesin heavy chain consists of three domains: an N-terminal pair of ~10 nm globular head domains, an α-helical coiled-coil stalk domain, and a C-terminal fan-like or feather-like tail domain.[1,9,12,13] The finer structural aspects of this heterotetrameric motor are depicted in Figure 2.[3]

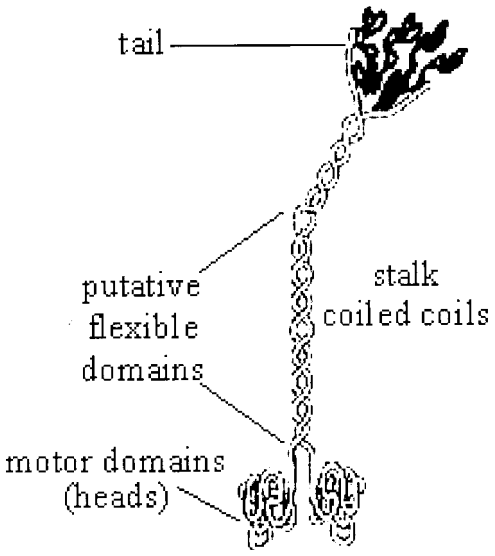

Figure 1: Kinesin Domains

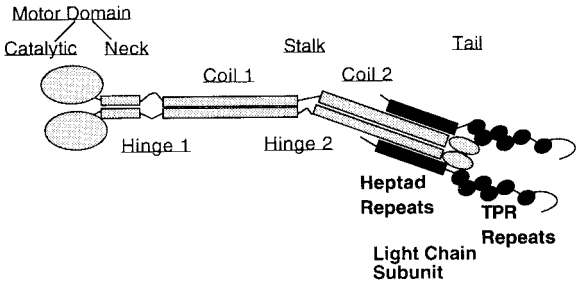

Figure 2: Domain Organization (KHCs are shown in grey with underlined labels, and KLCs are shown in black with bold labels)

The N-terminal ~325 amino acids constitute the catalytic core of the motor domain, which contains the nucleotide and microtubule binding sites. Alanine-scanning mutagenesis studies[14] suggest that several regions of the kinesin motor contribute amino acid residues to the tubulin binding interface. The critical residues are primarily positively charged, and interact with the negatively charged tubulin molecule, primarily through electrostatic attractions. This domain is highly conserved throughout the kinesins, and recent studies reveal that the crystal structures of the motor domain of kinesin and kinesin-related protein (KRP) Ncd show structural similarities with the motor domain of myosin and dynein. Three major types of kinesin proteins have been identified according to the position of the motor domain on the polypeptide chain,[1] namely, NH_2-terminal motor domain type (N-type), middle (centrally located) motor domain type (M-type), and COOH-terminal motor domain type (C-type). Although the N- and M- type

kinesins are plus-end directed, and the C-type are minus-end-directed, the directionality is not determined by the domain location, instead, the kinesin directionality is the function of the neck region.[6] The "small" size of its motor domain (which is less than one-half the size of myosin's motor domain) and the ability to express active motor in bacteria has made kinesin an attractive system for structural studies.[14]

Immediately following the motor domain is the neck domain (Figure 2),[3] comprising 46-50 amino acid residues. The first 10-15 residues of the neck form a β-sheet structure that makes contact with the catalytic core and is thought to be important for kinesin mechanics. The subsequent portion of the neck forms a coiled-coil that is sufficient to dimerize the two motor domains. The neck region mediates a sophisticated communication between the two heads of kinesin. The neck of the kinesin motors is essential, not only for motor directionality and velocity, but for other aspects of motor function. Alternating catalysis of ATP hydrolysis by the two heads of kinesin may be regulated by conformational changes in the neck that occur with specific steps of the nucleotide hydrolysis cycle. Apart from mediating the motor-processivity, the neck may also determine the path taken by the motor along the MT track. Following the neck, there is a glycine and proline-containing region (hinge 1) that may allow the motor domains to swivel with respect to an attached cargo. Beyond hinge 1 is an extended coiled coil or the stalk domain, which contains two segments (coil 1 and 2) that are interrupted by glycine and proline-rich hinge 2. This hinge enables the KIF5 molecule to adopt a folded conformation in which the tail interacts with the head. Coils 1 and 2 have distinct melting (unwinding) properties, and coil 2 contains highly conserved sequence that may bind to the light chains. The C-terminal of coil 2 is a well conserved, ~100 amino acid globular tail domain. A neuronal conventional kinesin isoform contains an ~70 amino acid C-terminal extension in the tail.[3] The tail domain is

involved in kinesin light chain (KLC) and cargo-binding interactions. The overall structure of KLCs is conserved among various species. A long series of N-terminal heptad repeats and six tetratricopeptide (TRP) repeats close to the C-termini were identified in KLCs. The TRP repeats could be part of a protein interaction interface with a target molecule on the organelles, whereby the KHC isoforms may target kinesin to specific cargos. It is also believed that KLCs regulate the ATPase activity of KHCs *in vivo*.

Kinesin Functions: An Overview

Kinesins are involved in numerous cell biological processes.[1,10,15] They are essential for mitotic and meiotic spindle organization, chromosome alignment and segregation, endocytosis, exocytosis, secretion and membrane trafficking. The associated cargos include, endoplasmic reticulum, mitochondria, lysosomes, peroxyzomes, tubulin oligomers, intracellular vesicles (e.g. Golgi-derived vesicles), chromosomes, kinetochores, intermediate filaments, mRNA, signaling proteins, membrane associated complexes (e.g. rafts or intraflagellar transport particles), virus particles, neuro-protective and repair molecules and even other motors. The movements of these essential components are critical for many developmental functions.

Although all eukaryotic cells need an active system to generate intracellular movement along the MT tracks, the neurons have a much more pronounced demand.[16] The neuronal axon lacks protein synthesis machinery, and therefore, all the proteins and lipids required in the axon and the synaptic terminal must be transported from the cell body (Figure 3). Kinesins are responsible for such anterograde (from cell body to synapse) transport of organelles and vesicles necessary to support the axon. As a result of this axonal transport, neurons can communicate at long distances and can form the complex cellular networks of the nervous system. The axons of some motor neurons can be as long as 1 m and can have volumes that are at least 1000 times that

of the supporting cell body. Kinesins in coordination with cytoplasmic dyneins (CDs) play a vital role in maintaining neuronal well being. KIF5 is responsible for the fast axonal transport necessary for neuronal functioning. For example, it transports vesicles containing ApoER2, the receptor for Reelin, which might function in neuronal development.[17,18] While in the dendrite, KIF5 transports vesicles containing α-amino-3-hydroxy-5-methylisoxazole-4-propionic acid (AMPA)-type glutamate receptors from the cell body to the postsynaptic site, apart from carrying mRNAs for an activity-regulated protein called Arc and the α subunit of Ca/calmodulin-dependent protein kinese II (CaMKIIα), both of which play roles in long-term potentiation.[19] Kinesins also transport various tubovesicular structures that may be precursors of axonal plasma membrane, synaptic vesicles and synaptic plasma membranes. Chemical signaling between the cell body and synapse or the target cell relies on neurotropic factors and signals, which also use this MT-based mode of axonal transport.[16]

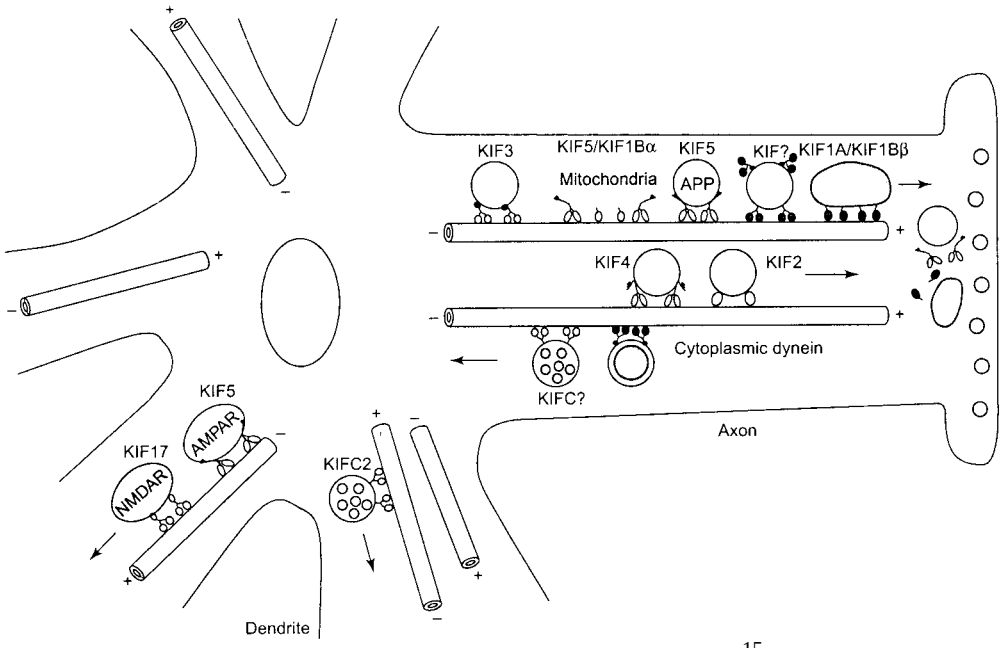

Figure 3: Motor Protein-Mediated Axonal and Dendritic Transport[15]

More recently, it has been shown that, apart from transporting cellular cargos, the kinesins also modulate the dynamics of the underlying MT network, couple the movement of cargo with the MT polymerization or depolymerization, and crosslink the MTs in dynamic structures.[17]

Kinesins and Human Diseases

As stated earlier, the smooth functioning of kinesin is pivotal for processes like mitosis and axonal transport; hence, disruption in its activity would lead to a disease state. Studies of intracellular transport and kinesins are beginning to shed light on several human diseases and therapeutic opportunities. The disease-related roles of kinesins are grouped as follows:[18]

1) Problems with long distance traffic: Especially in neurons or other asymmetric cells where diffusion would be ineffective. In this case the physiological cargos are not delivered appropriately. This applies mainly to KIF5.
2) Uncontrolled cell division and cancer: Various kinesins are involved in mitosis. Therefore, their malfunction can cause undesired cell proliferation. Conversely, kinesins of transformed cells represent targets for drug intervention.
3) Entry and exit of pathogens: Viruses and parasites and their components are too large for diffusion, and hence, their movement in and out of the cells is dependent on motor proteins. This is a case where non-physiological cargos make use of the transport system.

Since kinesins play a vital role in maintaining axons, any disruption of kinesin-mediated axonal transport can cause neurodegenerative diseases like the Alzheimer's disease, spastic paraplagia or dementia, and other neuronal disorders. Due to their involvement in cell division, the malfunctioning of kinesin like Eg5 can result in cancer. Since, kinesins are such an important

part of cell physiology, various aspects of human health are also dependent on the smooth functioning of kinesin motor proteins.

There is an obvious relationship between kinesin-driven axonal transport and neuronal well being. There are numerous neurodegenerative diseases in which there is formation of protein-aggregates, which can inhibit/slow down the axonal transport and cause the disease progression. The possible functional interaction between KIF5 and amyloid precursor protein (APP) may implicate KIF5 based transport for the development of Alzheimer's disease.[11,20-22] This is because the overexpression of APP causes protein aggregates in patients with Alzheimer's disease, and inhibits the axonal transport. An N256S missense mutation in the KIF5A gene is known to cause autosomal dominant hereditary spastic paraplegia type 10 (SPG10). A missense mutation is a genetic change involving the substitution of one base in the DNA for another. This results in the substitution of a codon for one amino acid into a codon for a different amino acid, and introduces an incorrect amino acid in the protein sequence. Patients with N256S mutation in KIF5A develop axonal degeneration of the motor and the sensory neurons.[23]

Glucose homeostasis in humans is dependent on the catalytic activity of a glucose transporter protein, GLUT4. The vesicles containing this protein are transported by KIF5B, a Kinesin-1 family member. An aberrant GLUT4 transport might result in the pathogenesis of diabetes.[24]

Kinesin also plays a role in tumor generation or suppression. KIF5B is identified as a part of a complex with two neurofibromatosis tumour suppressors, NF1 and NF2. It has been observed that, the aberrant KIF5/NF1-mediated trafficking might affect the normal development of cerebral cortex.[25] In epithelial cancers, there is a crosstalk between anti-cancer drugs Taxol®

and cisplatin, mediated by KIF5. Cisplatin is necessary for the growth arrest induced by Taxol®, but it preferentially damages the genes encoding KIF5, thus reducing the efficacy of Taxol®.[26]

Viral cytoplasmic transport is mediated by the cytoskeleton, and hence, viruses can hijack the kinesin-dependent transport.[27] Such transport is essential in the case of neurotropic herpes simplex viruses (HSVs), which have to be transported over long distances from the cell body to the axon terminals of dorsal root ganglion neurons. There is a direct interaction between human ubiquitous kinesin husKHC and HSV capsid tegument protein US11.[28] In the case of vaccinia virus, a close relative of the causative agent of smallpox, KIF5 transports the viral protein A36R from the perinuclear site to the plasma membrane.[29]

Apart from KIF5, other kinesin superfamily members are also associated with human diseases. A variant of KIF1B that belongs to Kinesin-3 family is downregulated in some neuroblastomas, and has the potential to function as a tumor suppressor.[30] In the treatment of pancreatic cancer with a vitamin A derivative like retinoic acid, Eg5, a mitotic kinesin of the Kinesin-5 family was downregulated, consistent with its role in cell division.[31] Retinoids inhibit cell proliferation, induce differentiation and promote apoptosis. Retinoic acid mediates its biological effects by binding to nuclear, ligand–active receptors like retinoic acid receptors (RARs). These receptors repress the activity of activating protein-1 (AP-1) transcription factor, which plays an important role in activating genes responsible for cell division. Rheumatoid arthritis is caused by transformed synovial fibroblasts that destroy the articular cartilage. One of the key genes upregulated in these cells is KIF10/CENP-E, a Kinesin-7 family member critical for cell division.[32] KIF10/CENP-E is a kinetochore-based mitotic motor, which modulates chromosome movement and spindle elongation; kinetochore being the chromosomal attachment point for the spindle fibers located within the centrosomes. An interaction between KIF3A of the

Kinesin-2 family and the growth arrest and DNA-damage inducible (GADD) proteins, which protect the differentiated cells against apoptosis, has been observed.[33] During the neuronal development, KIF2A (Kinesin-13 family) plays a significant role in the regulation of axon-collateral branch extension, which is essential for brain wiring.[22] KIF1Bβ transports synaptic vesicle precursors in the axon. A mutation in KIF1Bβ causes a human peripheral neuropathy, Charcot-Marie-Tooth disease type 2A (CMT2A).[34] KIF17 is localized in the dendrites, and is specifically involved in transporting the *N*-methyl-D-aspartase (NMDA) receptor from the cell body to the postsynaptic sites. This transport is physiologically important for learning and memory.[22,35] In some neurodegenerative diseases, such as senile dementia, neuronal cell death caused by defects in the transport of synaptic vesicle precursors by KIF1A (Kinesin-3 family) may be involved.[11] KIF21A, a member of the Kinesin-4 family, is a neuronally expressed protein. Mutations in human KIF21A appear to exclusively affect the development and functioning of the oculomotor nerve. The autosomal dominant strabismus disorder congenital fibrosis of extraocular muscle type 1 (CFEOM1) is due to heterozygous missense mutations in KIF21A.[36] CFEOM1 results from the inability of mutated KIF21A to successfully deliver a cargo that is essential to the development of the oculomoter axons or neuromuscular junction. Patients suffering from this disease cannot raise their eyelids above the midline. One of the roles of KIF3 (Kinesin-2 family) is to conduct intraflagellar transport (IFT), which is necessary to form and maintain cilia.[15,37] Many mammalian organs are placed in left-right asymmetry. The left-right anomalies are called *situs invertus*. An absence of Kinesin-2 family members, namely, KIF3A and KIF3B is known to result in *situs invertus*.[38] The KIF3 complexes also transport opsin, a retinal protein at the connecting cilium at the junction of the inner and outer segments of the photoreceptor cells.[39,40] Impairment of transport owing to KIF3A causes blindness due to the

degeneration of photoreceptor cells. All these facts underscore the importance of kinesin proteins.

Kinesin Motor Protein Inhibitors

Selectively abolishing activity *in vivo* to a whole family of kinesins, while retaining function in other families, would afford an insight into the enzyme mechanism.[41] Although a great deal is known about the function of kinesins, some questions are still unanswered. Specific inhibitors of kinesin motor proteins would be important research tools, specifically for their ability to disrupt essential processes of cell chemistry. Currently, specific motor protein inhibitors are scarce (nucleotide analogs are excepted as they are non specific *in vivo*). Also, the development of kinesin inhibitors may ultimately have clinical applications. This can have strong implications in restoring human health, given the importance of kinesins in numerous life-threatening diseases.

There are two approaches to target the kinesin activity. One approach would involve the toxin action at the level of cargo attachment.[20] As mentioned earlier, viruses hijack MT-based transport systems. As the mechanism for motor-virus attachment becomes clear, it might be possible to interfere with these associations and provide therapeutic benefits (e.g. anti-HIV drugs). Given the diversity of cargo adaptors and receptors, this approach should afford good inhibitor specificity. But toward this end, little attention has been paid. The popular approach, on the other hand, involves the targeting of the conserved motor domain of kinesin.[14,42] This domain offers several opportunities for inhibition, including competitive or allosteric inhibition of the interactions with nucleotides or MTs[43] and causing interference with the conformational changes associated with motility.[44]

The screening of natural products for cytotoxic activity has led to the identification of numerous mitotic spindle poisons, like taxanes, podophyllotoxin, colchicines, and others, which target β-tubulin.[45] Apart from being crucial for mitotic spindles, the tubulin polymers are essential for non-mitotic cytoskeletal functions. Hence, this mode of action of tubulin poisons can cause peripheral neurotoxicity.[43] The dose-limiting toxicity and pharmacology of these agents is unpredictable, and their efficacy is a major limiting factor. Therefore, there is a need to explore an alternative approach to achieve the mitotic spindle inhibition by targeting the function of enzymes that are specific to mitotic spindles, rather than targeting tubulin. In this way one can mimic the anti-mitotic action of taxanes without the side effects associated with the disruption of tubulin function in non-dividing cells. In recent times there have been some efforts to target mammalian kinesins with small molecule inhibitors that could prove beneficial in cancer chemotherapy. The same strategy can be extended to other diseases, for example arthritis, where the disease features the pathological proliferation of certain cell types.[20]

The mitotic kinesins, such as Eg5, a member of Kinesin-5 family, are required for spindle bipolarity. Since Eg5 is involved in the assembly and maintenance of the mitotic spindle, it is a natural target for cytostatic drugs. Mayer *et al*.[46,47] used phenotype-based screens to identify compounds that affect mitosis. When mammalian cells were treated with a cell-permeable 1,4-dihydropyrimidine-based compound, their bipolar mitotic spindle was replaced by a monastral MT array. The perturbation of bipolar spindle assembly by this small molecule caused monopolar aster formation (a single star-shaped figure at the end of prophase in mitosis), and arrested cells during mitosis. The researchers aptly named the molecule monastrol for its ability to produce a monastral phenotype. Monastrol is specific to Eg5, and inhibits the

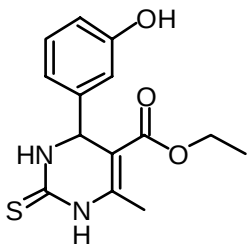

Monastrol

motility of Eg5, but not its MT-binding ability. It was the first known small molecule inhibitor of mitotic machinery that did not target tubulin. Monastrol can serve as a prototype for the development of anticancer drugs, apart from providing a valuable tool for dissecting the function of Eg5 in the establishment of spindle bipolarity, and other cellular processes. Subsequent studies showed that monastrol was an allosteric inhibitor of Eg5,[48] and that the *S* enantiomer is more potent than the *R* form. These findings kindled the hope of developing selective inhibitors of specific mitotic kinesins.

Vale *et al.*[42] used structure-based computer screening to identify small molecule ligands for kinesin. They probed potential binding sites of kinesin inhibitors by docking several classes of compounds. In addition to the obvious nucleotide-binding pocket, other sites that are sensitive to mechanochemical switching were considered as targets. Their studies showed that a pocket cradled by loop 8 and β5 was a novel site for kinesin inhibitors. During this study Rose Bengal lactone (RBL) was identified as a potent kinesin inhibitor. RBL disrupts the interaction between kinesin and MTs, but does not interfere with kinesin's affinity for ATP. This result showed that the RBL-induced inhibition occurred via RBL's binding at a kinesin site involved in MT stimulation. Since RBL also reduced the affinity of kinesin's strongly bound, AMP-PNP state for MTs, it was concluded that RBL competed with MTs for kinesin binding. The other inhibitors that were identified were actually inhibiting the ATPase via MT binding, destabilization, or both. Thus, the computer aided screening proved to be a rapid method for identifying several submillimolar kinesin inhibitors.

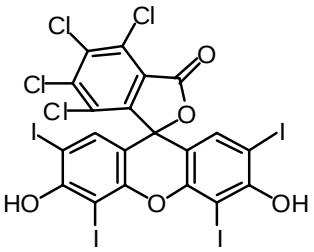

Rose Bengal Lactone (RBL)

Based on their ability to inhibit growth, and induce differentiation, retinoids have received attention in oncology. One of the most widespread effects of retinoic acid is its ability to arrest growth in various types such as, melanoma, lymphoma, neuroblastoma and carcinoma cells. Since HsEg5 plays an important role in spindle assembly and spindle function during mitosis, studies have been conducted[31] in various pancreatic carcinoma cell lines and HaCat keratinocytes to elucidate the mechanism by which all-*trans*-retinoic acid (ATRA) inhibits HsEg5 expression, wherein the effects of ATRA on HsEg5 gene transcription and mRNA stability have been evaluated. It was observed that ATRA did not inhibit HsEg5 gene transcription. Instead, pretreatment with ATRA significantly decreased HsEg5 mRNA stability ($t_{1/2}$ 5.6 h *versus* 14.0 h in untreated controls), suggesting that ATRA significantly inhibits HsEg5 gene expression by a posttranscriptional inhibitory mechanism. This decrease in the HsEg5 concentration results in retardation of centrosome separation and bipolar spindle formation, leading to a strongly retarded mitosis. Thus, ATRA acts as a cytostatic drug.

Local anesthetics like tetracaine and lidocaine inhibit neuronal axoplasmic transport in a dose-dependent manner.[44] At the concentrations that led to such inhibition, these anesthetics neither depolimerize MTs, nor do they decrease the intracellular ATP, as much as they inhibit the axoplasmic transport. This leads to the possibility of direct inhibition of kinesin motility. The motility assays show that the charged forms of the local anesthetics directly and reversibly inhibit the MT-based kinesin motility without lowering its ATPase activity. The charged forms of these anesthetics interfere with the charged residues of the kinesin neck region, and inhibit the unwinding of the neck, thereby preventing the free head from rotating and

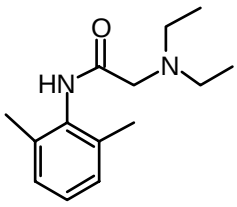

Lidocaine

stepping forward along the MT. Thus, the inhibition of kinesin motility by local anesthetics is the major cause of fast axoplasmic transport inhibition.

Recently Wood *et. al.*[48] identified a quinazolinone compound (*R*)-CK0106023 as a potent and specific allosteric inhibitor of Eg5 ATPase with a K_i of 12 nM. This compound effectively inhibited cell cycle progression, and *in vitro* produced a phenotype similar to the one by monastrol. CK0106023 is the first agent targeting mitotic kinesin to demonstrate anticancer activity, and the article was the first to demonstrate the feasibility of targeting mitotic kinesins for the treatment of cancer. The *in vivo* antitumour activity exhibited by CK0106023 was comparable to or exceeded that of paclitaxel.

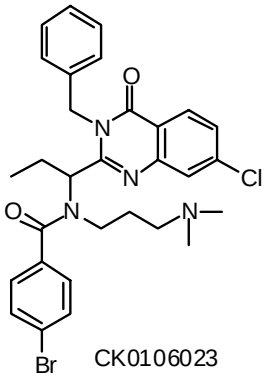

CK0106023

One important approach for the discovery of small molecule inhibitors involves a simultaneous derivatization of the small molecule and the engineering of the target protein. This "one-ligand/one-protein" system creates an excellent specificity.[49] To clarify the specific role of individual kinesins, Kapoor *et al.*[50] developed mutant motors capable of interacting only with the unnatural ATP analogs. By using KIF5 as a model system, they have developed an approach to activate or inhibit a specific kinesin allele in the presence of other similar motors. They prepared ATP analogs, e.g. cyclopentyl-ATP (Cp-ATP), that did not activate either KIF5 or Eg5. However, a KIF5 allele (R14A), mutated in its nucleotide-binding pocket could use this nucleotide analog to drive MT gliding. While a nonhydrolyzable form of the Cp-ATP analog, namely, cyclopentyl-AMPPNP, inhibited the mutant allele in a nonmotile MT-bound rigor state, but did not inhibit either KIF5 or Eg5. The incorporation of kinesin mutants and allele specific activators and inhibitors in the *in vitro* assays can be used to deconvolute the function of KIF5 in complex cellular processes in the presence of other kinesins. This approach can be extended for

studying other kinesins as well. Continuing with this theme of kinesin inhibitors, a class of small molecules has been discovered,[41,51] namely, polycyclic natural products, adociasulfates.

Adociasulfates as Kinesin Inhibitors

The adociasulfates (Figure 4, herein AS) are a recently discovered group of sulfated hexaprenoid hydroquinones isolated from a *Haliclona* (*aka* adocia) species marine sponge from Palau, Western Caroline Islands. These compounds inhibit the MT-stimulated kinesin ATPase activity by interfering with the kinesin binding to MT. This mechanism is unique among known motor protein inhibitors, and results from the AS binding to the kinesin-MT binding site. Thus, the kinesin-MT interaction site could be a useful target for small molecule modulators. Hence, AS represent lead compounds in the search for specific inhibitors of these ATPases.

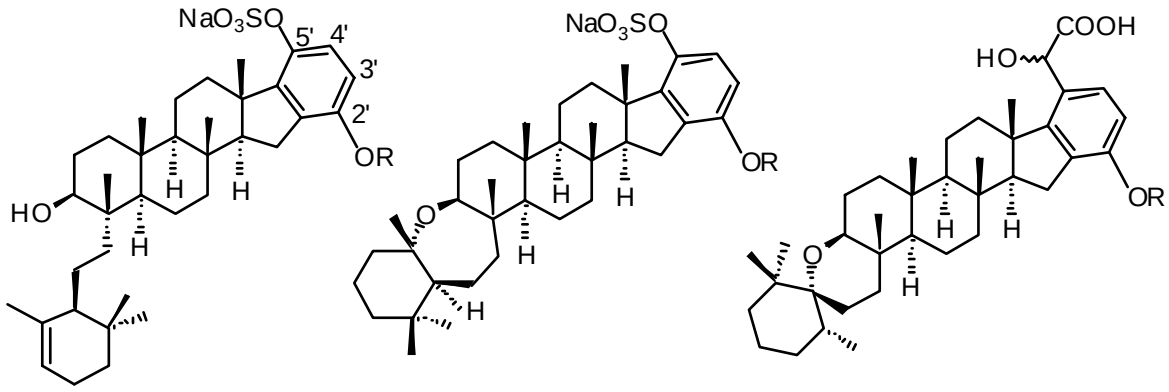

AS-1, R = SO_3Na AS-2, R = SO_3Na AS-10, R = SO_3Na
AS-5, R = H AS-6, R = H

Figure 4: Some AS Derivatives

Extraction of AS from the natural source affords meager quantities of material,[51] not surprisingly, because any potent kinesin inhibitor would be highly toxic even to the organism

producing it. The natural AS are not cell permeable due to the presence of the sulfate moiety. When made membrane permeable, AS-2 and its derivatives can be effective antimitotic and antitransport drugs for studying kinesin functions. Also, the ability of AS-2 and its derivatives to mimic the activity of the MT may allow modification of surfaces to create artificial kinesin tracks.[41] To date, only AS-1 has been synthesized through a twenty eight step route.[52]

Based on the above discussion, it is clear that kinesins play an important role in various intracellular activities, and are important for cellular morphogenesis. Human health is dependent on kinesins, and their malfunctioning can lead to cancer, Alzheimer's disease, neuropathies, and viral infections, to name a few. Thus, an understanding of the role of individual kinesin members is essential from the standpoint of cell biology and therapeutics. This can be achieved by inhibiting specific kinesin members so as to elucidate their role in different physiological events. In the last five to six years there have been efforts directed toward inhibiting the activity of certain kinesins by small organic molecules, such as, monastrol, RBL and others. Some of these compounds can serve as prototypes in developing life saving drugs. Continuing with this theme of small molecule inhibitors of kinesins, the marine natural products adociasulfates have emerged as candidates of interest, as AS inhibit the kinesin activity by a unique mechanism, namely, by binding to the kinesin-MT binding sites. Our plan was to synthesize useful quantities of AS analogs having bioactivity comparable to their natural counterparts in order to answer important biological questions. The following chapter gives an account regarding the design of the proposed AS analog and the synthesis conducted toward achieving the target molecule.

CHAPTER 2

RESULTS AND DISCUSSION

PROGRESS TOWARD THE SYNTHESIS OF ADOCIASULFATE ANALOGS

Introduction

The adociasulfates (AS) are kinesin motor protein inhibitors. The availability of AS from their natural sources is vanishingly low. Their lack of cell-permeability makes their use *in vivo* difficult. Improving the pharmacological properties of AS would provide interesting compounds for biological studies. Hence, the goal of this research project is to employ synthetic schemes of less than ten steps to furnish substantial amounts of AS analogs for studies aimed at understanding the mechanism of AS-induced kinesin inhibition.

Realizing that the Overman synthesis (28 steps) of AS-1 is not suitable for producing useful quantities of material, we envisioned a shorter pathway, having the potential for generating AS analogs possessing bioactivity comparable to the natural AS. Our focus has been on modifying the commercially available steroidal core, instead of attempting a *de novo* synthesis of the tetracyclic moiety of the target molecule, thereby shortening the multi-step synthetic sequence. The design of small molecule inhibitors often times requires insight from molecular modeling studies, wherein protein-ligand docking is conducted to optimize the structural features of the small molecule based on the binding energy values generated during the docking exercise.

Molecular Modeling

We rationalized the choice of our target molecule by means of computer-aided molecular modeling. The structural information[53-55] of human kinesin motor domain was used to screen some analogs that could act as potential inhibitors.

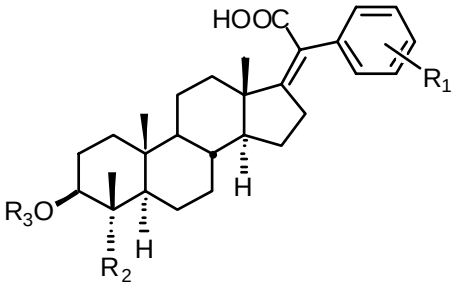

Figure 5: Proposed AS Analog

Figure 6: AS Analog Docked On 1BG2

When the AS analog, shown in Figure 5 (R_1 = CO_2H), was overlaid on AS-2, it was observed that there was little difference in the topology of the anionic units of AS-2 and our analog. Using the SYBYL® force-field, AS-2 and its analogs were then docked (Figure 6) on to the crystal structure of human ubiquitous kinesin motor domain (1BG2). The search for potential binding sites was restricted to the contact points of kinesin-microtubule interaction, namely, loop 11 (amino acid residues 238-254), loop 12 (272-280), α-helix 5 (281-290), and α-helix 4 (257-269). Based on the steric and electrostatic considerations, we identified loop 11 and α-helix 4 as the potential binding sites for AS-2 and its analogs (R_1 = *m*-CO_2^-, *p*-CO_2^-, R_2 and R_3 matches the AS-1 structure). Based on the literature, it can be said that the 2´-sulfate in the AS molecule (AS-

6, Figure 4) is superfluous from a biological point of view, but the sulfate group at the 5´-position on the aromatic ring, and the ring itself are essential in binding to the kinesin motor domain. Hence, we decided to install an unsubstituted aromatic ring in the proposed analog (where R_1 = H, Figure 5), along with the necessary allylic/benzylic -COOH functionality that would not only act as a surrogate for 5´-sulfate, but would also mimic its topology. This was consistent with our goal of identifying the key structural elements of AS necessary for disrupting the kinesin ATPase activity; and ultimately providing a small molecule inhibitor for probing a biologically important motor. The following discussion deals with the aspect of organic synthesis associated with this research project.

Organic Synthesis

The proposed AS analog was pared down (Scheme 1) to the cyclohexyl unit, a steroidal scaffold and the aryl/anionic moiety.

Scheme 1: Simplifying the AS analog

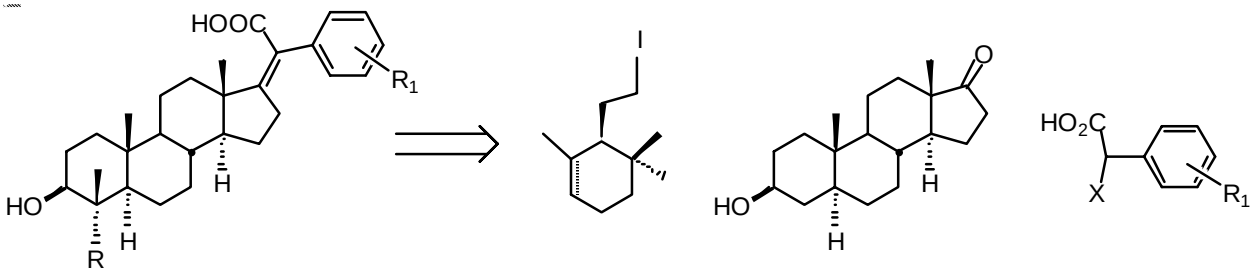

Based on this retrosynthetic scheme, the idea of alkylating the steroidal core with a readily attainable terpene iodide was conceived, and compound **5** was synthesized from 2,4,4-trimethyl-2-cyclohexen-1-one (**1**) (Scheme 2).

Scheme 2: Synthesis of (2,6,6-Trimethyl-2-cyclohexenyl)-1-iodoethane (**5**)

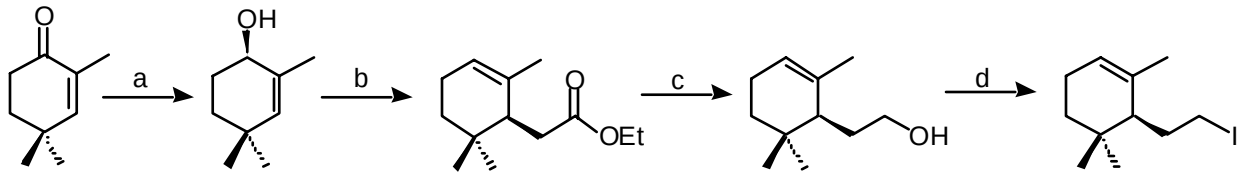

1 **2** **3** **4** **5**

(a) CBS oxazaborolidine, $BH_3 \cdot SMe_2$, THF, rt, 82%, >95% ee; (b) $(EtO)_3CCH_3$, propionic acid, 140-150 °C, 79%; (c) $LiAlH_4$, THF, 5 °C - rt, 78%; (d) I_2, imidazole, PPh_3, CH_3CN, ether, 0 °C, 35%

Asymmetric reduction of **1** to afford alcohol **2** was achieved with Corey's oxazaborolidine catalyst in high yields.[56] The optical purity of **2** was confirmed by synthesizing the corresponding Mosher's esters[57] using (*R*)- and (*S*)-MTPA chlorides, and was found to be greater than 95%. Alcohol **2** gave **3** upon orthoester Claisen rearrangement,[58] and a sequential $LiAlH_4$ reduction[58] and an iodination[59] furnished iodide **5** by a known method. This route, though successful, has drawbacks. First, the starting material **1** is expensive, as are the oxazaborolidine catalyst and MTPA chlorides. Secondly, the intermediates leading to this iodide are highly volatile, and cause difficulties during work-up and purification, which results in a low overall yield.

The goal of any synthetic project is to get to the target molecule from inexpensive substrates and reagents. Since the synthesis of **5** was contrary to this idea, we turned to a similar iodide **10** that was synthesized from β-ionone (**6**),[60,61,59] an inexpensive precursor (Scheme 3).

Scheme 3: Synthesis of (2,6,6-Trimethyl-1-cyclohexenyl)-1-iodoethane (**10**)

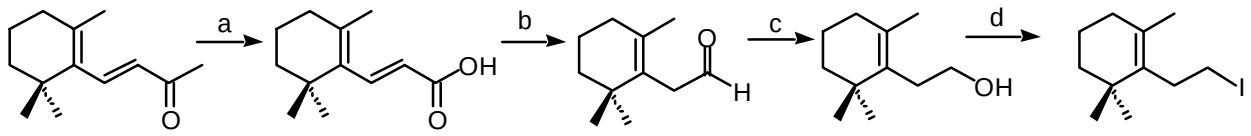

6 **7** **8** **9** **10**

(a) NaOH, Br_2, H_2O, dioxane, 0 °C - rt, 88%; (b) DPPA, Et_3N, dioxane, 0.5 N HCl, 120 °C, 65%; (c) $LiAlH_4$, ether, 35 °C - rt, quantitative; (d) I_2, imidazole, PPh_3, CH_3CN, ether, rt, 55%, DPPA = diphenylphosphorylazide

A haloform reaction was performed on **6** to furnish acid **7**, which underwent a modified Curtius reaction with DPPA to yield aldehyde **8** in moderate yield. Again, $LiAlH_4$ reduction and iodination gave **10**. Concurrent to synthesizing the terpenoids **5** and **10**, the steroidal backbone (4,5α-dihydrotestosterone **11**) of the prospective AS analog was being modified with a view to conducting a key alkylation, at the C4 position of **13** with iodide **10** (Scheme 4).

Thus, the TBS protection[62] of the C17 hydroxyl group of steroid **11**, followed by an oxidation with IBX[63] gave enone **13**. (Previously this enone was synthesized in two steps by the Segusa oxidation[64] of the TMS enol ether of TBS protected **11** with $Pd(AcO)_2$). Since C2 of steroid **13** was now blocked, the methylation using LiHMDS/CH_3I was directed at C4, and was expected to occur from the alpha face due to angular C19 methyl group.[65] Thus, compound **14** was obtained in modest yield. Though the alkylation of **14** with model alkylating agents like benzyl bromide and even *n*-butyl iodide furnished the respective products,[65] the reaction with **10** returned the starting materials. There was no evidence for the base promoted elimination of the homoallylic iodide **10**. Also, the Mukaiyama cross aldol reaction[66] (not shown) between TMS enol ether of **14** and aldehyde **8** returned the starting materials.

Scheme 4: Attempted alkylation of the steroidal core with iodide **10**

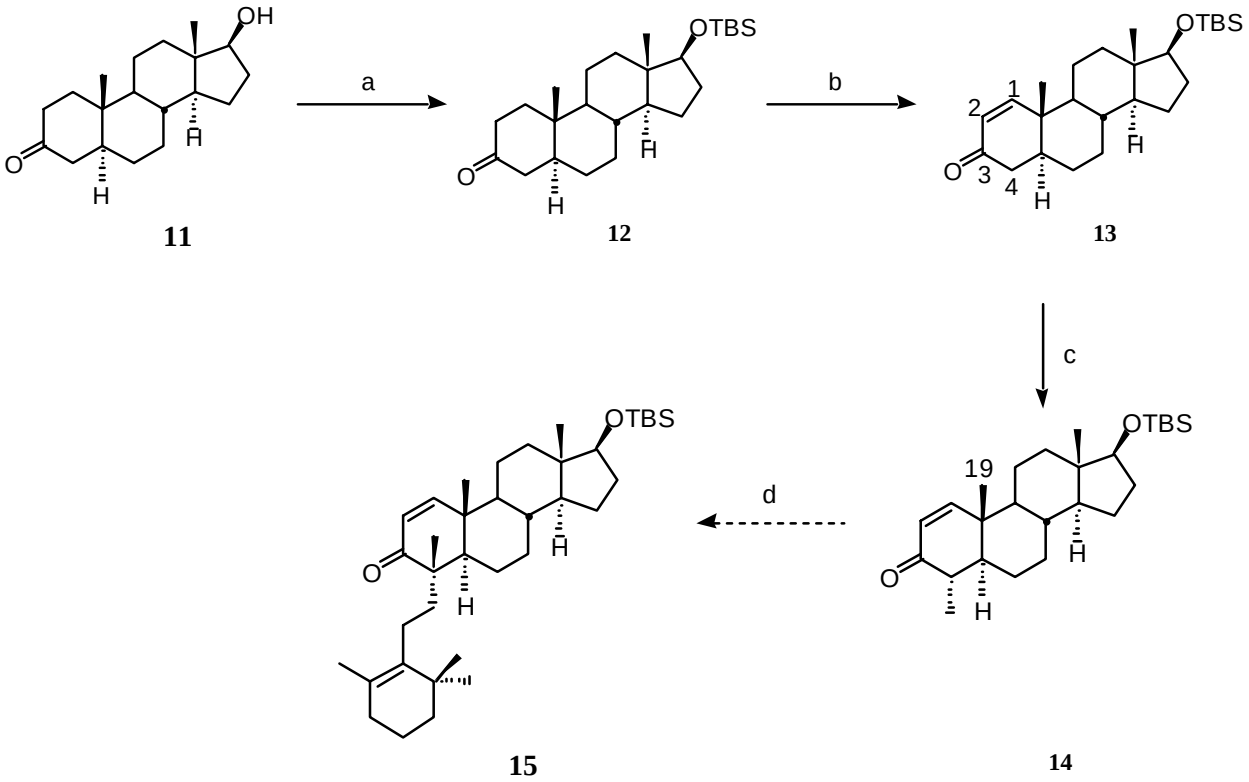

11 **12** **13** **14** **15**

(a) TBSOTf, 2,6-lutidine, $CHCl_3$, rt, 93%; (b) IBX, toluene, DMSO, 55-75 °C, 71%; (c) LiHMDS, CH_3I, THF, 0 °C - rt, 59%; (d) LiHMDS, **10**, THF, 0 °C – reflux;
TBSOTf = tertbutyldimethylsilyltriflate, IBX = *o*–iodoxybenzoic acid, LiHMDS = lithium hexamethyldisilazide

Since attempts to perform the desired transformations via Scheme 4 failed, a pathway based on the Overman synthesis,[52] was undertaken. Schemes 5 and 6 depict this convergent route, wherein the reaction between a nucleophile and an electrophile is meant to install the cyclohexyl unit. Scheme 5 was initiated to obtain the nucleophile (compound **18**).

Scheme 5: Toward the synthesis of iodide **17**

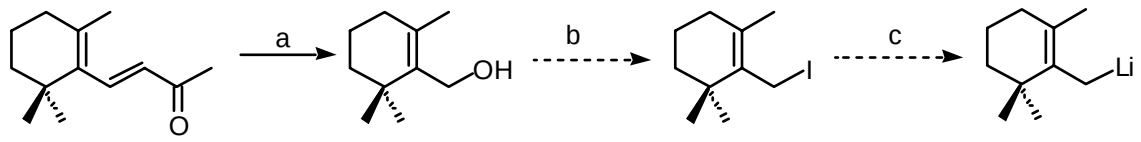

6 **16** **17** **18**

(a) O_3, MeOH, -78 °C, $NaBH_4$, rt, 39% (b) I_2, imidazole, PPh_3, CH_3CN, ether, rt; (c) *t*-BuLi, hexane, ether, - 78 °C – rt

β-Ionone (**6**) on reductive ozonization[67] afforded alcohol **16**. This alcohol can then be converted to iodide **17** by a previously explored method[59] (see Schemes 2 and 3). The *in situ* generated lithio derivative of **17** could then act as a good nucleophile in the proposed synthesis in generating alcohol **21**, the key intermeditate.

Simultaneously, intermediate **14** from Scheme 4 was employed in Scheme 6 so as to generate aldehyde **20**, the electrophilic counterpart of **18**.

Scheme 6: Toward aldehyde **20**

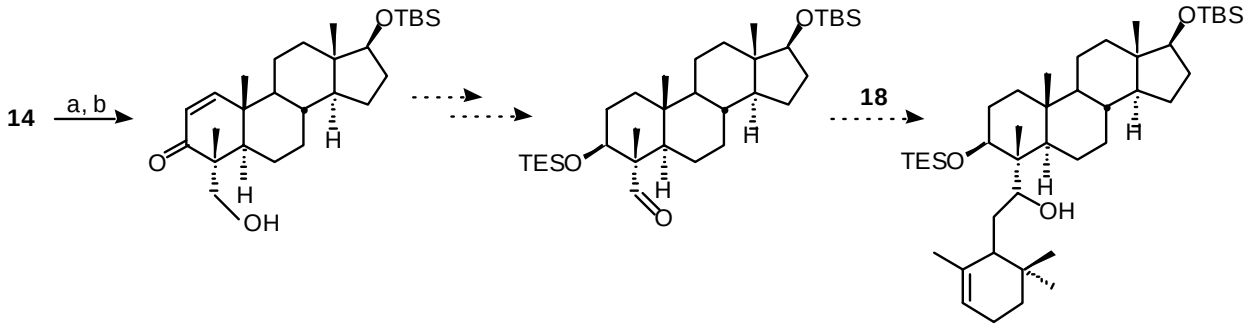

19 **20** **21**

(a) TMSCl, LDA, THF, -78 °C; (b) $HCHO_{(g)}$, TBAT, CH_2Cl_2, -78 °C – rt, 37%;

The TMS enol ether of **14** (not shown) was synthesized using LDA at –78 °C, and then reacted with gaseous formaldehyde (generated by heating paraformaldehyde to 135 ºC) to append a primary alcohol at C4 of **14** to yield compound **19**.[64] Subsequent synthetic operations would then lead to aldehyde **20**, thereby providing the site for nucleophilic attack by **18** that would result in giving pentacycle **21**. However, this is a winding path, and we were inclined to circumvent it. Therefore, modifications on another steroid, testosterone **22**, were initiated (Scheme 7) with a view to realizing aldehyde **20**, via a pathway shorter than the one proposed in Scheme 6.

Scheme 7: Modifying testosterone by alkylation chemistry

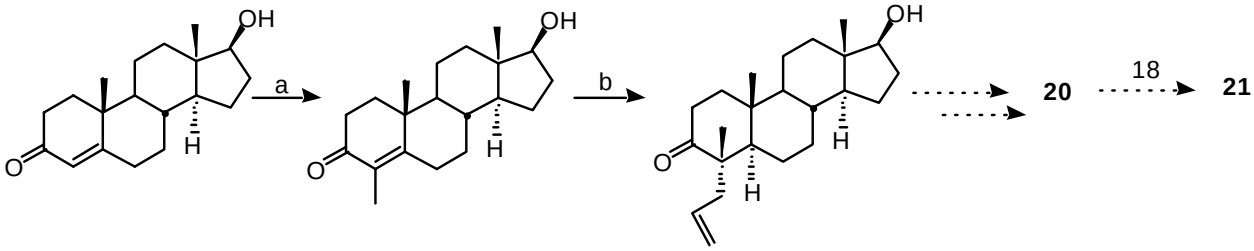

22 **23** **24**

(a) *t*-BuOK, *t*-BuOH, CH_3I, 85 °C, 54%; (b) Li/NH_3, allyl bromide, THF, -33 °C – rt; 47%;

Testosterone (**22**) was methylated under thermodynamic conditions at its C4 position,[68] and then put through a reductive allylation[69] to give **24** in modest yield. Compound **24** can then be transformed to **21** via a series of reactions as in Scheme 6.

At this point, the delay in generating the desired cyclohexyl unit prompted us to reassess the original synthetic strategy. All the routes (except Scheme 3) lack a quick turn-around. This was contrary to the goal of obtaining an AS analog through short synthetic operations. Moreover, the biological role of the cyclohexyl moiety of the AS is yet unclear. The anionic unit at the other end of the molecule is essential for binding with the motor domain of kinesin, as suggested by literature[42] and our modeling studies. Hence, an effort was initiated toward building the anionic portion of our AS analog. The change in our strategy was meant to speedily test the bioactivity of the AS analog, and to provide a quick turn-around.

Accordingly, pregnenolone (**25**) was converted to **27** in good yield by a sequential double bond hydrogenation,[70] and the TBS protection of the C3 hydroxyl group[71] (Scheme 8). Tertiary alcohol **28** was realized by a nucleophilic addition of phenyllithium to the keto functionality of **27**.[73]

Scheme 8: Building the anionic unit

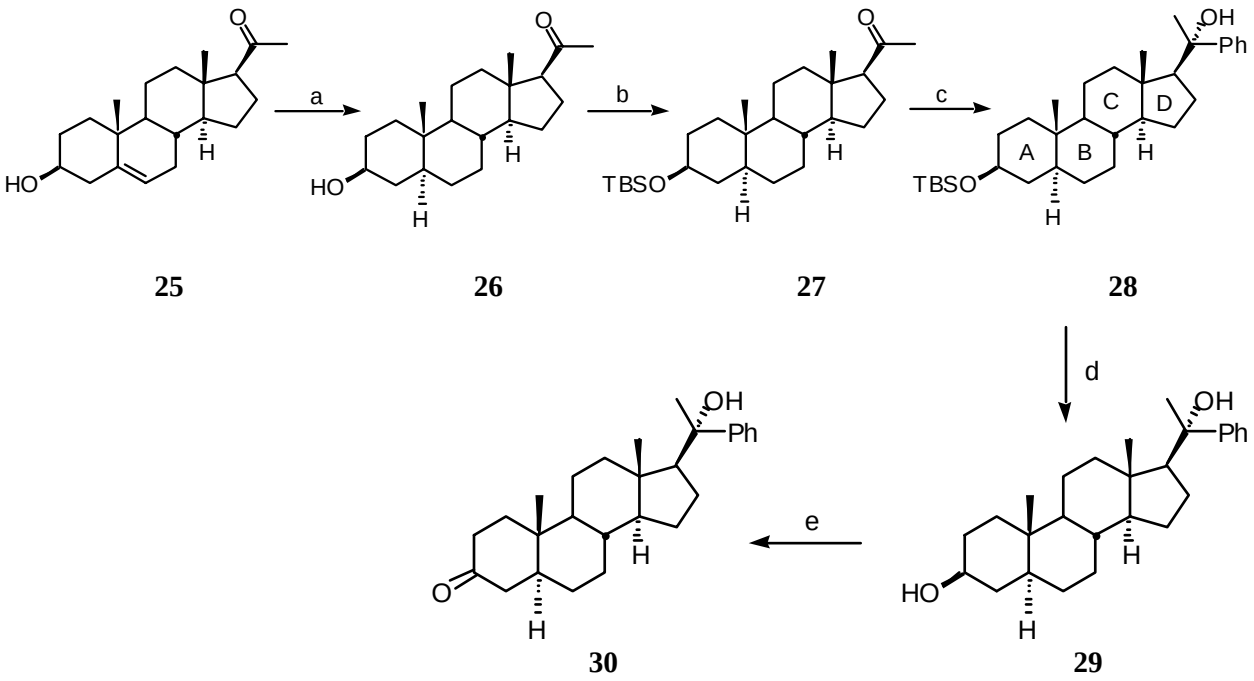

25 **26** **27** **28** **29** **30**

(a) Pd/C (10%), $H_{2(g)}$, 1 atm, EtOH, rt, 48 h, 90% or Pd/C (10%), $H_{2(g)}$, 50 psi, THF, rt, 15 h, 90% (b) TBSCl, Et_3N, DMAP, DCM, rt, 8 h, 90%; (c) *n*-BuLi, PhBr, Et_2O, toluene, rt, 2 h, 84%; (d) TBAF (1M in THF), THF, rt, 24 h, 83%; (e) CrO_3·pyr, DCM, rt, 1 h, 78%

Compound 2**8** was converted to ketone **30** in two sequential steps, namely, a TBAF deprotection of the TBS group,[73] and the Collins oxidation[74] of the free secondary alcohol at C3 of **29**. Hereafter, the key step involved an acid catalyzed dehydration of the tertiary hydroxyl group of **30** to afford tetrasubstituted alkene **31** (Scheme 9). The double bond between C17 and C20 is important for generating a rigid anionic moiety, necessary to mimic the one in natural AS.

Scheme 9: Attempted synthesis of the tetrasubstituted alkene

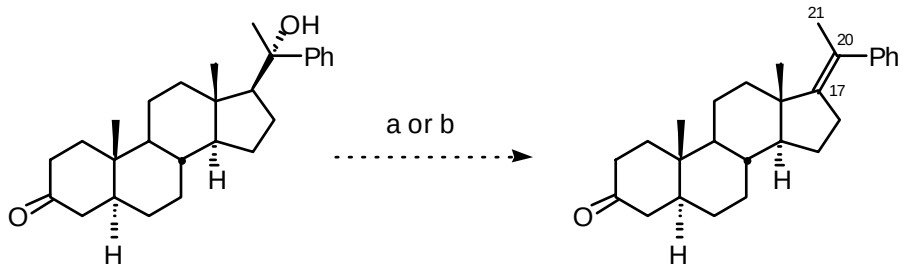

30 **31**

(a) $BF_3 \cdot OEt_2$, DCM, rt, 1 h; or (b) *p*TSA, benzene reflux, 1 h; *p*TSA = *para*-toluenesulfonic acid

Subjecting **30** to $BF_3 \cdot OEt_2$[75] and *p*TSA[76] catalyzed dehydration reactions afforded a compound(s) that showed a single spot by tlc analysis. The gas-chromatographic analysis of the compound(s) exhibited two peaks in the ratio 3:2. ESI-MS showed a peak at *m/z* = 376 (which is the molecular weight of **31**), but the LC-MS spectrum did not exhibit this peak. This is possible if the boiling point of the compounds(s) is >250 °C. The ^{1}H NMR spectrum displayed the aromatic peaks and 6 peaks (instead of just 3) in the aliphatic/methyl region, including two pairs of doublets at ~1 ppm.

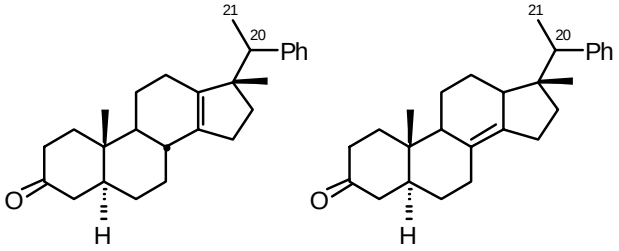

by-products formed due to the carbocation rearrangement

The characteristic allylic methyl peak was absent. This led us to believe, based on the above spectral analyses, that tetrasubstituted alkene **31** was not formed; instead the benzylic/tertiary carbocation generated at C20 under acidic conditions underwent rearrangement to form two compounds. The pair of doublet at ~1 ppm can be attributed to the C21 methyl group, which is being split as a doublet due to the benzylic proton in both the compounds. Further investigations were not carried out to ascertain the identity of the by-products.

Another dehydrating agent that was then employed was $MeSO_2Cl$ in presence of a base. According to the literature,[77] $MeSO_2Cl$ dehydrates a tertiary alcohol without affecting the TBS ether present within the substrate. Hence, compound **27** was reacted with $MeSO_2Cl/Et_3N$ so as to form either the C17-C20 or C20-C21 alkene. Unfortunately, in our hands, not only did $MeSO_2Cl$ generate the C20-C21 alkene, but it also attacked the C3-TBS ether. In spite of using IR, ^1H NMR and ESI-MS, the nature of the modification in the "A" ring of the steroid was not ascertained. Hence, we decided to replace the TBS protecting group with a robust functionality, namely, benzyl (Scheme 10), and then conduct the dehydration with $MeSO_2Cl$.

Scheme 10: Synthesis of benzyl ether of hydrogenated pregnenolone

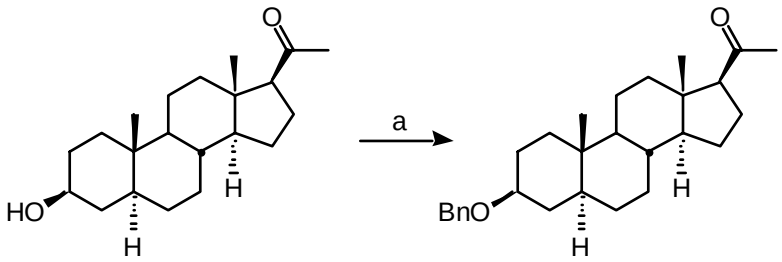

26 **32**

(a) benzyltrichloroacetimidate, TMSOTf, DCM, 0 °C -reflux, 72 h, 39%; Tf = triflic, Bn = benzyl

The benzylation of alcohol **26** with standard method (BnBr, NaH, THF)[78] did not afford the benzyloxy ether. Finally, benzyl ether **31** was synthesized by employing benzyl-2,2,2-trichloroacetimidate and TMSOTf,[79] albeit in low yield. Using freshly distilled reagents, varying the duration and the temperature of the reaction, and maintaining anhydrous conditions did not improve the yield. Also, no starting alcohol was recovered. A low yield at an early stage of the pathway was undesirable, forcing us to continue with Scheme 8.

Scheme 11: Synthesis of disubstituted alkene

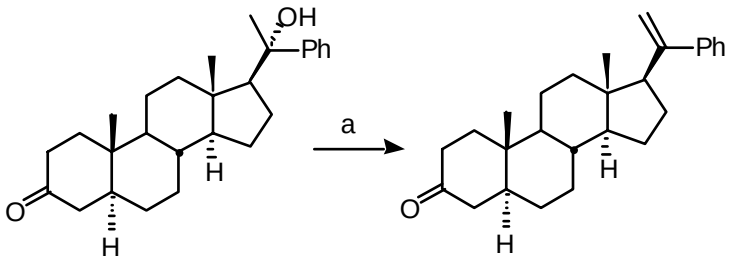

30 **33**

(a) $MeSO_2Cl$, Et_3N, DMAP, DCM, 0 °C -reflux, 1 h, 87%

Subjecting ketone **30** to prescribed amounts[77] of $MeSO_2Cl/Et_3N$ at room temperature produced alkene **33** in <40%. But increasing the molar ratios of reagents and elevating the reaction temperature generated **32** in 87% yield (Scheme 10).

The next step involved a hydroboration-oxidation[80] of the terminal alkene unit of **33** to form a primary alcohol **34** (Scheme 12). However, the hydroboration of **33** to generate primary alcohol **34** resulted in a very poor yield. Instead, the major product was secondary alcohol **35** obtained by the reduction of the C3 ketone.

Scheme 12: Poor chemoselectivity: hydroboration of alkene vs. reduction of ketone

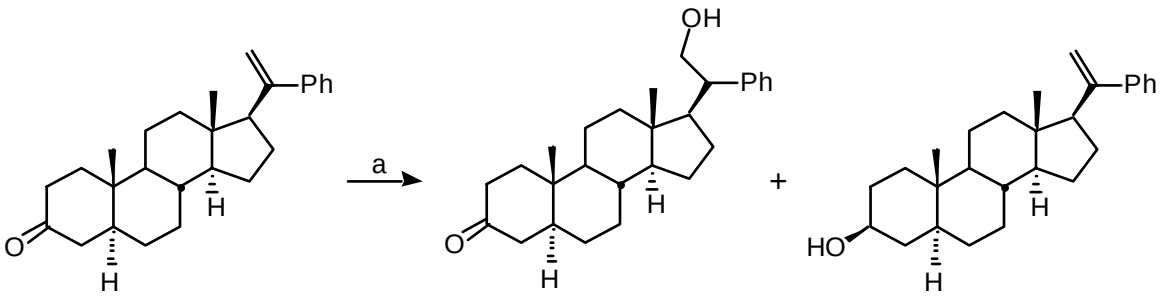

33 **34** **35**

(a) BMS, THF, 0°C→ rt, 3 h, NaOH (3N), H_2O_2, reflux, 56% overall; BMS = borane-methyl sulfide

Since the desired chemoselectivity was not achieved during the reaction, ketone **33** was protected as the acetal in high yield[81] to obtain intermediate **36**. The hydroboration of **36** formed primary alcohol **37** in 56% yield (Scheme 13).

Scheme 13: Protection of C3 ketone leads to the desired primary alcohol

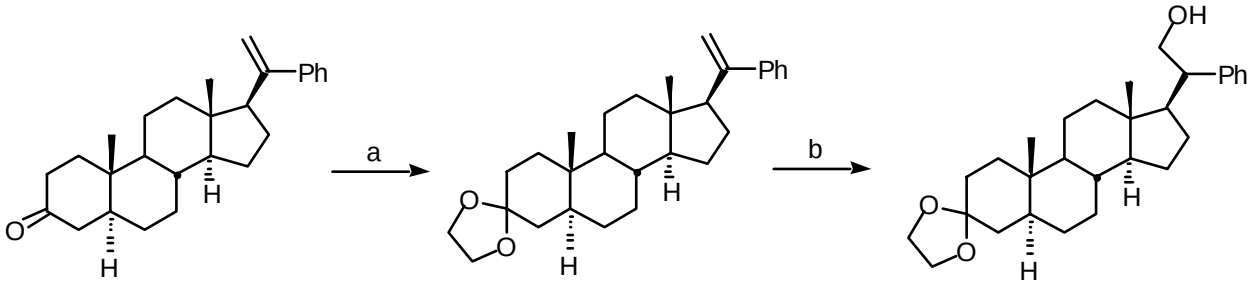

33 **36** **37**

(a) ethylene glycol, TMSCl, DCM, reflux, 24 h, 87%; (b) BMS, THF, 0°C→ rt, 3 h, NaOH (3N), H_2O_2, reflux, 56%

The next step involves, either a one-pot oxidation of primary alcohol **37** to the corresponding carboxylic acid **39**, or producing the acid via aldehyde **38** (Scheme 14).

Scheme 14: Oxidation of primary alcohol or aldehyde: toward the target carboxylic acid

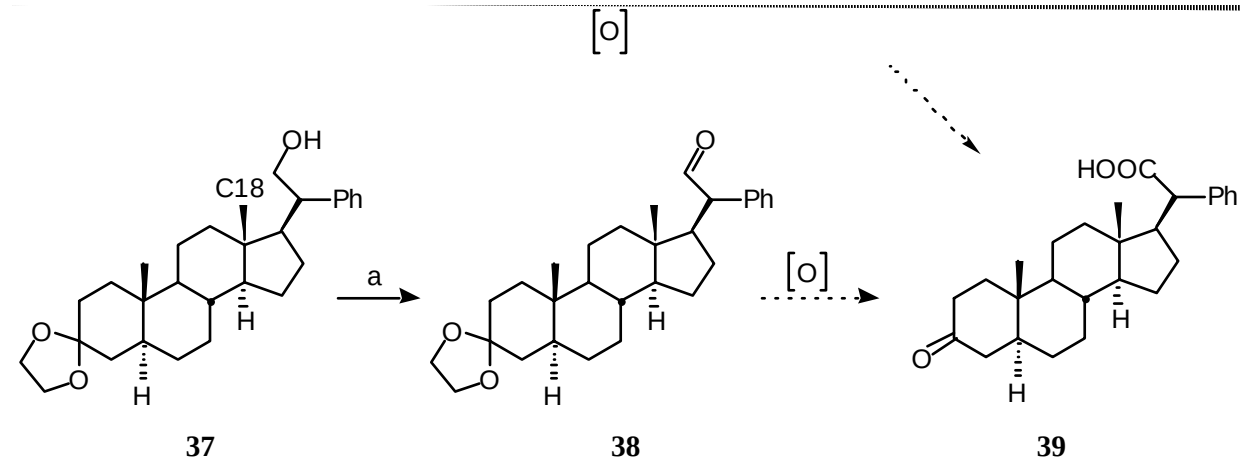

37 **38** **39**

(a) CrO_3.pyr., DCM, rt, 1 h, 70%; (b) various oxidants

There are a number of methods available for the oxidation of a primary alcohol or an aldehyde to the carboxylic acid, but many of these oxidations are conducted either in acetonitrile

or acetone, ethyl acetate or DMSO. The solubility of compounds **37** and **38** in acetone is quite poor (2 mg in ~5 mL), and in the rest of these solvents they are practically insoluble. Fortunately, these compounds are soluble in dichloromethane (DCM), DMF and THF. The choice of solvents influences the reactivity profile. In one case, the solvent THF itself is converted to δ-butyrolactone by the oxidant.[82] Considering these factors, oxidants that could cleanly convert an alcohol or aldehyde into an acid in acetone, DCM, DMF or THF were chosen. In spite of investigating various oxidation conditions, the desired acid could not be synthesized. In most cases, the oxidation stopped at the intermediate aldehyde stage (that is, compound **37**, entries 1, 6, 7 and 9). Subjecting **37** to further oxidation returned the unreacted starting material (entries 9-11). This is most likely due to the steric hindrance caused by the C18 steroidal methyl group. In many cases, these oxidants readily converted a structurally similar alcohol, namely, 2-phenylethanol to 2-phenylacetic acid, in very high yield. The following table depicts the results obtained from the attempted oxidation reactions.

Table 1: The Oxidation Reactions: Conditions and Results

Entry	Substrate	Experimental conditions	Results
1.	alcohol **37**	acetone, aq. $NaHCO_3$, phosphate buffer, NaBr, TEMPO, TCCA, reflux[83]	aldehyde **34**
2.	**37**	Replacing acetone with THF	decomposition
3.	**37**	TEMPO, bleach (5%), $NaClO_2$, THF, 35 ° C[84]	SM recovered
4.	**37**	Benzotriazole·CrO_3 complex, C_6H_6, reflux[85]	SM recovered
5.	**37**	Ag(II)O, THF:H_2O (9:1)[86]	SM recovered
6.	**37**	$NaMnO_4.H_2O$, DCM, reflux[87]	aldehyde **34**
7.	**37**	TEMPO, bleach (13%), $NaClO_2$, THF, reflux[88]	aldehyde **34**
8.	**37**	TEMPO, bleach (13%), $NaClO_2$, DCM, reflux[88]	decomposition
9.	**37**	Ru-Co$(OH)_2$-CeO_2, $O_{2(g)}$, trifluorotoluene[89]	aldehyde **34**
10.	aldehyde **38**	(bipy)H_2CrOCl_5 complex, DCM, reflux[90]	SM recovered
11.	**38**	acetone, aq. $NaHCO_3$, phosphate buffer, NaBr, TCCA, reflux[83] (conducted with & without TEMPO)	SM recovered
12.	**38**	Oxone®, DMF, Δ (other solvents ineffective)[91]	SM recovered
13.	**38**	PDC, DMF, Δ[92]	decomposition
14.	**38**	Ru-Co$(OH)_2$-CeO_2, $O_{2(g)}$, trifluorotoluene[89]	SM recovered

Benzotriazole·CrO_3, (bipy)H_2CrOCl_5 and Ru-Co$(OH)_2$-CeO_2 were synthesized by a known procedure, TCCA = trichlroisocyanuric acid, SM = starting material

Apart from this, compound **37** was also subjected to the Jones oxidation (2.67 M) at low temperatures.[93] A dilute solution of substrate (0.025 g, 0.057 mmol) in acetone (~50 mL) was

titrated against the reagent, which was added dropwise in the reaction vessel till the orange-brown color of the reaction mixture persisted. The reaction was further stirred at that temperature for ~2 h before working it up in a standard fashion. In addition to reacting at the primary alcohol, the aqueous acid present in the Jones reagent cleaved the acetal group to regenerate the C3 ketone. The acid (**39**) thus obtained would have a molecular weight of 408, i.e. M^+ = 408. The results are reported in the table below.

Table 2: The Jones Oxidation

Entry	Substrate	Temperature.	Result
i.	alcohol **37**	0 °C	ESI-MS (negative ion mode): (M^+-1) = 407, ^{1}H NMR: aromatic, C18 & C19 methyl peaks present. Also, a doublet (at ~3.4 ppm) observed, possibly due to the presence of a benzylic proton
ii.	**37**	-78 °C (till reaction mixture turned orange)	SM recovered
iii.	**37**	-78 °C (till reaction mixture turned orange-brown)	Decomposition
iv.	aldehyde **38**	0 °C	same as in entry (i).

The reactions conducted at 0 °C gave a crude solid (entry i), who's ESI-mass spectrum (negative ion mode) shows modestly intense peak at M^+-1 = 407. However, no peak corresponding to MH^+ was seen in the positive ion mode. Its ^{1}H NMR spectrum, displayed the aromatic and the two steroidal methyl peaks. Also, all the spectra show a doublet at ~3.4 ppm,

which could be attributed to the benzylic proton conjugated with the –COOH group. However, based on this speculation, no conclusion can be drawn regarding the presence or absence of such a proton. The IR data is inconclusive due to the poor quality of the instrument. The crude product is very moderately soluble in DCM or $CHCl_3$, and quite soluble only in THF (and DMSO). Attempts to purify the "carboxylic acid" by the standard method, namely, aqueous $NaHCO_3$ wash, followed by acidification with HCl, and a subsequent extraction with an organic solvent, were futile. Also, column chromatography seems to be of little help, given the complex nature of the tlc picture. The same result as in entry (i) was obtained when aldehyde **38** was exposed to the Jones reagent. As this oxidation impasse continued, we conducted a sulfation reaction on the hydroxyl group of **37** (Scheme 15).[94]

Scheme 15: Sulfation of the primary hydroxyl group

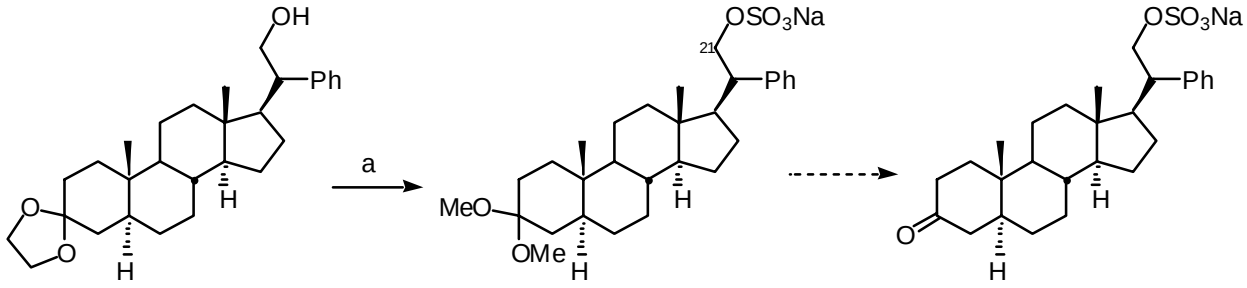

37 **40** **41**

(a) $Et_3N{\cdot}SO_3$, DMF, rt, 3 h, 50%

The sulfation strategy was meant to avoid the problematic oxidation step, and yet afford an anionic unit. The sulfation complex ($Et_3N{\bullet}SO_3$) was synthesized from triethylamine and chlorosulfonic acid.[95] Exposing **37** to the sulfation conditions afforded, based on ^1H NMR analysis, the sulfated dimethyl acetal sulfate ester **40**, instead of ketone **41**. This is rationalized by the opening up of the 1,3 dioxolane ring under the influence of amberlyst, an acidic cation exchange resin, and methanol, which were used for chromatographic purposes. The

deacetalization[96] of **37** to afford **34**, followed by the sulfation step again resulted in **40** under the same chromatographic conditions.

Screening for Kinesin ATPase Inhibition

Having installed an anionic functionality on the steroidal backbone, sulfate **40** was subjected to a phosphatase assay using EnzChek® phosphate assay kit (Molecular Probes, E-6646).[97] This assay was conducted for the quantitation of the inorganic phosphate (P_i) released when ATP is enzymatically hydrolyzed to ADP during the processive motion of human ubiquitous kinesin (KIF-1) on microtubule tracks. In the presence of purine nucleoside phosphorylase (PNP), P_i converts 2-amino-6-mercapto-7-methylpurine ribonucleoside (MSEG) into 2-amino-6-mercapto-7-methylpurine, which is chromophoric. The reaction can be monitored by UV-VIS spectrophotometry to obtain an IC_{50} or a K_i for the test compound. A decrease in the concentration of the released phosphate would indicate that the ligand (sulfate **40** in the present case), after binding to the protein, was capable of effectively inhibiting the microtubule-stimulated ATPase activity of the motor protein. Since no decrease in the concentration of the released P_i was observed, even at high compound concentration, it was concluded that sulfate **40** was ineffective as a K560 inhibitor. This presumably is due to the additional carbon (C21) in the anionic unit that adversely affects its rigidity, and prevents **40** from binding to the kinesin motor domain.

Future Directions

In view of this negative result, the following two routes warrant attention for their potential to yield more rigid anionic functionality. Continuing with the sulfation theme, a new approach would involve a key organocuprate reaction to produce compound **43** (Scheme 16). Thereafter, a three-step sequence is necessary to form **45**.

Scheme 16: Alternative sulfation scheme

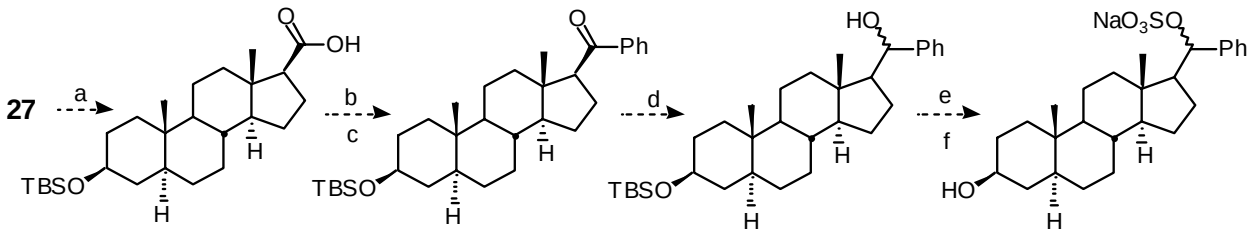

42 **43** **44** **45**

(a) NaOH, Br_2, H_2O, dioxane, 0 °C – rt; (b) $SOCl_2$, $CHCl_3$ (c) *n*-BuLi, PhBr, ether, -78° C, Cu(I)I; (d) $LiAlH_4$, ether; (e) $Et_3N{\cdot}SO_3$, DMF, rt ; (f) TBAF, THF, rt

A haloform reaction on compound **27** would lead to carboxylic acid **42**, which can be converted to acid chloride by treatment with $SOCl_2$,[98] followed by a Gilmann reaction to install the phenyl ring of **43**.[99] The diastereomeric secondary alcohol **44** would result from a subsequent $LiAlH_4$ reduction of the carbonyl group of phenyl ketone **43**. The diastereomers should be separable by column chromatography. The pure diastereomers can then be sulfated to obtain both the diastereomers of the sulfate **45**.

A second strategy, devoid of an oxidation, that could be explored to obtain the unsaturated carboxylic acid functionality is shown in scheme 17. This proposed route involves the triflation reaction on phenyl ketone **43**,[100] wherein the C17-C20 double bond can also be installed to generate a diastereomeric (*E/Z*) mixture of triflate **46**. Then, a Pd(0) catalyzed methoxycarbonylation of the diastereomeric triflate would form the methyl carboxylate **47**.[101] This ester on saponification would furnish the carboxylic acid functionality. Photoisomerization of this unsaturated carboxylic acid will favor the desired *Z* diastereomer,[102] which should afford unsaturated *Z* acid **48** on TBAF deprotection of the TBS group.

Scheme 17: Proposed route to generate the unsaturated carboxylic acid unit

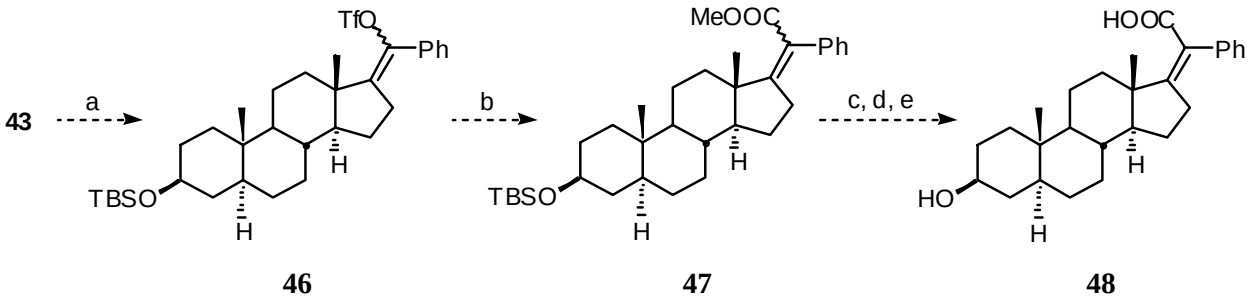

(a) $(TfO)_2O$, 2,6-di-*tert*-butylpyridine, DCM, reflux; (b) $Pd(OAc)_2$, $CO_{(g)}$, Et_3N, PPh_3, MeOH, DMF, rt; (c) aq. K_2CO_3, MeOH, reflux; (d) hv, THF; (e) TBAF, THF, rt

This scheme involves the triflation reaction on phenyl ketone **43**,[100] wherein the C17-C20 double bond can also be installed to generate a diastereomeric (*E/Z*) mixture of triflate **46**. Then, a Pd(0) catalyzed methoxycarbonylation of the diastereomeric triflate could form the methyl carboxylate **47**.[101] This ester on saponification would furnish the carboxylic acid functionality, which should favor the desired *Z* diastereomer upon photoisomerization.[102] Unsaturated *Z* acid **48** should be produced upon on TBAF deprotection of the TBS group.

The above discussion mainly deals with the organic chemistry conducted in our laboratory toward the synthesis of AS analogs by short routes. During this endeavor, the AS carboxyl analog **39** could not be identified unambiguously, and the sulfate **40** did not possess the biologically active necessary to inhibit the human ubiquitous kinesin. However, the proposed synthetic strategies toward the end of the discussion section (Schemes 16 and 17) hold the promise of furnishing potentially active AS analogs through few synthetic manipulations. Further studies along these lines could afford molecules of scientific importance and aid our understanding regarding the mechanism of AS-induced kinesin inhibition.

CHAPTER 3

EXPERIMENTAL SECTION

General

All moisture-sensitive reactions were carried out using standard syringe-septum techniques under an atmosphere of dry nitrogen or argon with oven-dried (140 °C) or flame-dried glassware. All solvent extracts were dried over anhydrous $MgSO_4$. Concentrations were performed under reduced pressure with a rotary evaporator followed by placement on a vacuum (<1 torr) line for several minutes, except in case of volatile compounds. Reaction temperature of -78 °C was achieved using an acetone-dry ice bath. The percentage yields of the products are rounded off to the nearest whole numbers and refer to the compounds isolated after purification.

Reagents and Solvents

Dichloromethane (DCM), iodomethane (both distilled over P_2O_5), diisopropylamine (distilled over NaOH), trimethylsilylchloride and acetonitrile (both distilled over CaH_2), pyridine (pre-dried over solid NaOH) and hexamethyldisilazane were distilled at atmospheric pressure. β–Ionone, $BF_3.OEt_2$, benzyl bromide (pre-dried over $CaCl_2$), bromobenzene (distilled over CaH_2), allyl bromide, methanesulfonyl chloride (distilled over P_2O_5), ethylene glycol and 2,6-lutidine (latter distilled over CaH_2) were distilled under reduced pressure. Liquid ammonia was distilled over metallic sodium. Lithium metal was washed with hexanes prior to use. Chromium trioxide was dried in a desiccator over P_2O_5 under reduced pressure. Tetrahydrofuran (THF), chloroform, benzene, toluene and diethyl ether were dried by passing through an activated alumina column under positive nitrogen pressure (assembly from Solv-Tek Inc. purification system) prior to use.

IBX[103] and TBAT[104] were prepared according to literature procedures. All other starting materials and reagents were obtained commercially or prepared as per literature procedure, and were used as such or purified by standard means.[105]

Chromatography

Thin-layer chromatography (tlc) was carried out on pre-coated glass plates with 0.25 mm silica gel 60 with 254 nm fluorescent indicator purchased from EM Science or Sorbent technologies. The plates were developed in a covered chamber. Materials were detected by visualization, either under UV light or by dipping the plate into phosphomolybdic acid (PMA) stain or 10% ethanolic H_2SO_4 stain, followed by gentle heating. Column chromatography refers to the flash column technique.[106] Normal phase column chromatography was performed using silica gel 60, 230-400 mesh, (0.04-0.063 mm particle size) from EM Science or Sorbent technologies. Reverse phase column chromatography was conducted using C18 silica gel, 60 Å, 0.04-0.06 mm particle size, from Sorbent technologies. The cation exchange resin, amberlite® CG-120, 200-400 mesh, was obtained from Mallinckrodt chemical works. Chromatographic solvent proportions are expressed on a volume:volume basis.

Physical and Spectroscopic Measurements

^1H and ^{13}C spectra were recorded on a Varian Mercury Plus 400 MHz and a 100 MHz spectrometer (with automation), respectively, using tetramethylsilane (TMS) as the internal standard and $CDCl_3$ as the solvent, except as noted. For ^1H NMR, the following abbreviations are used: s singlet, d double, t triplet, q quartet and m multiplet. ^1H and ^{13}C Chemical shifts are reported in parts per million (δ) relative to the internal standard TMS (δ 0.00). The coupling constants (*J*) are given in Hz. FT-IR spectra were recorded on a Bio-Rad® Excalibur Series spectrophotometer, and the absorption frequencies are reported in cm^{-1}. Mass spectrometry was

performed on a Sciex API-1 Plus quadrupole mass spectrometer with an electospray ionization source. Melting points are recorded on a Mel-Temp® apparatus and are uncorrected.

Experimental Details

(*R*)-2,4,4-Trimethyl-2-cyclohexen-1-ol (2):[56]

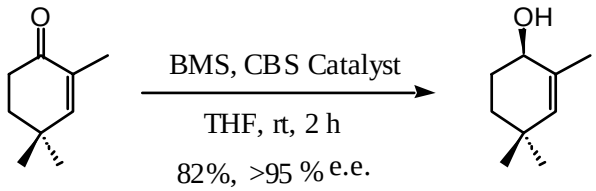

1 **2**

A 15-mL round bottom flask was charged, at room temperature with a solution of borane-dimethylsulfide (BMS) complex (170 μL) in THF (1.6 mL). To this was added the CBS oxazaborolidine catalyst (180 μL). To this mixture was added, dropwise over a period of 30 minutes, a solution of enone **1** (0.27 mL, 1.86 mmol) in THF (7 mL). The reaction mixture was stirred for 2.5 h, after which methanol (4 mL) and 0.1 N HCl (10 mL) were added to the mixture. The organic and the aqueous layers were separated and the aqueous layer was extracted with ether (3 x 10 mL). The combined ether extracts were washed with H_2O (2 x 5 mL), brine (5 mL), dried, and evaporated under reduced pressure to give a yellow oil that was purified by short-path distillation under reduced pressure (6 torr at 76 °C) to give alcohol **2** as a colorless oil (0.21 g, 1.52 mmol, 82%).

^{1}H NMR δ 5.24 (s, 1H), 3.93 (t, *J* = 5, 1H), 1.71 (s, 3H), 2.13-1.0 (m, 5H), 0.99 (s, 3H), 0.93 (s, 3H).

[Boiling point and spectral date match with the literature values. The enantiopurity of **(*R*)-2** was determined by converting it to the corresponding Mosher's ester].

(*R,R*)-Mosher's ester of alcohol 2:[57]

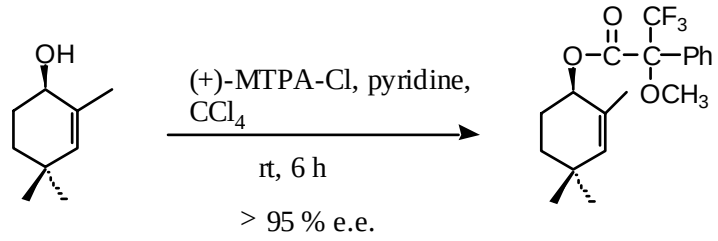

2 **(*R,R*)-Mosher's ester**

A 1-dram vial, fitted with a septum, was sequentially charged with pyridine (150 μL), (+)-MTPA-Cl (20 mg, 0.07 mmol), CCl_4 (150 μL), and alcohol **2** (70 mg, 0.05 mmol). This mixture was shaken and allowed to stand for 6 h at room temperature until the reaction was complete as evidenced by no more formation of pyridinium hydrochloride. Then excess 3-dimethylamino-1-propylamine (12 μL, 0.01 mmol) was added, and the mixture was allowed to stand for 5 minutes. The mixture was extracted with ether (2 x 1 mL), and the combined ether layers were washed with cold dilute HCl (2 x 0.5 mL), cold saturated Na_2CO_3 (2 x 0.5 mL), brine (0.5 mL), dried, and evaporated under reduced pressure to give a pale yellow oil, which was purified by elution through a short (~1 inch) silica gel bed using hexanes:ethyl acetate (90:10) system to give the diastereomeric Mosher's esters as a colorless oil. Based on the $–OCH_3$ peaks in the NMR spectrum of this oil, the enantiomeric excess of **(*R*)-2** was determined to be >95%.

^{1}H NMR (Bruker AMX-400 MHz) δ 7.55-7.39 (m, 5H), 5.40-5.34 (m, 1H), 3.56 (s, 3H, $–OCH_3$), 1.94-1.25 (m, 5 H), 1.66 (s, 3H), 0.95 (s, 3H), 0.93 (s, 3H).

(R,R)-Mosher's ester of 2

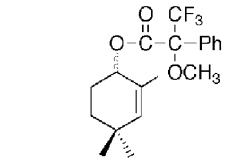

Mosher's ester of racemic **2**

Ethyl [(*S*)-2,6,6-trimethy-2-cyclohexenyl] ethanoate (3):[58]

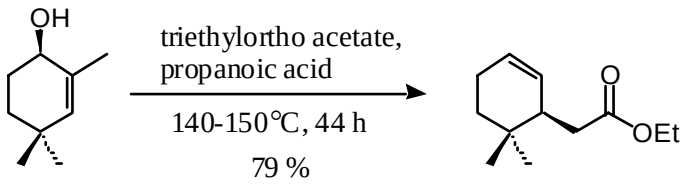

2 **3**

A 10-mL round bottom flask fitted with a Dean-Stark apparatus was charged at room temperature, with alcohol **2** (0.30 g, 1.65 mmol), triethylorthoacetate (2.64 g, 16.27 mmol), and freshly distilled propanoic acid (0.4 mL), and the reaction was heated to 140-150 °C for 20 h, after which an additional charge of propanoic acid (0.2 mL) was added. The heating was continued for further 24 h, after which the solution was concentrated under reduced pressure. The resultant residue was diluted with diethyl ether (5 ml), and the ether layer was washed with H_2O (2 x 1 mL), saturated aqueous Na_2CO_3 (2 x 1 mL), brine (1 mL), dried, and evaporated under reduced pressure to give a yellow oil (0.29 g) that was purified by short-path distillation (6 torr at 118 °C) to give ester **3** as a colorless oil (0.28 g, 1.31 mmol, 79%).

^{1}H NMR δ 5.33 (s, 1H), 4.14 (q, *J* = 7.2, 2H), 2.55-2.15 (m, 2H), 2.18-1.50 (m, 3H), 1.72-1.58 (m, 3H), 1.25 (t, *J* = 7.2, 2H), 1.51-1.00 (m, 2H), 0.92 (s, 3H), 0.84 (s, 3H).

[Boiling point and spectral date match with the literature values].

2-[(*S*)-2,6,6-Trimethy-2-cyclohexenyl] ethanol (4):[58]

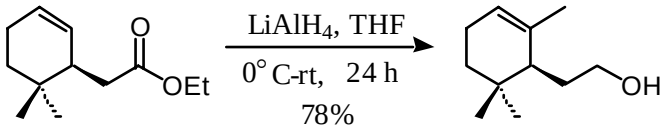

3 **4**

A 10-mL round bottom flask was charged with a solution of **3** (0.38 g, 1.83 mmol) in THF (4 mL). To it was added $LiAlH_4$ (50 mg, 1.32 mmol) at 0-5 °C, and the reaction mixture was stirred for 24 h at room temperature. The reaction was quenched with 10% aqueous NaOH (0.4 mL) and H_2O (0.4 mL). The precipitated lithium salt was filtered off, and the filtrate was extracted with diethyl ether (2 x 5 mL). The combined organic layers were washed with H_2O (2 x 2 mL), brine (2 mL), dried, and evaporated under reduced pressure to give a pale yellow oil (0.29 g) that was purified by short-path distillation (6 torr at 99 °C) to give alcohol **4** as a colorless oil (0.24 g, 1.43 mmol, 78%)

^{1}H NMR δ 5.31 (s, 1H), 3.66 (t, J = 7.2, 2H), 2.10-1.80 (m, 3H), 1.70 (s, 3H), 1.79-0.99 (m, 5H), 0.91 (s, 3H), 0.89 (s, 3H).

[Boiling point and spectral date match with the literature values].

(2,6,6-Trimethyl-2cyclohexenyl)-2-iodoethane (5):[59]

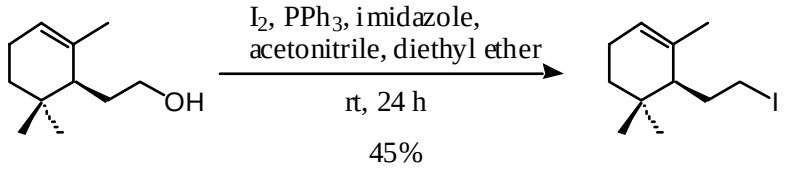

4 **5**

A 15-mL round bottom flask was charged, at room temperature, with alcohol **4** (50 mg, 0.29 mmol), triphenyl phosphine (0.10 g, 0.38 mmol), imidazole (30 mg, 0.39 mmol), acetonitrile (2.7 mL) and diethyl ether (4.5 mL). To this mixture was added, at 0 °C, iodine crystals (0.10 g, 0.41 mmol), and the solution was stirred for 24 h at room temperature. The mixture was diluted with diethyl ether (15 mL), and the organic layer was washed with saturated aqueous $Na_2S_2O_3$ (2 x 5 mL), saturated aqueous $CuSO_4$ (2 x 5 mL), H_2O (5 mL), dried, and evaporated under reduced pressure to give a colorless oil (0.05 g) that was purified by short-path distillation (6 torr at 125 °C) to give iodide **4** as a colorless oil (36 mg, 0.13 mmol, 45%).

^{1}H NMR δ 5.33 (s, 1H), 3.23 (t, *J* = 8.2, 2H), 2.10-2.03 (m, 1H), 1.95-1.85 (m, 3H), 1.70 (s, 3H), 1.46-1.43 (m, 1H), 1.39-1.34 (m, 1H), 1.20-1.15 (m, 1H), 0.92 (s, 3H), 0.88 (s, 3H).

[Boiling point and spectral date match with the literature values].

3-(2,6,6-Trimethyl-1-cyclohexen-1yl)-2-propenoic acid (7):[60]

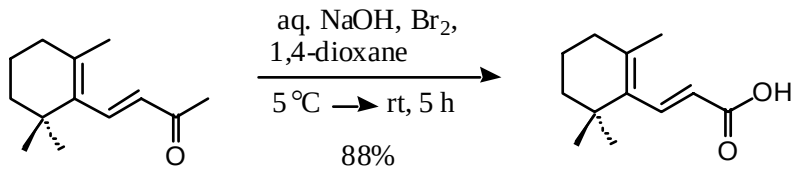

6 **7**

A 250-mL Erlenmeyer flask was charged with NaOH (17 g) and H_2O (70 mL). This solution was cooled in an ice-bath and to it was added Br_2 solution (5.5 mL) and the mixture was stirred for 1 h in ice-bath. A solution of β-ionone (**6**) (4.5 g, 23.4 mmol) in 1,4-dioxane (10 mL) was then added to it and then the reaction was stirred for 4 h. at room temp. Subsequently 10% aqueous sodium bisulfite (100 mL) was added and the mixture was extracted with diethyl ether (3 x 40 mL). The two layers were separated and the aqueous layer was acidified with concentrated HCl. The precipitated acid (**7**) was removed by suction filtration, washed with cold water, and dried *in vacuo* to give a white solid (4.0 g, 20.62 mmol, 88%, m.p. 104-106 °C) that was used in the next step without further purification.

^{1}H NMR δ 7.57 (d, *J* = 16, 1H), 5.86 (d, *J* = 16, 1H), 2.09 (m, 2H), 1.80 (s, 3H), 1.62 (m, 2H), 1.47 (m, 2H), 1.07 (s, 6H).

[Melting point and spectral date match with the literature values].

2,6,6-Trimethyl-1-cyclohexene-1-acetaldehyde (8):[60]

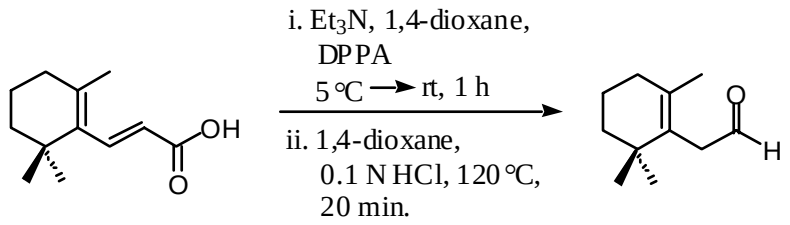

65%

7 **8**

A 25-mL round bottom flask was charged with compound **7** (1.94 g, 10 mmol), triethylamine (1.52 mL, 11 mmol) and 1,4-dioxane (7 mL). To this, over a period of 5 minutes at 5 °C, was added diphenylphosphorylazide (DPPA) (2.36 mL, 11 mmol). This solution was stirred for 1 h at room temperature, after which brine (50 mL) was added and the mixture was extracted with diethyl ether (3 x 25 mL). The ether extracts were dried and evaporated under reduced pressure to give yellow oil, to which was added 1,4-dioxane (15 mL) and 0.1N HCl (10 mL). This mixture was refluxed in a pre-heated (120 °C) oil bath for about 20 minutes under N_2 and then immediately cooled in an ice-bath, diluted with brine (50 mL), and then extracted with *n*-pentane (2 x 25 mL). The combined pentane extracts were dried, and evaporated under reduced pressure to give a yellow oil (1.20 g) that was purified by short-path distillation (5 torr at 115 °C) followed by column chromatography using *n*-pentane:diethyl ether (98:2) system to give aldehyde **8** as a colorless oil (1.09 g, 6.55 mmol, 65%).

^{1}H NMR δ 9.52 (t, *J* = 2.2, 1H), 3.09 (s, 2H), 2.0 (m, 2H), 1.59 (m, 2H), 1.57 (s, 3H), 1.49 (m, 2H), 0.97 (s, 6H).

[Boiling point and spectral date match with the literature values].

2,6,6-Trimethyl-1-cyclohexene-1-ethanol (9):[61]

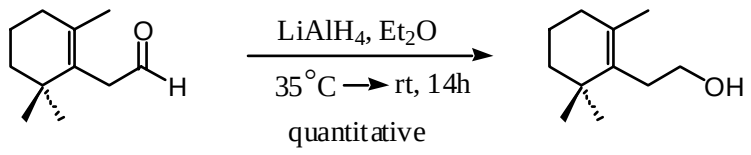

8 **9**

A 250-mL, 2-neck round bottom flask was charged with compound **8** (1.07 g, 6.44 mmol) and dry diethyl ether (86 mL). To it was added lithium aluminiumhydride (LAH) (0.16 g, 4.21 mmol). The mixture was refluxed at 35 °C for 2 h and then stirred at room temperature for 12 h. LAH was destroyed by adding 10% aqueous NaOH (1.6 mL) and H_2O (2 mL). After filtering off the precipitated lithium salt, the filtrate was dried, and evaporated under reduced pressure to give an oil (0.66 g) that was purified by column chromatography using hexanes:ethyl acetate (79:21) system to give alcohol **9** as a colorless solid (1.08 g, 6.43 mmol, quantitative, m.p. 51-53 °C) [reported yield 49%].

^{1}H NMR δ 3.62 (t, J = 8.0, 2H), 2.35 (t, J = 8.0, 2H), 1.95-1.90 (m, 2H), 1.64 (s, 3H), 1.58-1.52 (m, 2H), 1.42-1.22 (3H), 1.0 (s, 6H).

[Melting point and spectral date match with the literature values].

(2,6,6-Trimethyl-1-cyclohexenyl)-1-iodoethane (10):[59]

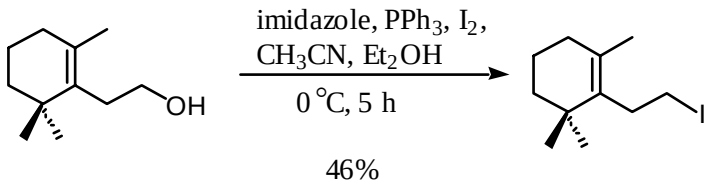

9 **10**

A 100-mL round bottom flask was charged with compound **9** (0.25 g, 1.485 mmol), triphenylphosphine (0.51 g, 1.93 mmol), imidazole (0.138 g, 2.02 mmol), acetonitrile (14 mL) and dry diethyl ether (23 mL). To this was added, at 0 °C, iodine (0.54 g, 2.11 mmol) in portions. This mixture was stirred at 0 °C for 5 h and then diluted with diethyl ether (40 mL). The organic layer was washed with saturated aqueous $Na_2S_2O_3$ (2 x 15 mL), saturated aqueous $CuSO_4$ (2 x 15 mL), H_2O (10 mL), brine (5 mL), dried, and evaporated under reduced pressure to give a yellow oil that was purified by column chromatography using hexanes (100%) system followed by short-path distillation under reduced pressure (6 torr at 65 °C) to give iodide **10** as a colorless oil (0.19 g, 0.68 mmol, 46%).

^{1}H NMR δ 3.08 (t, *J* = 8.5, 2H), 2.62 (t, *J* = 8.5, 2H), 1.90-1.85 (m, 2H), 1.59 (s, 3H), 1.58-1.52 (m, 2H), 1.43-1.39 (m, 2H), 0.99 (s, 6H).

^{13}C NMR δ 137.75, 130.30, 39.44, 34.84, 34.61, 32.74, 28.50, 20.08, 19.27, 5.00.

FT-IR (neat) 2927, 1470, 1359, 1202, 1164, 1114, 716, 543.

ESI-MS (*m/z*) calculated ($C_{11}H_{19}I$, M^+-127) 151, observed 151.

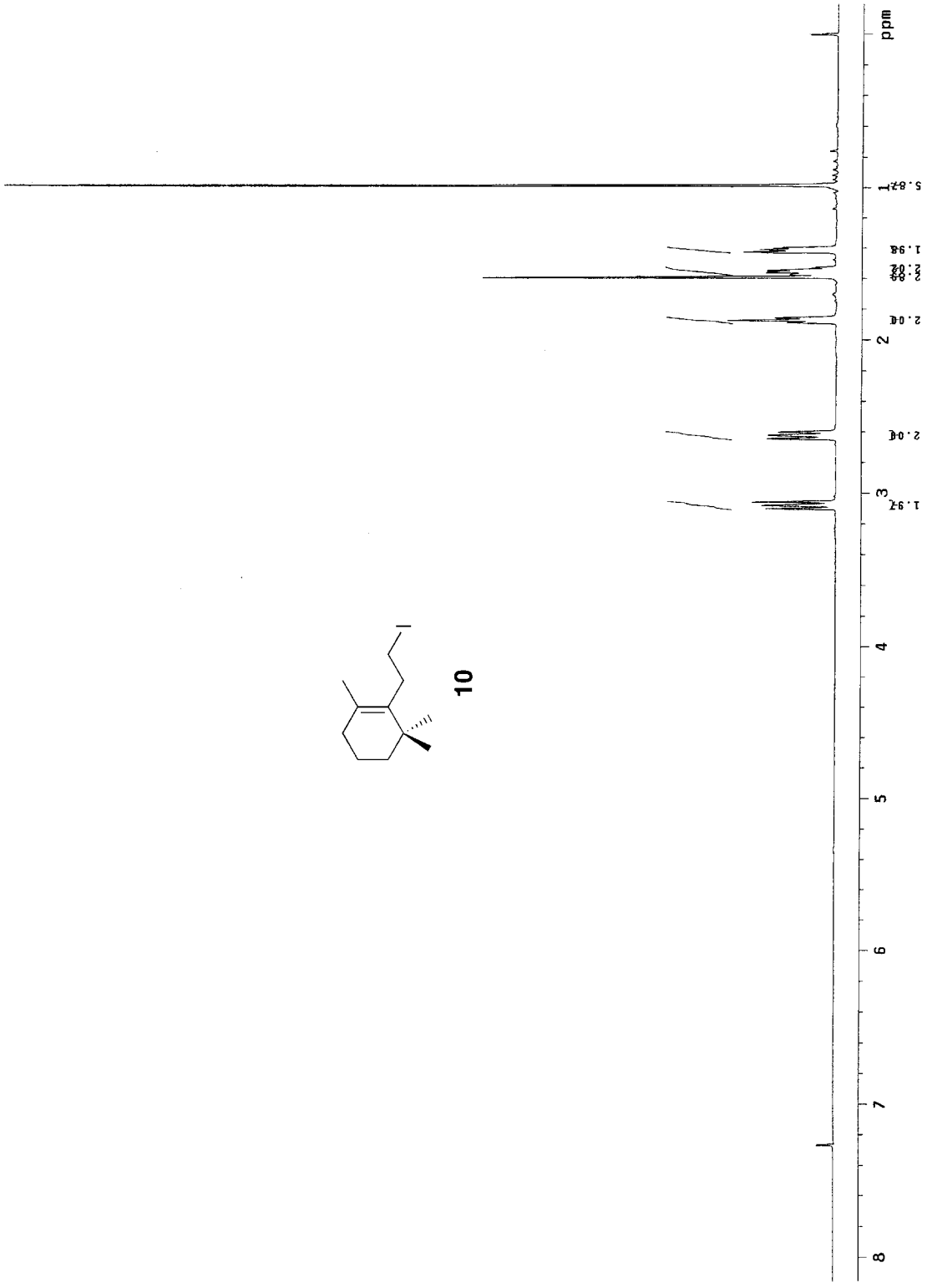

10

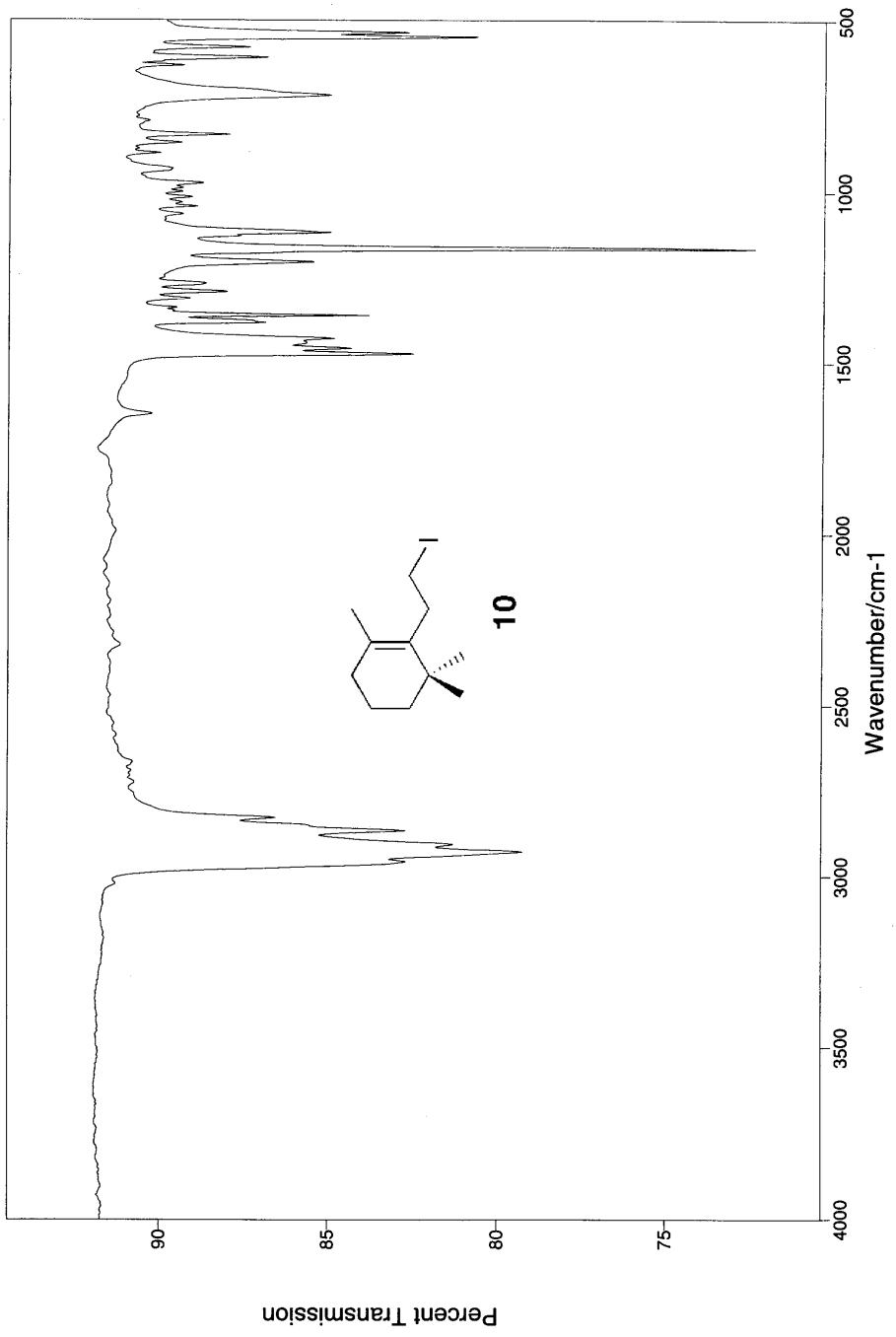
Percent Transmission
90
85
80
75
4000
3500
3000
2500
2000
1500
1000
500
Wavenumber/cm-1
I
10

17β-(*Tert*-butyldimethylsilyl)oxy-5α-androstan-3-one (12):[62]

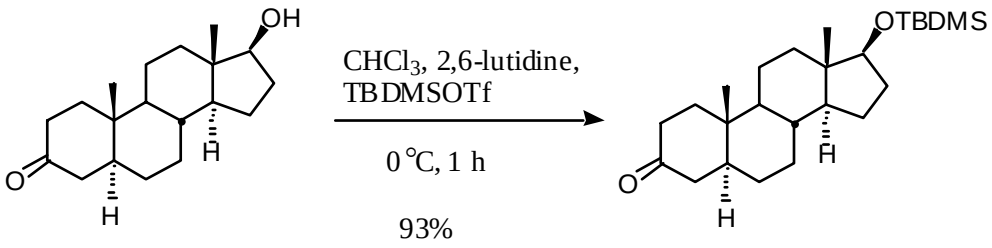

11 **12**

A 100-mL round bottom flask was charged, at room temperature, with 4,5α-dihydrotestosterone (**11**) (1.80 g, 6.20 mmol), chloroform (25 mL), 2,6-lutidine (2.52 mL, 21.68 mmol). To this mixture was added at 0 °C, TBDMS triflate (3.6 ml, 15.66 mmol). The reaction mixture was stirred for 1 h at 0 °C and quenched with saturated aqueous NH_4Cl (10 mL). The organic and aqueous layers were separated, and the aqueous layer was extracted with chloroform (3 x 10 mL). The combined chloroform layers ware washed with 1M HCl (2 x 15 mL), H_2O (2 x 15 mL), brine (10 mL), dried, and evaporated under reduced pressure to give a reddish brown solid (2.5 g) that was purified by column chromatography using hexanes:ethyl acetate (90:10) system to give TBS protected steroid **12** as a white solid (2.32 g, 5.75 mmol, 93%, m.p. 134-135 °C).

^{1}H NMR δ 3.55 (m, *J* = 8.0, 1H) 1.02 (s, 3H), 0.88 (s, 9H), 0.72 (s, 3H), 0.007 (s, 6H).

[Melting point and spectral date match with the literature values].

17β-(*Tert*-butyldimethylsilyl)oxy-5α-androst-1-en-3-one (13):[63]

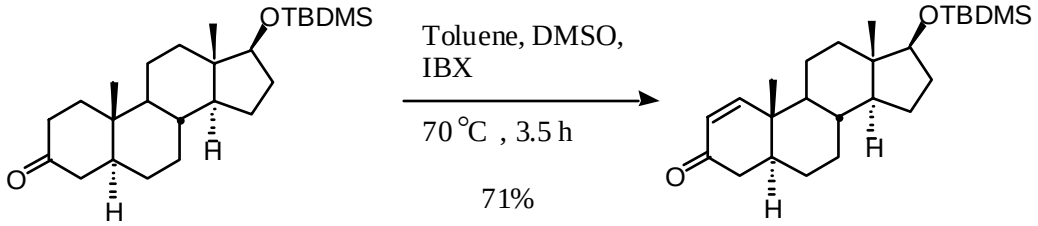

12 **13**

A 50-mL, 2-neck round bottom flask was charged with compound **12** (0.90 g, 2.23 mmol), toluene (15 mL), dimethylsulfoxide (DMSO) (7.5 mL) and *o*-iodoxybenzoic acid (0.82 g, 2.90 mmol). The reaction mixture was heated to 70 °C for 3.5 h. It was then diluted with diethyl ether (20 mL) and the organic layer was washed with 5% aqueous $NaHCO_3$ (2 x 10 mL), H_2O (2 x 10 mL), brine (5 mL), dried, and evaporated under reduced pressure to give a white solid (0.7 g) that was purified by column chromatography using hexanes:ethyl acetate (90:10) system to give enone**13** as a white solid (0.64 g, 1.58 mmol, 71%, m.p. 144-145 °C).

^{1}H NMR δ 7.15 (d, *J* = 10.4, 1H), 5.85 (d, *J* = 10.4, 1H), 3.55 (m, *J* = 8.0, 1H), 1.02 (s, 3H), 0.88 (s, 9H), 0.80 (s, 3H), 0.017 (s, 6H).

[Melting point and spectral date match with the literature values].

4α-Methyl-17β-(*tert*-butyldimethylsilyl)oxy-5α-androst-1-en-3-one (14):[64]

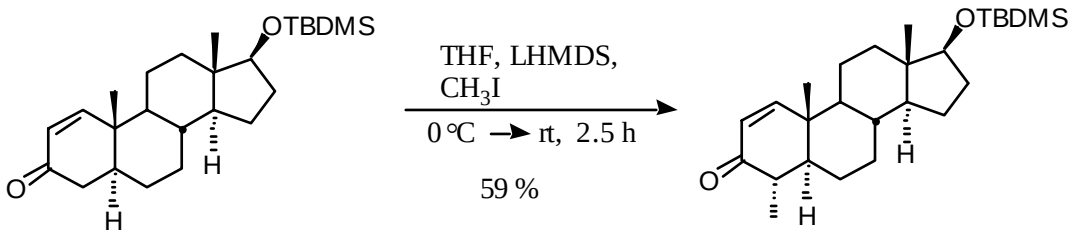

13 **14**

A 100-mL round bottom flask was charged with THF (13.5 mL). To it was added, at 0 °C, *n*-butyllithium (1.07 mL, 1.71mmole) and then, dropwise, hexamethyldisilazane (0.39 mL, 1.71 mmol). This solution was stirred for 30 minutes at 0 °C. To the LHMDS thus formed, was added, dropwise at 0 °C, a solution of compound **13** (0.13 g, 0.33 mmol) in THF (4 mL). The reaction mixture was stirred for 1 h at 0 °C, and iodomethane (6.8 mL, neat) was added rapidly. The solution was then stirred for 30 minutes at that temperature and for 1 h at room temperature. The reaction was quenched by adding a few drops of saturated aqueous NH_4Cl. THF was evaporated under reduced pressure to give a solid residue. To this residue was added aqueous NH_4Cl (10 mL) and ether (25 mL). The ether layer was washed with aqueous $Na_2S_2O_3$ (2 x 10 mL), H_2O (2 x 10 mL), brine (10 mL), dried, and evaporated under reduced pressure to give a yellow oil (0.12 g) that was purified by column chromatography using hexanes:ethyl acetate (92:8) system to give methylated enone **14** as a white solid (80 mg, 0.19 mmol, 59%, m.p. 152-156 °C).

^{1}H NMR δ 7.10 (d, *J* = 10.4, 1H), 5.85 (d, *J* = 10.4, 1H,), 3.56 (m, *J* = 8.0, 1H), 2.30 (m, *J* = 6.8, 13, 1H), 1.11 (d, *J* = 6.80, 1H), 1.04 (s, 3H), 0.88 (s, 9H), 0.72 (s, 3H), 0.008 (s, 6H).

^{13}C NMR δ 202.37, 157.55, 126.89, 81.82, 50.87, 50.73, 50.66, 43.61, 42.39, 39.63, 37.23, 35.52, 31.30, 31.16, 26.07, 24.56, 23.64, 21.04, 18.32, 13.98, 12.30, 11.75, -4.27, -4.60.

FT-IR (neat) 2937, 2851, 1678, 1460, 1245, 1197, 1085, 885, 831, 774, 669.

ESI-MS (*m/z*) calculated ($C_{26}H_{44}O_2Si$, MH^+) 417, observed 417.

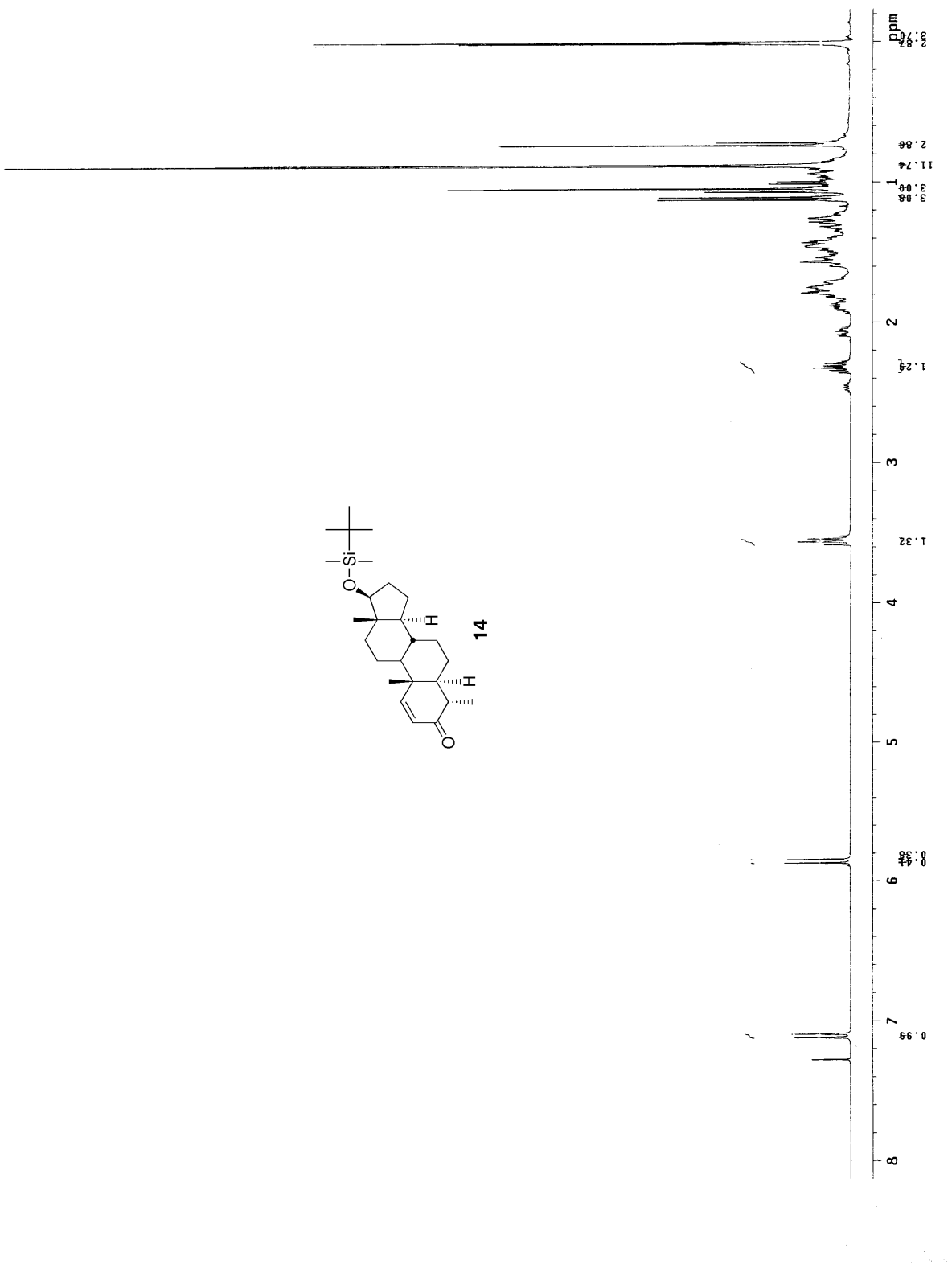

14

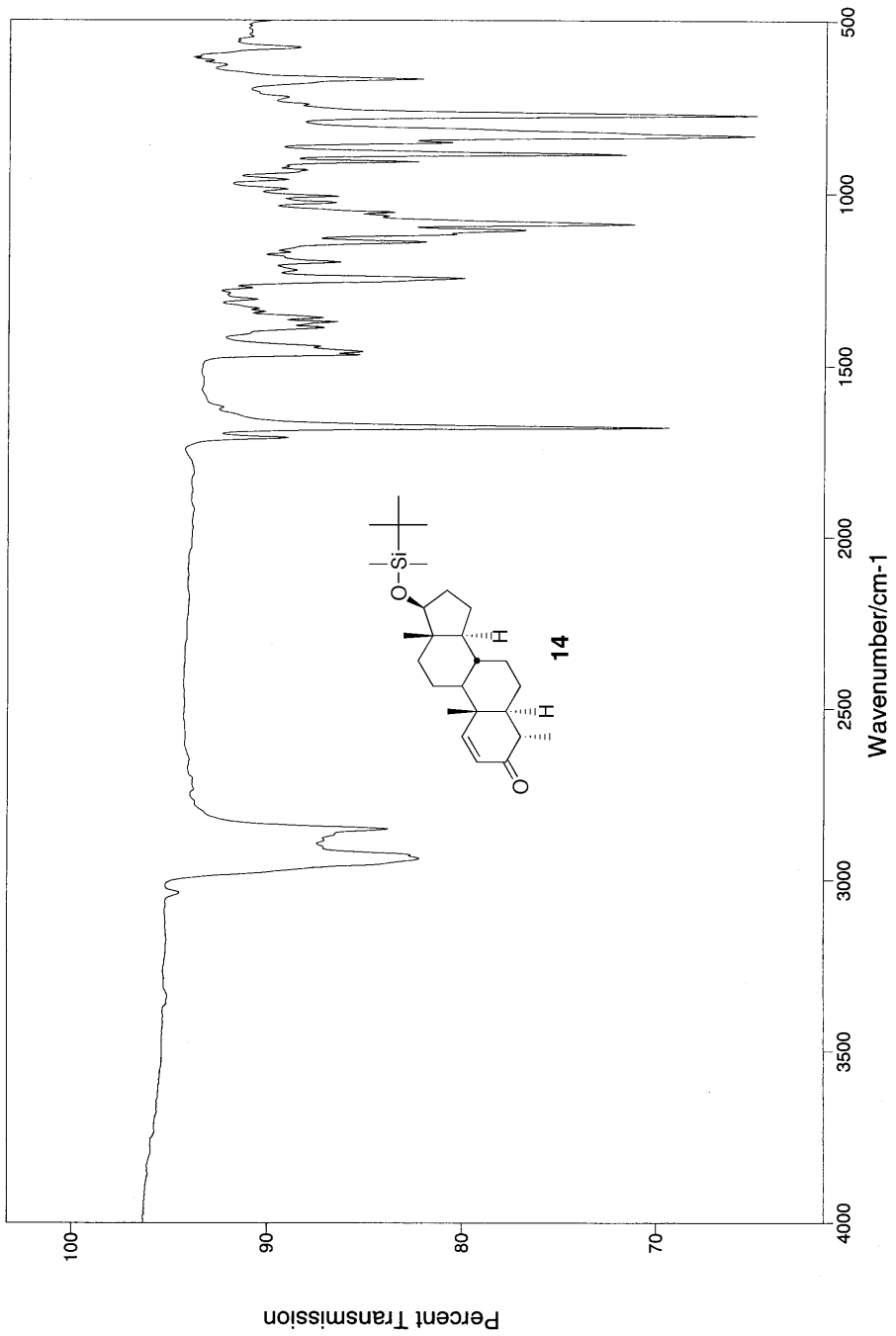
Percent Transmission
100
90
80
70
4000
3500
3000
2500
2000
1500
1000
500
Wavenumber/cm-1
O-Si
H
H
O
14

2,6,6-Trimethylcyclohex-1-ene methanol (16):[67]

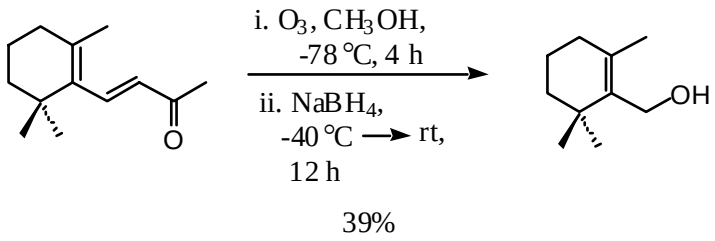

6 **16**

A 250-mL, 2-neck round bottom flask was charged with β-ionone **6** (0.96 g, 5 mmol) and methanol (9 mL). A stream of ozone was passed through this solution at –78 °C for 4 h. Excess ozone was flushed out with a stream of oxygen and then $NaBH_4$ (0.57 g, 15 mmol) was added while the temperature was maintained between –40 and –20 °C. The reaction mixture was then allowed to warm to room temperature and was stirred for 12 h. Evaporation of methanol under reduced pressure afforded a colorless residue that was acidified with 10% HCl and extracted with DCM (3 x 5 mL). The combined DCM extracts were washed with saturated aqueous $NaHCO_3$ (2 x 2 mL), brine (2 mL), dried, and evaporated under reduced pressure to give a colorless oil (0.37 g), that was purified by column chromatography using *n*-pentane:diethyl ether, first, 84:16 system to give unreacted **6** (0.4 g, 2.08 mmol) and then 75:35 system to afford the a colorless oil that was further purified by short-path distillation (6 torr at 83 °C) to give alcohol **16** as colorless oil (0.30 g, 1.95 mmol, 39%).

^{1}H NMR δ 4.12 (s, 2H), 1.92 (m, 2H), 1.74 (s, 3H), 1.65-1.20 (m, 4H), 1.04 (s, 6H).

[Boiling point and spectral date match with the literature values].

4α-Methanol-4β-methyl-17β-(*tert*-butyldimethylsilyl)oxy-5α-androst-1-en-3-one (19):[64]

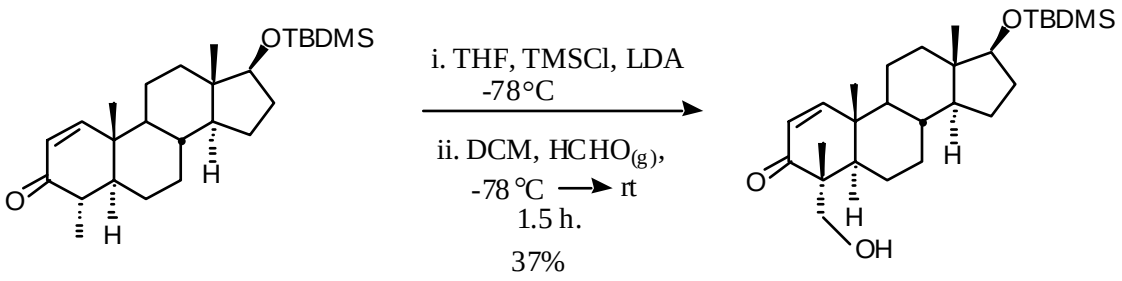

14 **19**

A 25-mL round bottom flask was charged with a solution of compound **14** (0.1 g, 0.24 mmol) in THF (6 mL). This solution was then cooled to –78 °C and to it was added, sequentially, trimethylsilylchloride (0.46 mL, 3.6 mmol), and dropwise, a solution of lithium diisopropylamide [LDA prepared at –78 °C from *n*-butyllithium (1.6 M in hexane) and diisopropylamine in THF]. The reaction mixture was stirred at that temperature for 30 minutes and then quenched with diethyl ether (5 mL) and H_2O (5 mL). The two layers were separated and the aqueous layer was extracted with ether (3 x 5 mL). Combined organic extracts were washed with H_2O (2 x 5 mL), brine (5 mL), dried, and evaporated under reduced pressure to give the crude TMS enol ether of **14** as a yellow solid (95 mg) that was used without purification or characterization.

Into a 25-mL, 2-neck round bottom flask that was charged with the crude TMS enol ether intermediate (0.04 g, 0.08 mmol) in DCM (10 mL), was bubbled formaldehyde gas (produced by depolymerization of paraformaldehyde, which was placed in a 2-neck round bottom flask dipped in an oil bath at ~135 °C, and carried by argon flow through a glass tube passed through a septum and dipped into the reaction mixture) during 15 to 20 minutes at –78 °C. To this mixture was added a solution of tetra-*n*-butylammonium difluorotriphenylsilicate (TBAT) (0.70 M in DCM, 0.30 mmol). Formaldehyde bubbling was continued for an additional 15-20 minutes and

then the mixture was stirred for 20 minutes at –78 °C without bubbling formaldehyde. The solution was warmed to room temperature over a period of 45 minutes, and then treated with brine (2 mL) and H_2O (2 mL). The layers were separated and the aqueous layer was extracted with ether (2 x 5 mL) and ethyl acetate (2 x 5 mL). The combined organic extracts were dried, and evaporated under reduced pressure to give a yellow oil that was purified by column chromatography using hexanes:ethyl acetate (92:8) system to recover the starting material (**6,** 0.015 g) and then 70:30 system to give alcohol **19** as a white solid (16 mg, 0.09 mmol, 37% from **14**, m.p. 178-180 °C).

^{1}H NMR δ 7.14 (d, *J* = 10.4, 1H), 5.84 (d, *J* = 10.4, 1H), 3.70 (d,d, *J* = 10.8, 7.6, 1H), 3.42 (d,d, *J* = 10.8, 7.2, 1H), 1.17 (s, 3H), 1.06 (s, 3H), 0.88 (s, 9H), 0.71 (s, 3H), 0.008 (s, 6H).

^{13}C NMR δ 206.08, 158.86, 126.44, 81.76, 67.75, 52.02, 50.85, 49.09, 46.43, 43.52, 39.47, 37.09, 35.69, 31.67, 31.12, 26.06, 23.69, 21.49, 20.76, 18.31, 17.56, 17.25, 11.74, -4.27, -4.60.

FT-IR (neat) 3398, 2941, 2848, 1656, 1471, 1371, 1258, 1248, 1143, 1085, 885, 837, 773, 668.

ESI-MS (*m/z*) calculated ($C_{27}H_{46}O_3Si$, MH^+) 447, observed 447.

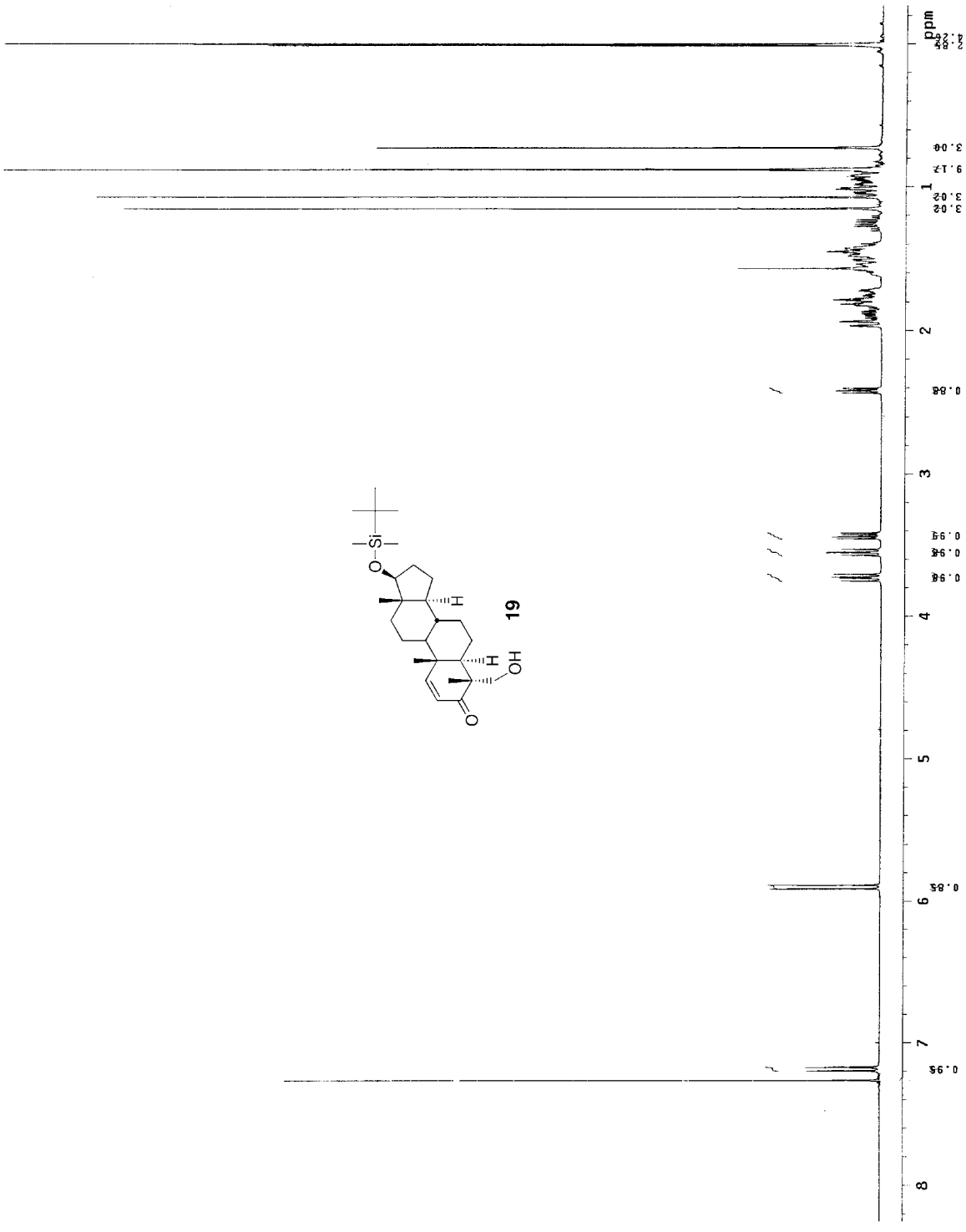
ppm
19

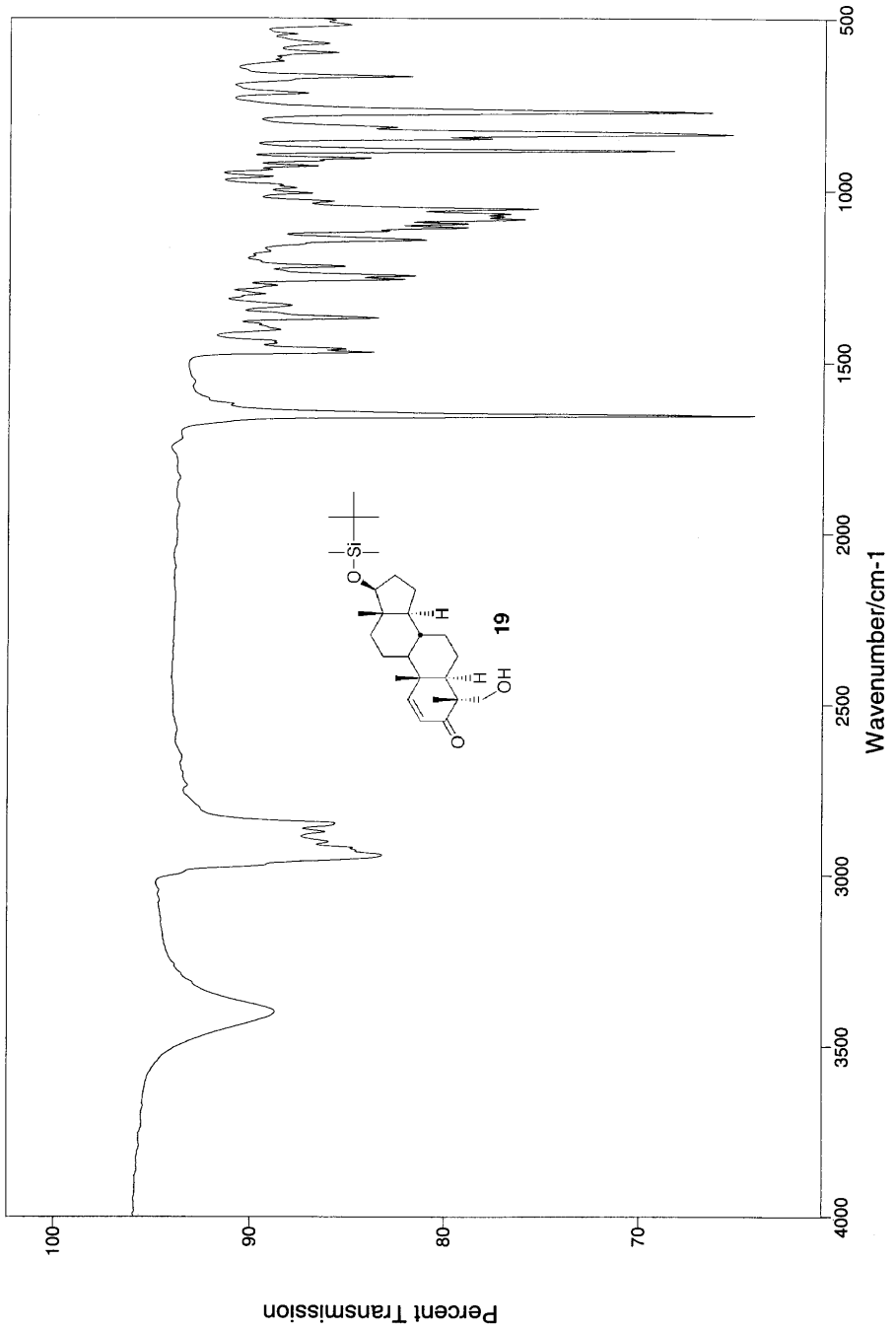
Percent Transmission
100
90
80
70
4000
3500
3000
2500
2000
1500
1000
500
Wavenumber/cm-1
O
Si
H
H
OH
O
19

4-Methyltestosterone (23):[68]

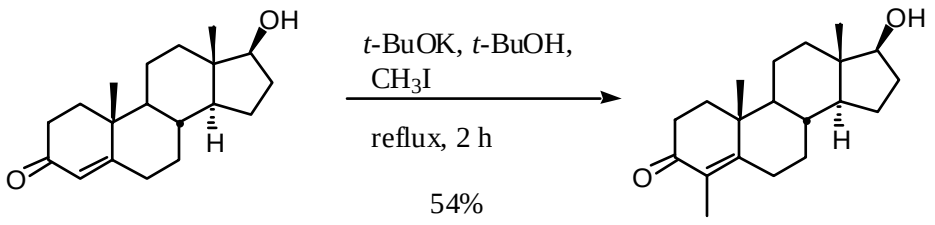

22 **23**

A 100-mL, 3-neck round bottom flask was charged with potassium *t*-butoxide (0.58 g, 5.20 mmol) and *t*-butanol (32 mL). This mixture was refluxed to dissolve all the *t*-BuOK. In another 50-mL, 2-neck round bottom flask was refluxed a solution of testosterone (**22**) (1.0 g, 3.47 mmole) in *t*-butanol (14 mL), and the latter was added, dropwise, to the boiling solution of the base. To this refluxing reaction mixture was added, dropwise, via a dropping funnel over a period of 45 minutes, a solution of iodomethane (251 μL, 3.46 mmol) in *t*-butanol (57 mL). After refluxing further for 30 minutes, the turbid solution was cooled and acidified with concentrated HCl. Some H_2O was added to dispel the turbidity and the resulting solution was stripped of *t*-butanol under reduced pressure. The organic material was extracted into benzene (2 x 20 mL) and the combined extracts were washed with H_2O (2 x 10 mL), brine (10 mL), dried, and evaporated under reduced pressure to give a yellow oil (0.83 g) that was purified by column chromatography using hexanes:ethyl acetate (60:40) system to give 4-methyltestosterone **23** as a white solid (0.43 g, 1.34 mmol, 54%, m.p. 165-167 °C) [reported yield 44%].

^{1}H NMR δ 3.65 (t, *J* = 8, 1H), 1.75 (s, 3H), 1.20 (s, 3H), 0.80 (s, 3H).

[Melting point and spectral date match with the literature values].

4-Allyl-4-methyl-4,5-dihydrotestosterone (24):[69]

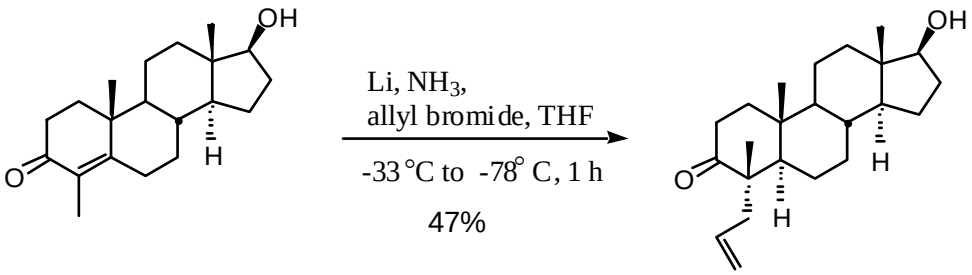

23 **24**

A 250-mL 3-neck round bottom flask, fitted with a cold-finger condenser was charged with finely cut Li metal (0.14 g, 18.98 mmol) and liquid NH_3 (90 mL) at -78 °C. To this stirring solution was added, dropwise at -78 °C, a solution of 4-methyltestosterone (**23**) (1.15 g, 3.8 mmol) in THF (15 mL) and distilled H_2O (70 μL). The reaction was then stirred at -33 °C for 1 h, re-cooled to -78 °C, and to it was rapidly added a solution of allyl bromide (1.64 ml, 1.40 mmol) in THF (5 mL). The liquid NH_3 was allowed to evaporated overnight. To the crude pale yellow solid thus obtained, was added saturated aqueous NH_4Cl solution (10 mL). The mixture was extracted with ether (3 x 20 mL). The combined ether extracts were washed with H_2O (2 x 10 mL), brine (10 mL), dried, and evaporated under reduced pressure to give a pale yellow oil (0.75 g) that was purified by column chromatography using hexanes:ethyl acetate (70:30) system to give allylated steroid **24** as a pale yellow solid (0.62, 1.79 mmol, 47%, m.p. 172-175 °C).

^{1}H NMR δ 5.66-5.54 (m, 1H), 5.0-4.95 (m, 2H), 3.55 (t, *J* = 8 Hz, 1H), 1.04 (s, 3H), 1.03 (s, 3H), 0.74 (s, 3H).

FT-IR (neat) 3271, 3069, 2947, 1701, 1638, 1449, 1047, 910.

ESI-MS (*m/z*) calculated ($C_{23}H_{36}O_2$, MH^+) 345, observed 345.

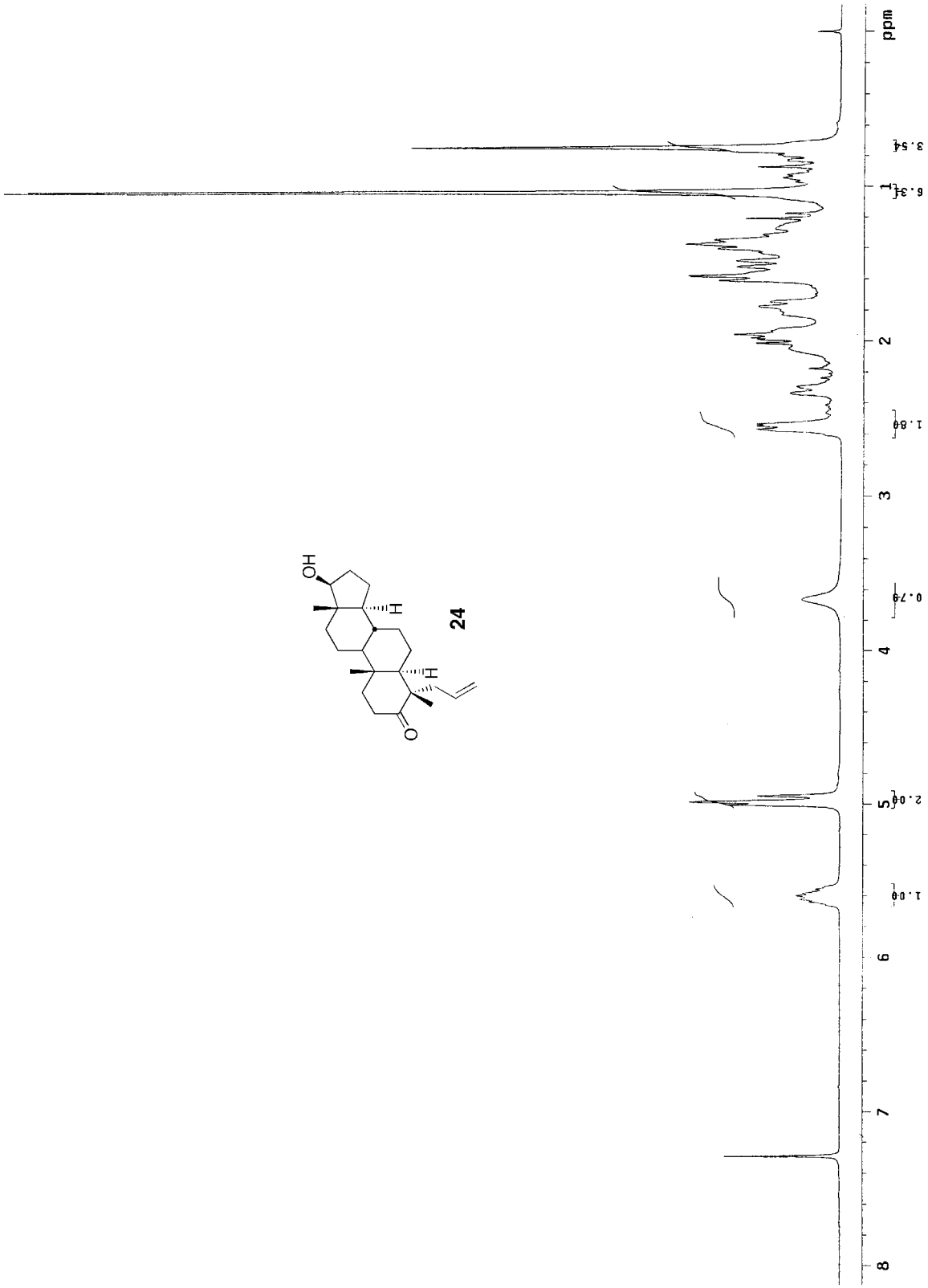
OH
H
H
O
24
ppm
1
2
3
4
5
6
7
8
3.54
6.31
1.80
0.79
2.00
1.00

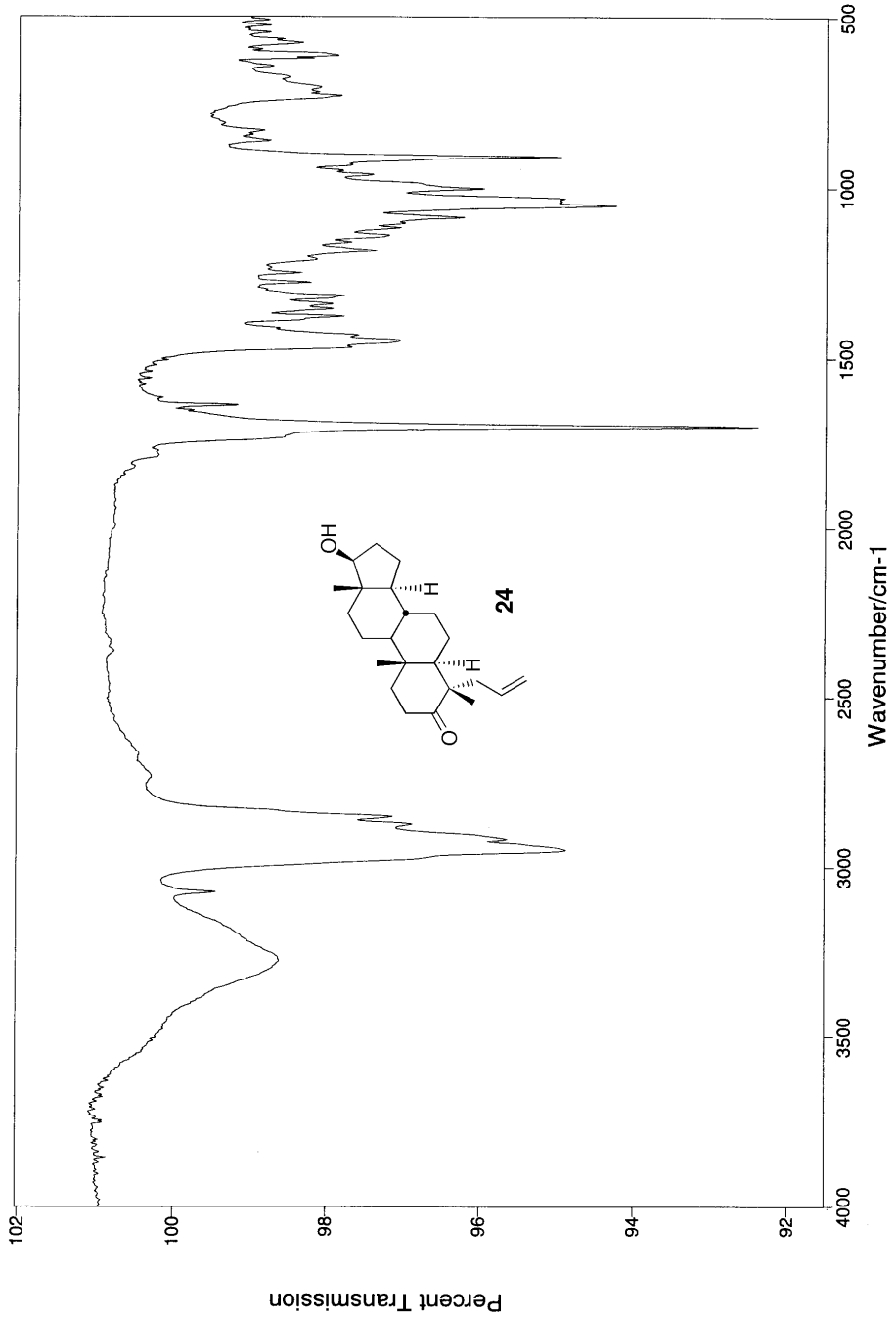
Percent Transmission
102
100
98
96
94
92
4000
3500
3000
2500
2000
1500
1000
500
Wavenumber/cm-1
OH
H
H
O
24

3β-Hydroxy-5α-pregnan-20-one (25):[70]

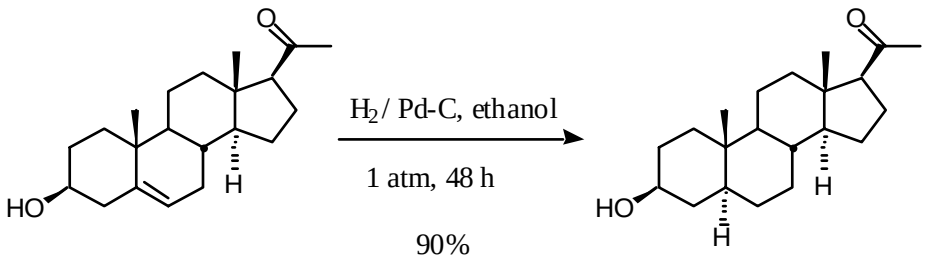

25 **26**

A 250-mL, 2-neck round bottom flask, fitted with a three-way stopper that was connected to a H_2 balloon, was charged with ethanol (11 mL) and 10% Pd-C (0.22 g). To this suspension was added a solution of pregnenolone (**25**) (1.0 g, 3.16 mmol) in ethanol (90 mL). The reaction vessel was repeatedly evacuated (using house vacuum) and filled with H_2 gas while stirring the reaction mixture. After 48 h of stirring at room temperature the solution was passed through a bed of celite to filter off the Pd-C. The celite pad was rinsed with little amount of ethanol and the combined filtrate was evaporated under reduced pressure to give a white solid (0.93 g) that was purified by column chromatography using hexanes:ethyl acetate (70:30) system to give hydrogenated pregnenolone **26** as a white solid (0.91 g, 2.86 mmol, 90%, m.p. 193-195 °C).

^{1}H NMR δ 3.56-3.45 (m, 1H), 2.10 (s, 3H), 0.82 (s, 3H), 0.60 (s, 3H).

[Melting point and spectral date match with the literature values].

3β-(*Tert*-butyldimethylsilyl)oxy-5α-pregnan-20-one (27):[71]

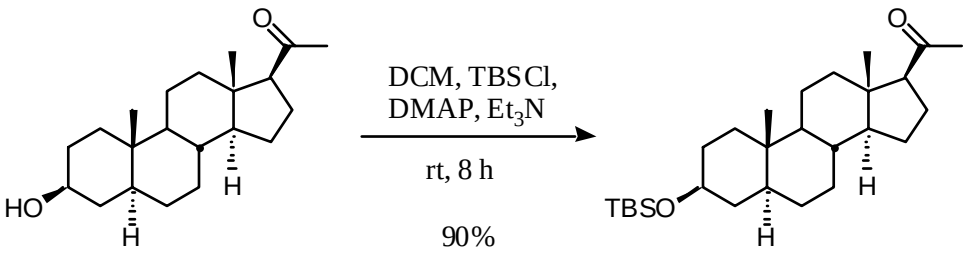

26 **27**

A 100-mL round bottom flask was charged, at room temperature, with compound **26** (0.63 g, 1.98 mmol), DCM (16 mL), TBSCl (0.84 g, 5.59 mmol), DMAP (0.50 g, 4.48 mmol) and Et_3N (0.62 mL, 4.42 mmol). This mixture was stirred for 8 h and then quenched with H_2O (5 mL). The aqueous layer was separated and extracted with DCM (2 x 15 mL). The combined DCM extracts were washed with saturated NH_4Cl (2 x 10 mL), brine (1 x 10 mL), dried, and evaporated under reduced pressure to give a pale yellow solid (0.86 g) that was purified by column chromatography using hexanes:ethyl acetate (93:7) system to give TBS protected steroid **27** as a white solid (0.78 g, 1.79 mmol, 90%, m.p. 137-139 °C]

^{1}H NMR δ 3.53-3.48 (m, 1H), 2.06 (s, 3H), 0.83 (s, 9H), 0.75 (s, 3H), 0.55 (s, 3H), 0.10 (s, 6H). [Melting point and the spectral date match with the literature values].

20-Methyl-20-phenyl -3β-(*tert*-butyldimethylsilyl)oxy-5α-pregnan-20-ol (28):[72]

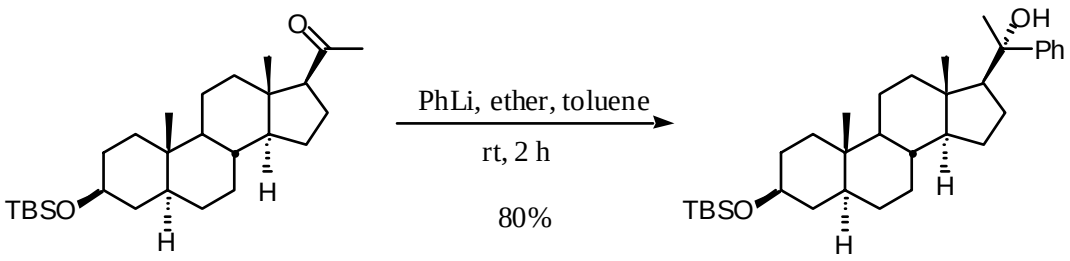

27 **28**

A 25-mL round bottom flask was charged with bromobenzene (0.32 mL, 3 mmol) and diethyl ether (3 mL). To this stirring solution was added, dropwise, *n*-BuLi (1.87 mL, 3 mmol, 1.6M in hexane). After stirring this mixture for 30 minutes at room temperature, the resultant phenyllithium was added slowly to a solution of **27** (0.43 g, 1 mmol) in toluene (14 mL). The stirring was continued for an additional 2 h, after which the reaction was quenched with H_2O (5 mL). The aqueous layer was separated and extracted with DCM (2 x 10 mL). The combined organic extracts were dried, and evaporated under reduced pressure to give a yellow solid (0.44 g) that was purified by column chromatography using hexanes:ethyl acetate (93:7) system to give tertiary alcohol **28** as a white solid (0.41 g, 0.80 mmol, 80%, m.p. 145-148 °C).

^{1}H NMR δ 7.39-7.14 (m, 5H), 3.50-3.45 (m, 1H), 1.62 (s, 3H), 0.87 (s, 3H), 0.86 (s, 9H), 0.77 (s, 3H), 0.07 (s, 3H).

^{13}C NMR δ 149.99, 127.85, 126.07, 124.51, 76.50, 72.17, 60.75, 56.68, 54.45, 45.02, 43.24, 40.37, 38.66, 37.19, 35.50, 34.87, 31.95, 29.82, 29.02, 28.73, 25.96, 23.42, 22.80, 21.13, 18.29, 13.70, 12.38, -4.56.

FT-IR (neat) 3578, 2929, 2858, 1491, 1443, 1250, 1135, 1095, 1068, 869, 835, 773, 700, 569.

ESI-MS (*m/z*) calculated ($C_{33}H_{54}O_2Si$, MH^+) 511, observed 511.

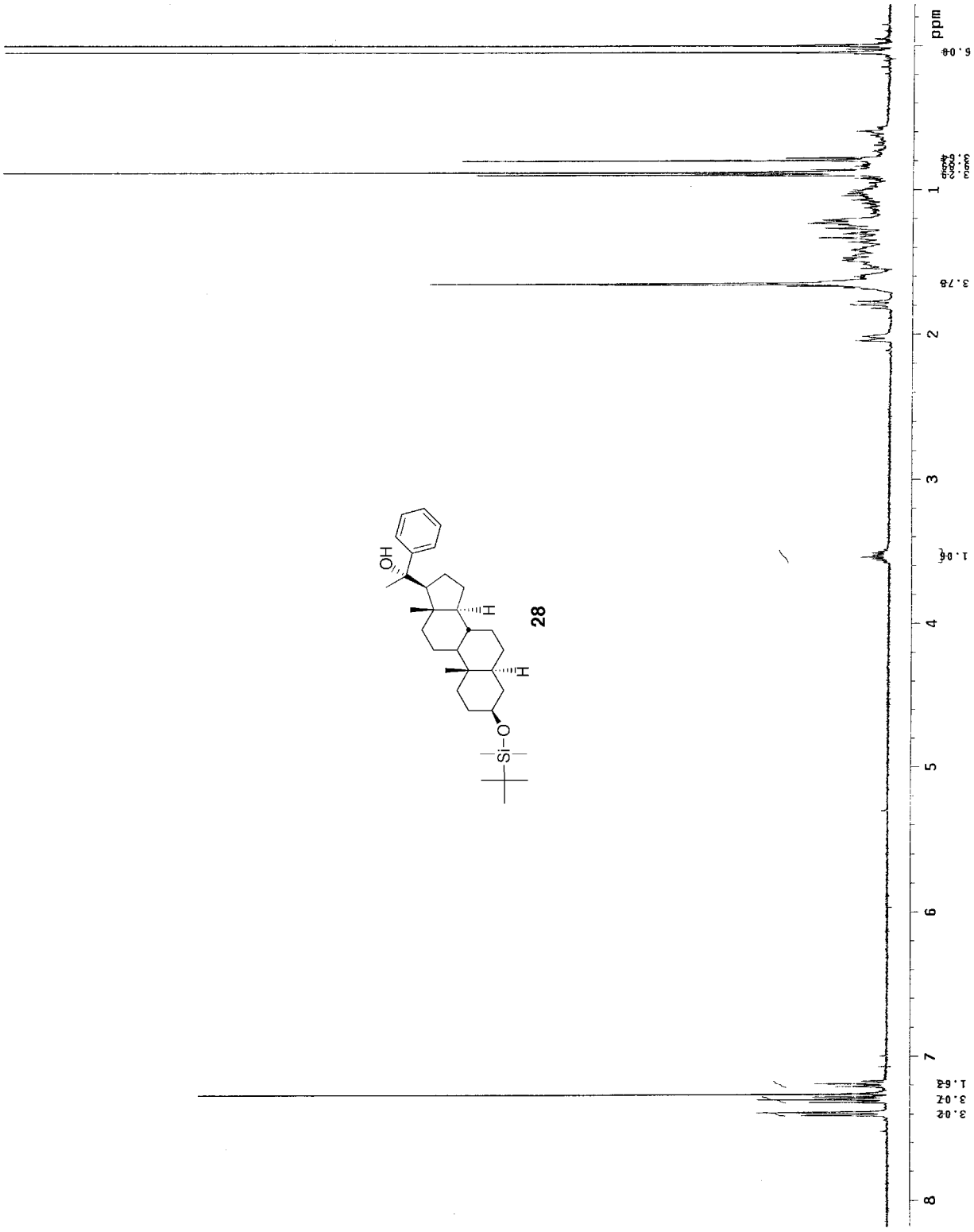
OH
H
H
Si
O
28
ppm
6.08
3.78
1.66
3.02
3.07
1.64

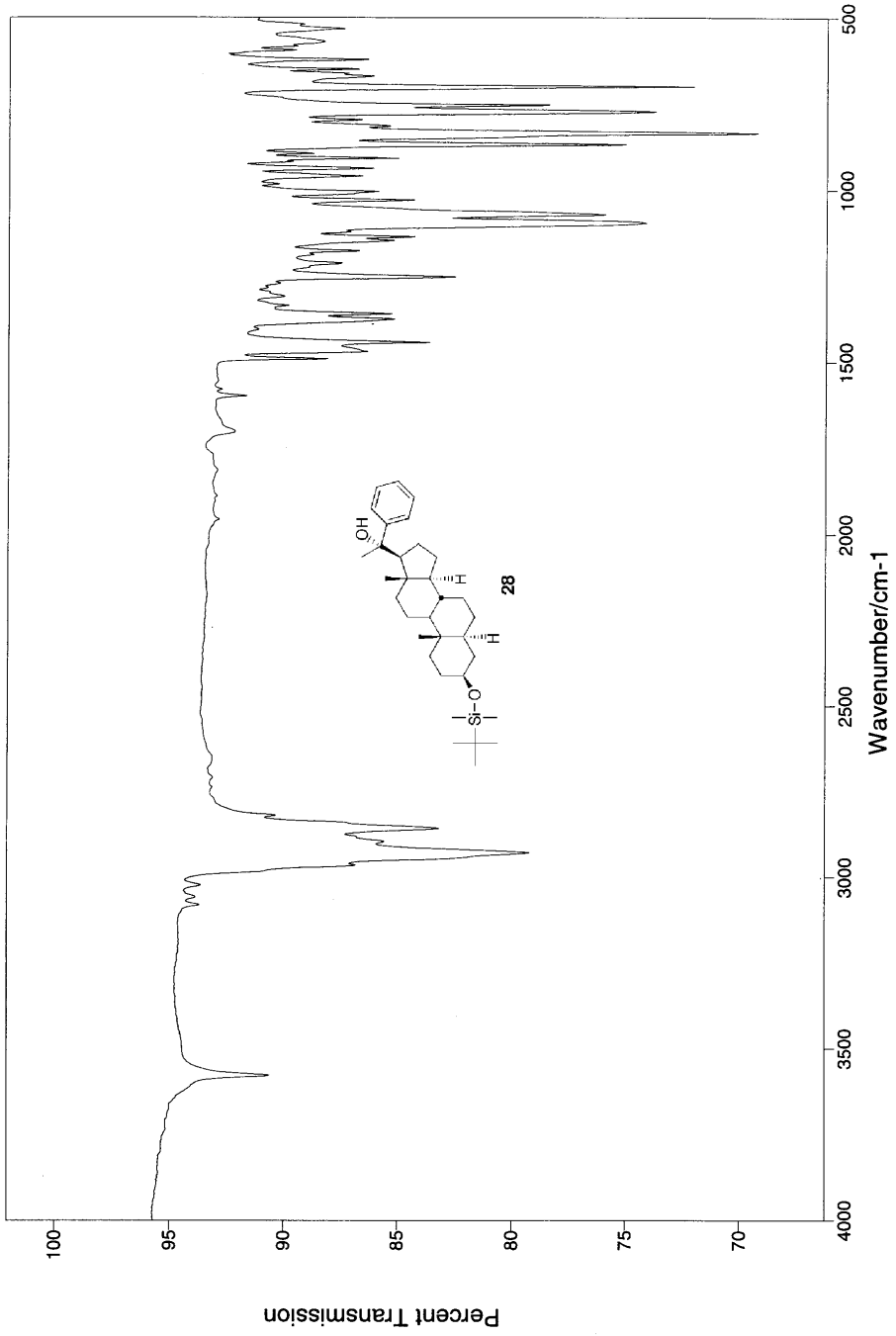
Percent Transmission
100
95
90
85
80
75
70
4000
3500
3000
2500
2000
1500
1000
500
Wavenumber/cm-1
OH
H
H
Si
O
28

3β-Hydroxy-20-methyl-20-phenyl-5α-pregnan-20-ol (29):[73]

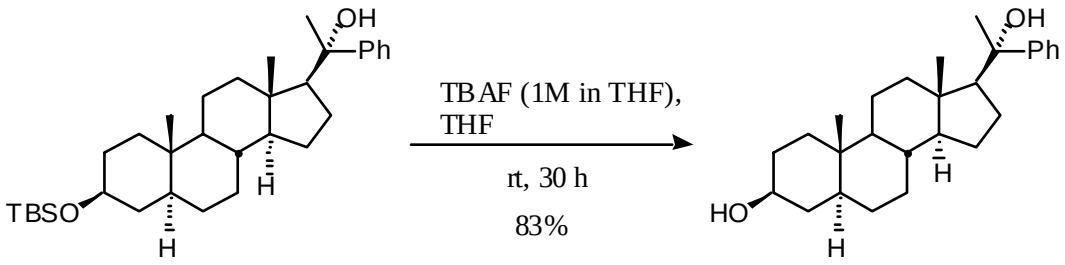

28 **29**

A 50-mL round bottom flask was charged, at room temperature, with compound **28** (1.83 g, 3.58 mmol.), THF (20 mL) and 1M solution of TBAF in THF (7.17 mL, 7.17 mmol). The reaction mixture was stirred for 30 h and then diluted with DCM (10 mL). The organic layer was washed with H_2O (2 x 10 mL), brine (10 mL), dried, and evaporated under reduced pressure to give a pale yellow solid (1.63 g) that was purified by column chromatography using hexanes:ethyl acetate (70:30) system to give deprotected secondary alcohol **29** as a white solid (1.18 g, 2.97 mmol, 83%, m.p. 151-153 °C).

^{1}H NMR δ 7.43-7.14 (m, 5H), 3.63-3.54 (m, 1H), 1.65 (s, 3H), 0.91 (s, 3H), 0.82 (s, 3H).

^{13}C NMR δ 149.99, 127.86, 126.09, 124.52, 76.50, 71.344, 60.77, 56.66, 54.37, 44.86, 43.24, 40.35, 38.21, 37.01, 35.38, 34.89, 31.90, 31.54, 29.82, 28.68, 23.42, 22.81, 21.16, 13.71, 12.34.

FT-IR (neat) 3434, 3292, 2930, 2864, 1651, 1443, 1359, 1136, 1035, 755, 699, 604.

ESI-MS (*m/z*) calculated ($C_{27}H_{40}O_2$, M^++Na) 396, observed 396.

OH
H
H
HO
29
ppm
1
2
3
4
5
6
7
8
3.00
2.78
2.90
1.05
1.92
1.95
0.96

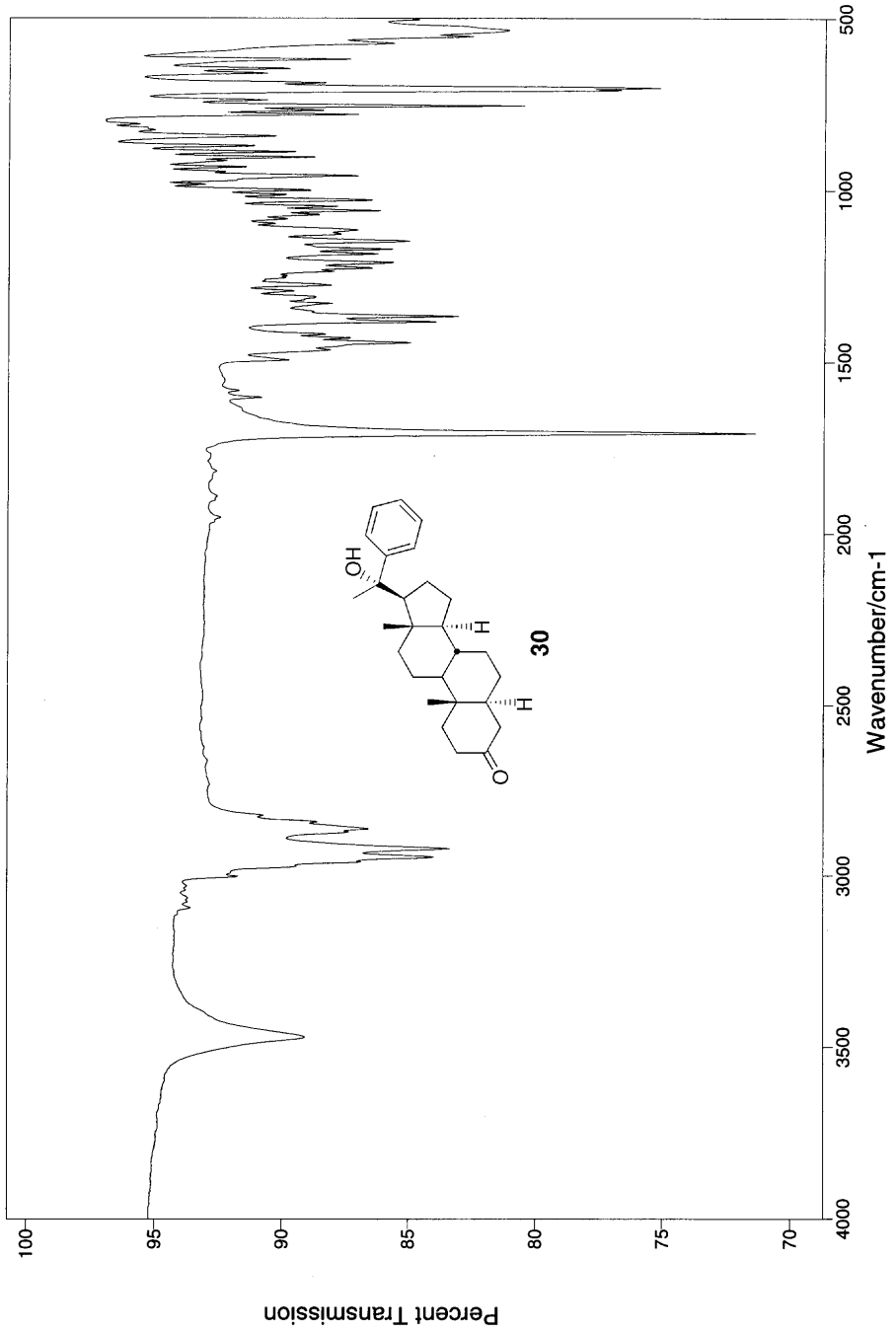
Percent Transmission
100
95
90
85
80
75
70
4000
3500
3000
2500
2000
1500
1000
500
Wavenumber/cm-1
OH
H
H
O
30

20-Methyl-20-phenyl-5α-pregnan-3-one-20-ol (30):[74]

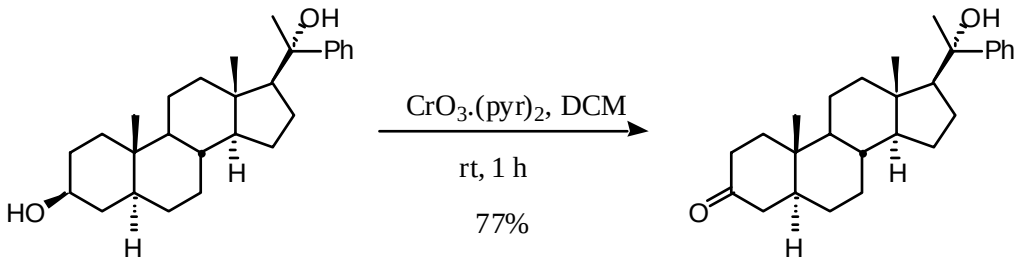

29 **30**

A 100-mL round bottom flask was charged, at room temperature, with DCM (35 mL), pyridine (2.25 mL, 27.90 mmol) and CrO_3 (1.40 g, 13.95 mmol). This mixture was stirred for 30 minutes, and to it was added, in one portion, a solution of compound **29** (0.92 g, 2.33 mmol) in DCM (15 mL). A tarry, black deposit separated immediately. After stirring for additional 30 minutes at room temperature, the solution was decanted from the residue, and evaporated under reduced pressure to give a deep brown solid, which was taken up in ether (15 mL), and washed with 5% aqueous NaOH solution (3 x 5 mL), H_2O (10 mL), brine (10 mL), dried, and evaporated under reduced pressure to give a pale brown solid (0.81 g) that was purified by column chromatography using hexanes:ethyl acetate (80:20) system to give ketone **30** as a white solid (0.71 g, 1.79 mmol, 77%, m.p. 162-164 °C).

^{1}H NMR δ 7.41-7.18 (m, 5H), 1.66 (s, 3H), 1.02 (s, 3H), 0.93 (s, 3H).

^{13}C NMR δ 212.12, 149.91, 127.89, 126.15, 124.50, 77.22, 76.46, 60.72, 56.43, 53.79, 46.69, 44.71, 43.20, 40.19, 38.55, 38.20, 35.64, 34.76, 31.53, 29.80, 28.90, 23.43, 22.79, 21.34, 13.70, 11.48.

FT-IR (neat) 3471, 2945, 2920, 2863, 1705, 1444, 1367, 842, 754, 702, 619.

ESI-MS (*m/z*) calculated ($C_{27}H_{38}O_2$, M^++Na) 417, observed 417.

OH
H
H
O
30
ppm
1
2
3
4
5
6
7
8
3.00
3.27
3.27
2.12
2.14
0.97

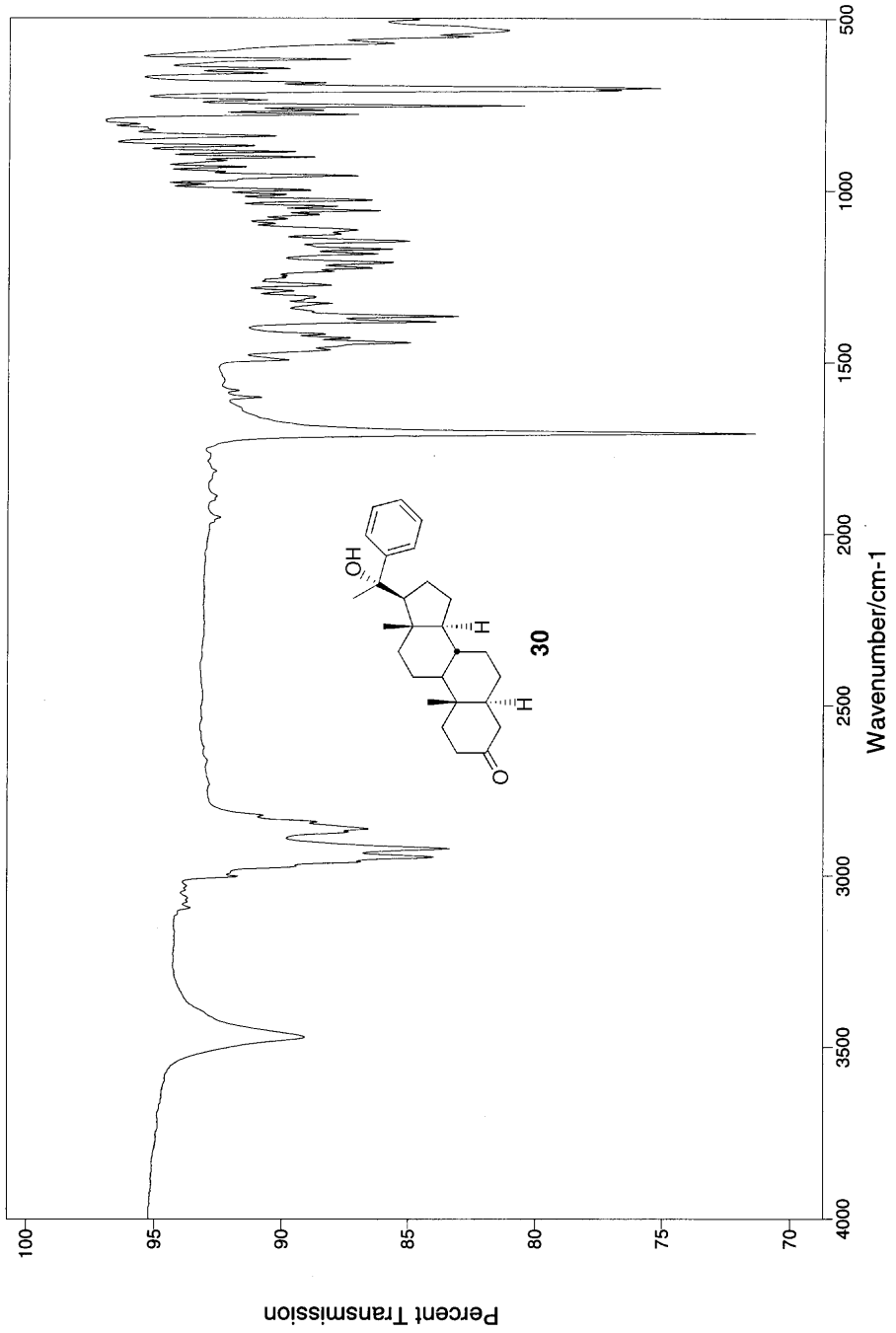
Percent Transmission
100
95
90
85
80
75
70
4000
3500
3000
2500
2000
1500
1000
500
Wavenumber/cm-1
OH
H
H
O
30

3β-(Phenylmethoxy)-5α-pregnan-20-one (32):[79]

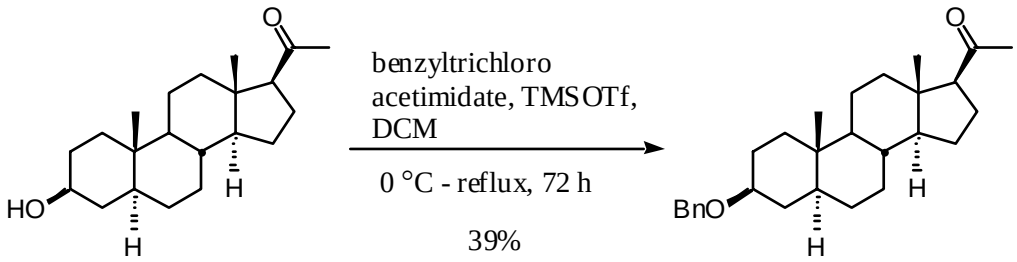

26 **32**

A 25-mL 2-neck round bottom flask fitted with a reflux condenser was charged, at room temperature, with compound **26** (0.10 g, 0.32 mmol), and DCM (8 mL), followed by benzyltrichloroacetimidate (90 μL, 0.47 mmol). This mixture was cooled to 0 °C, and to it was added TMSOTf (10 μL, 0.06 mmol). The resulting solution was refluxed for 72 h, after which it was cooled to room temperature, and washed with saturated $NaHCO_3$ (2 x 5 mL), H_20 (2 x 5 mL), brine (5 ml), dried, and evaporated under reduced pressure to give a pale yellow solid (0.08 g) that was purified by column chromatography using hexanes:ethyl acetate (93:7) system to give benzyl ether **32** as a white solid (50 mg, 0.12 mmol, 39%).

^{1}H NMR δ 7.40-7.25 (m, 5H), 4.60 (d, *J* = 5.0, 2H), 3.40-3.25 (m, 1H), 2.15 (s, 3H), 0.80 (s, 3H), 0.60 (s, 3H).

20-Phenyl-5α-pregn-20-en-3-one (33):[77]

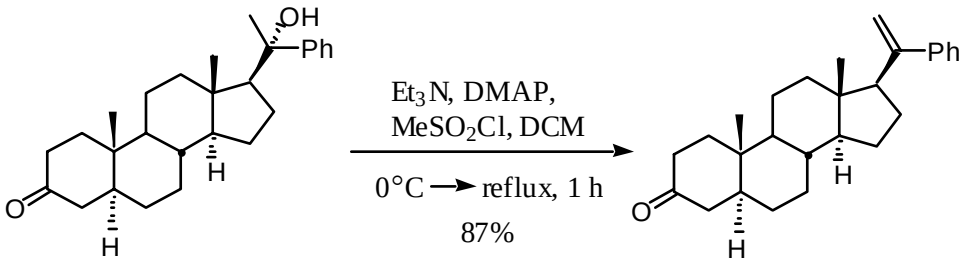

30 **33**

A 50-mL round bottom flask was charged, at room temperature, with compound **30** (1.0 g, 2.56 mmol), DCM (15 mL), Et_3N (4.26 mL, 30.33 mmol) and catalytic amount of DMAP. The solution was cooled to 0 °C, and $MeSO_2Cl$ (1.18 mL, 15.33 mmol) was added dropwise over a period of 15 minutes, after which the reaction was refluxed for 1 h. Crushed ice was then added to it, and stirring continued for 1 h, and then the mixture was extracted with DCM (3 x 10 mL). The combined DCM extracts were washed with H_2O (3 x 5 mL), brine (10 mL), dried, and evaporated under reduced pressure to give a white solid (0.95 g) that was purified by column chromatography using hexanes:ethyl acetate (85:15) system to give alkene **33** as a white solid (0.84 g, 2.22 mmol, 87%, m.p. 158-159 °C).

^{1}H NMR δ 7.29-7.22 (m, 5H), 5.17 (t, *J* = 1.6, 1H), 5.07 (t, *J* = 1.6, 1H), 0.94 (s, 3H), 0.57 (s, 3H).

^{13}C NMR δ 212.13, 150.02, 145.05, 127.88, 127.07, 126.86, 113.37, 56.25, 54.86, 53.88, 46.72, 44.70, 43.40, 38.71, 38.49, 38.18, 35.89, 35.63, 31.63, 28.91, 25.45, 24.01, 21.41, 12.78, 11.43.

FT-IR (neat) 3085, 2968, 2917, 2849, 1707, 1617, 1443, 1227, 885, 775, 702.

ESI-MS (*m/z*) calculated ($C_{27}H_{36}O$, MH^+) 377, observed 377.

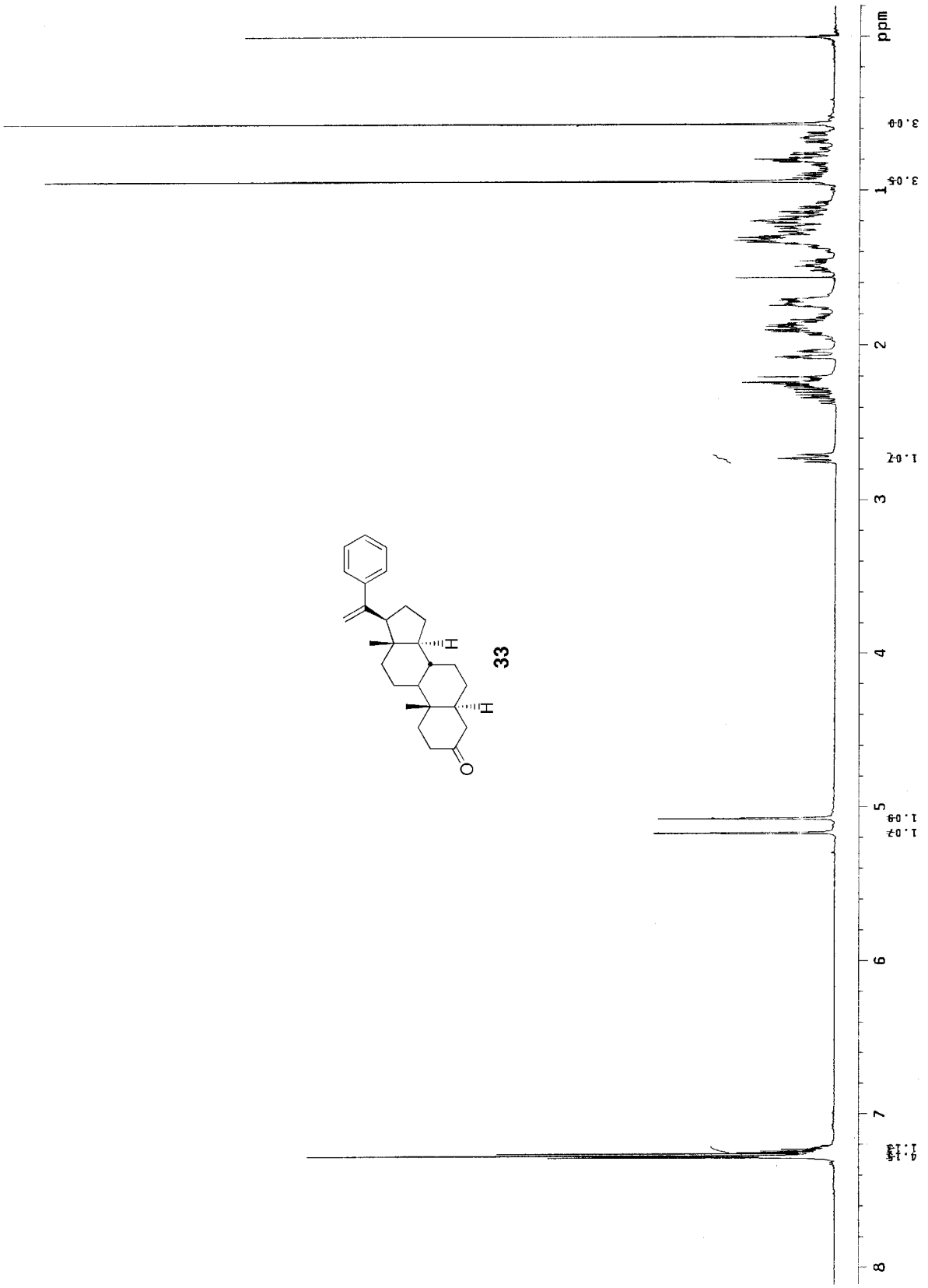
ppm
33
H
H
O

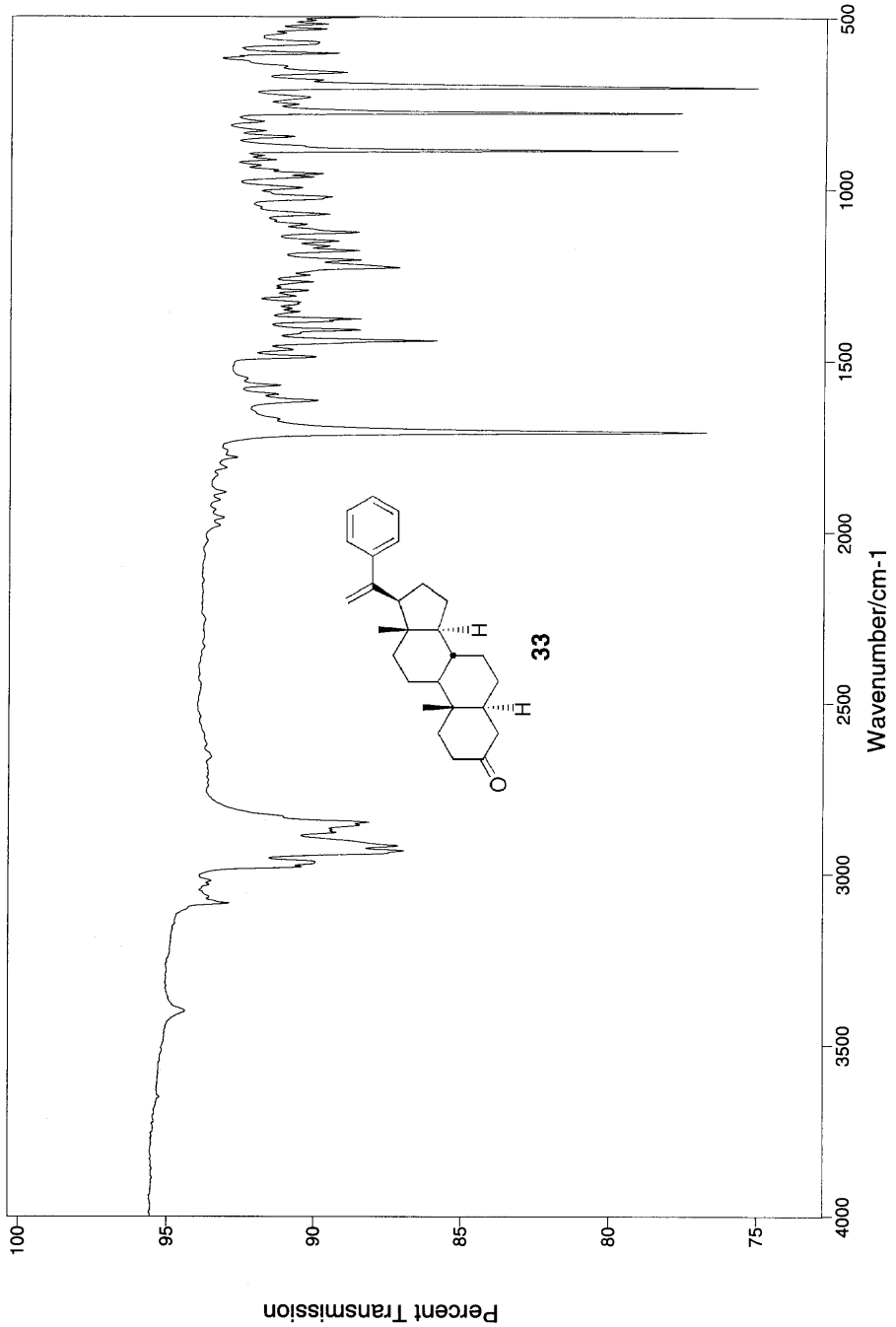
Percent Transmission
100
95
90
85
80
75
4000
3500
3000
2500
2000
1500
1000
500
Wavenumber/cm-1
H
H
O
33

Cyclic 3-(1,2-ethanediyl acetal)-20-phenyl-5α-pregn-20-en-3-one (36):[81]

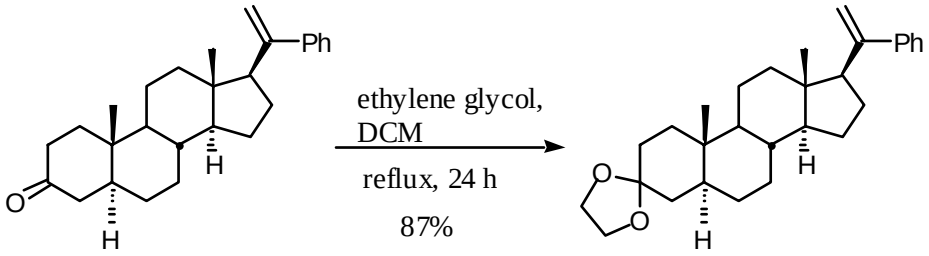

33 **36**

A 15-mL 2-neck round bottom flask, fitted with a reflux condenser, was charged with compound **33** (0.14 g, 0.37 mmol), DCM (5 mL), and ethylene glycol (45 μL, 0.82 mmol). To this mixture was added, dropwise, TMSCl (208 μL, 1.64 mmol). The reaction mixture was then refluxed for 24 h, and then quenched by adding a 5% aqueous solution of $NaHCO_3$ (15 mL). This mixture was extracted with diethyl ether (2 x 15 mL). The combined organic extracts were washed with brine (10 mL), dried, and evaporated under reduced pressure to give a pale yellow solid (0.14 g) that was purified by column chromatography using hexanes:ethyl acetate (90:10) system to give acetal **36** as a white solid (0.14 g, 0.32 mmol, 87%, m.p. 171-173 °C).

^{1}H NMR δ 7.29-7.22 (m, 5H), 5.16 (t, *J* = 1.6, 1H), 5.07 (t, *J* = 1.6, 1H), 3.92 (s, 4H), 0.75 (s, 3H), 0.54 (s, 3H).

^{13}C NMR δ 150.20, 145.16, 127.85, 127.09, 126.79, 113.26, 109.39, 64.13, 64.10, 56.42, 54.88, 54.05, 43.69, 38.83, 37.94, 36.00, 35.93, 35.46, 31.82, 31.13, 28.55, 25.50, 24.02, 21.15, 12.81, 11.35.

FT-IR (neat) 2932, 1619, 1444, 1371, 1138, 1088, 1017, 946, 905, 779, 700, 565.

ESI-MS (*m/z*) calculated ($C_{29}H_{40}O_2$, MH^+) 421, observed 421.

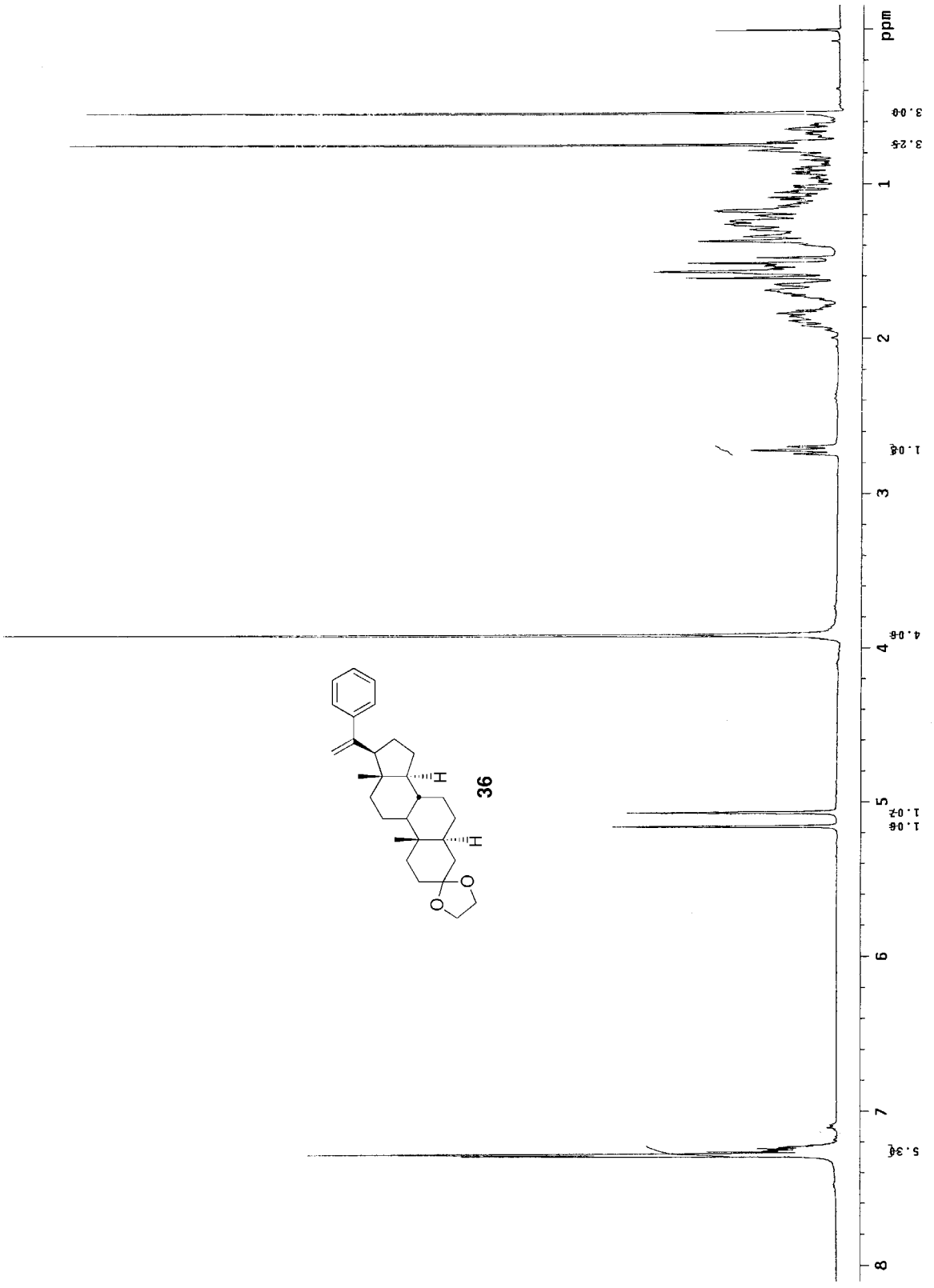
36
H
H
O
O
ppm
8
7
6
5
4
3
2
1
5.34
1.08
1.07
4.08
1.04
3.25
3.00

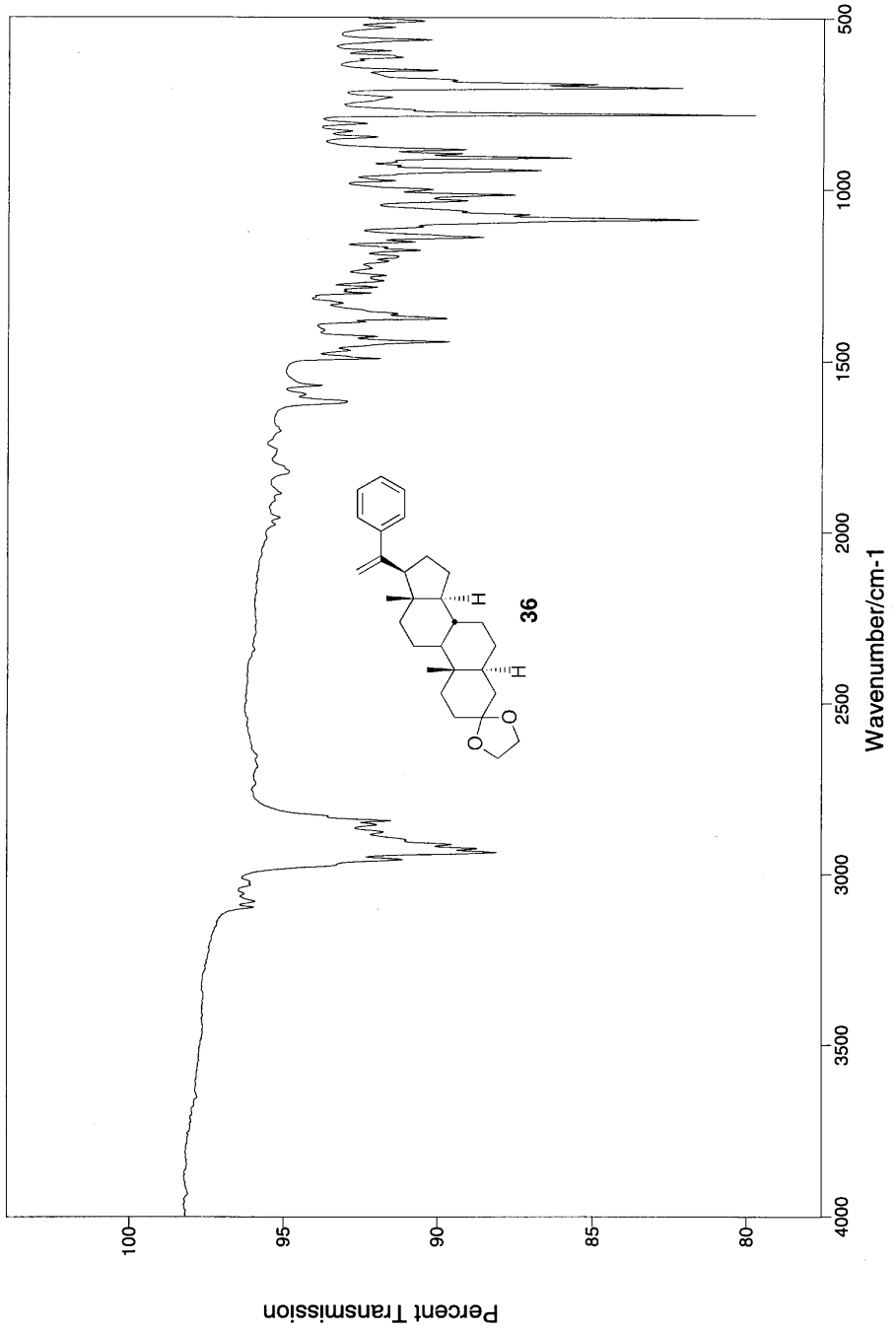
Percent Transmission
100
95
90
85
80
4000
3500
3000
2500
2000
1500
1000
500
Wavenumber/cm-1
H
H
O
O
36

Cyclic 3-(1,2-ethanediyl acetal)-21-hyroxyl-20-phenyl-5α-pregnane-3-one (37):[80]

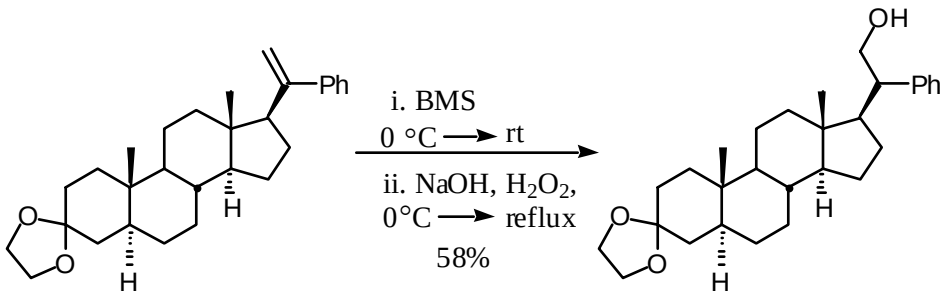

36 **37**

A 15-mL, 2-neck round bottom flask, fitted with a reflux condenser, was charged with compound **36** (0.13 g, 0.30 mmol) and THF (6 mL). This solution was cooled to 0 °C, and to it was added, dropwise, borane-dimethyl sulfide (BMS) complex (32 μL, 0.32 mmol). The reaction was stirred for 3 h at room temperature, and then cooled to 0 °C. To the mixture was added, a 3N aqueous solution of NaOH (59 μL), followed by dropwise addition of 30% aqueous H_2O_2 (59 μL). This solution was refluxed for 1 h, and then poured over crushed ice-water (~20 ml). The aqueous phase was extracted with diethyl ether (2 x 15 mL). The combined organic extracts were washed with brine (10 mL), dried, and evaporated under reduced pressure to give a white solid (0.10 g) that was purified by column chromatography using hexanes:ethyl acetate (70:30) system to give primary alcohol **37** as a white solid (77 mg, 0.18 mmol, 58%, m.p. 194-195 °C).

^{1}H NMR δ 7.33-7.20 (m, 5 H), 4.04-3.98 (m, 1H), 3.92 (s, 4H), 3.73-3.65 (m, 1H), 2.81-2.73 (m, 1H), 0.82 (s, 3H), 0.8 (s, 3H).

^{13}C NMR δ 142.40, 128.61, 126.68, 109.42, 77.59, 77.22, 65.65, 64.15, 56.47, 54.04, 52.23, 51.62, 43.67, 42.53, 39.77, 37.94, 36.04, 35.50, 35.48, 31.82, 31.15, 28.53, 23.98, 21.26, 12.38, 11.42.

FT-IR (neat) 3472, 2925, 1603, 1447, 1136, 1079, 1043, 946, 771, 729, 702.

ESI-MS (*m/z*) calculated ($C_{29}H_{42}O_3$, MH^+) 439, observed 439.

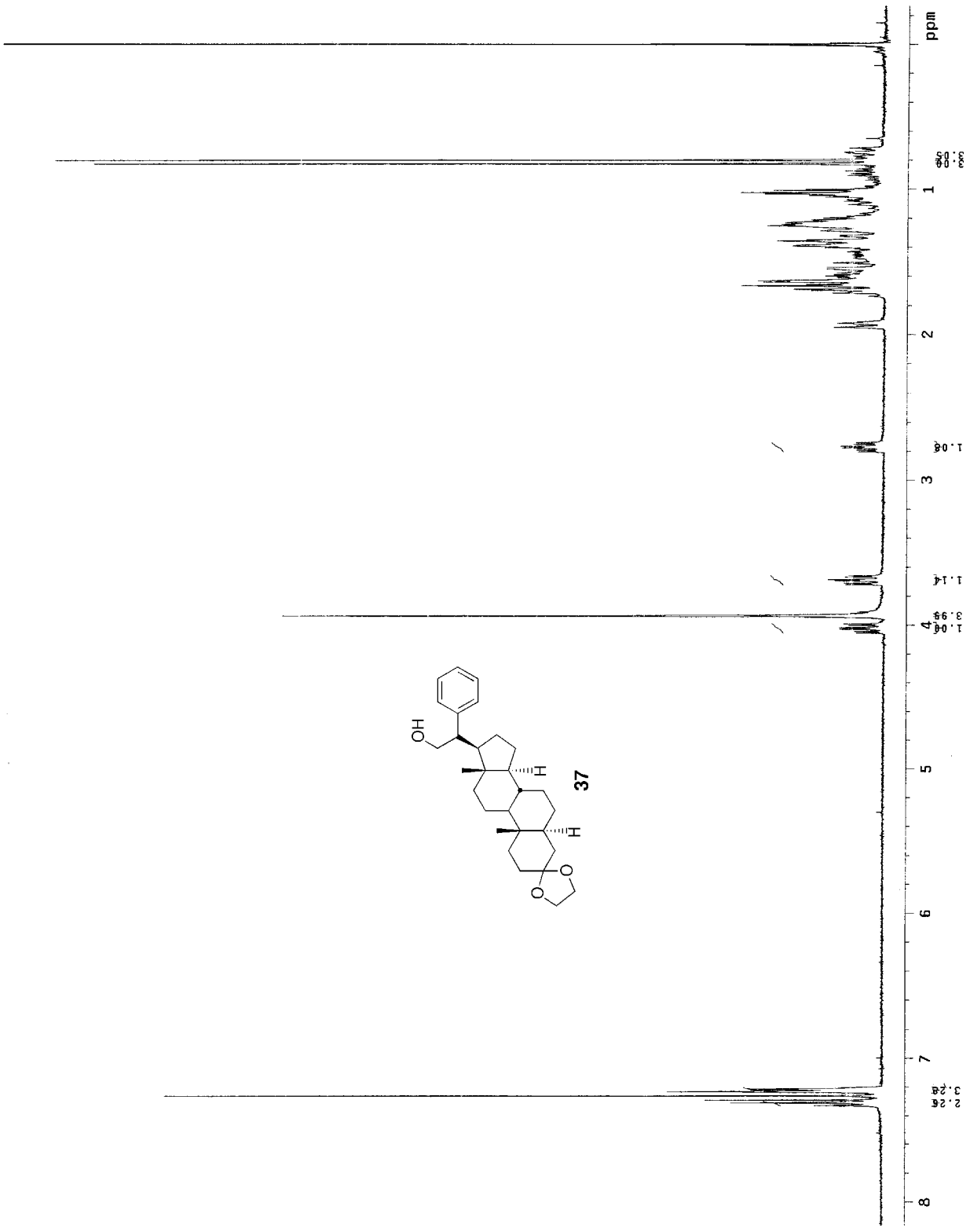
ppm
OH
H
H
O
O
37

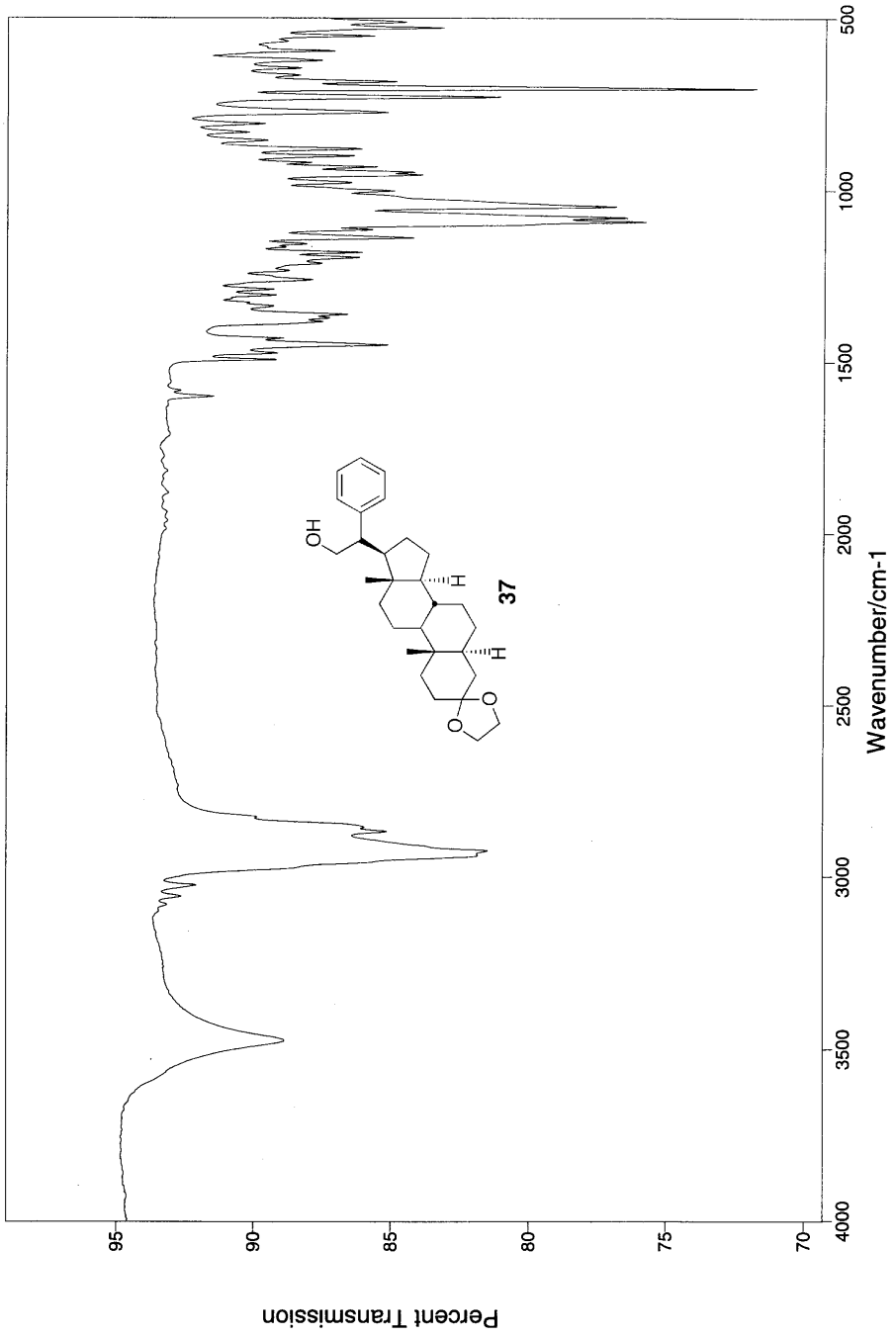
Percent Transmission
95
90
85
80
75
70
4000
3500
3000
2500
2000
1500
1000
500
Wavenumber/cm-1
OH
H
H
O
O
37

Cyclic 3-(1,2-ethanediyl acetal)-21-formyl-20-phenyl-5α-pregnane-3-one (38):[74]

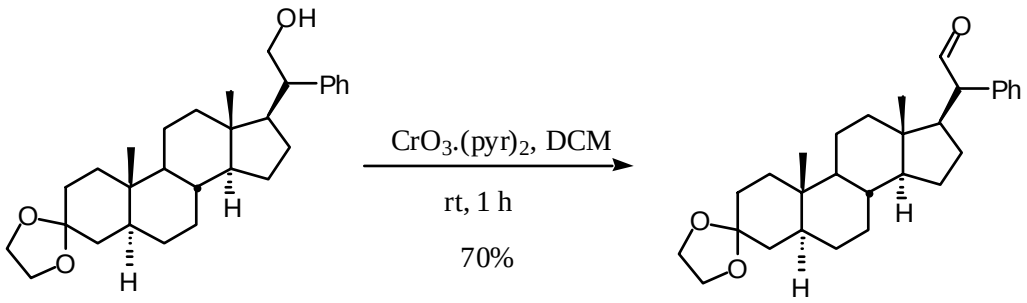

37 **38**

For procedure and molar ratios refer to the synthesis of ketone **30**. The reaction was performed on 30 mg (0.07 mmol) of compound **37**. The crude pale brown solid (30 mg) obtained after work-up was purified by column chromatography using hexanes:ethyl acetate (80:20) system to give the required compound (**38**) as a white solid (20 mg, 0.048 mmol, 70%, m.p. 168-169 °C).

^{1}H NMR δ 9.64 (d, *J* = 5.2, 1H), 7.35-7.24 (m, 5 H), 3.94 (s, 4H), 3.44 (dd, *J* = 11.2, 5.2, 1H), 0.82 (s, 3H), 0.77 (s, 3H).

^{13}C NMR δ 201.31, 135.82, 128.99, 128.87, 127.41, 109.39, 64.16, 61.75, 56.05, 54.07, 50.69, 43.69, 42.14, 38.79, 37.97, 36.04, 35.52, 35.49, 31.85, 31.14, 28.50, 26.83, 23.72, 20.96, 13.04, 11.43.

FT-IR (neat) 2930, 2712, 1719, 1597, 1449, 1360, 1181, 1096, 1072, 949, 883, 762, 731, 702.

ESI-MS (*m/z*) calculated ($C_{29}H_{40}O_3$, MH^+) 437, observed 437.

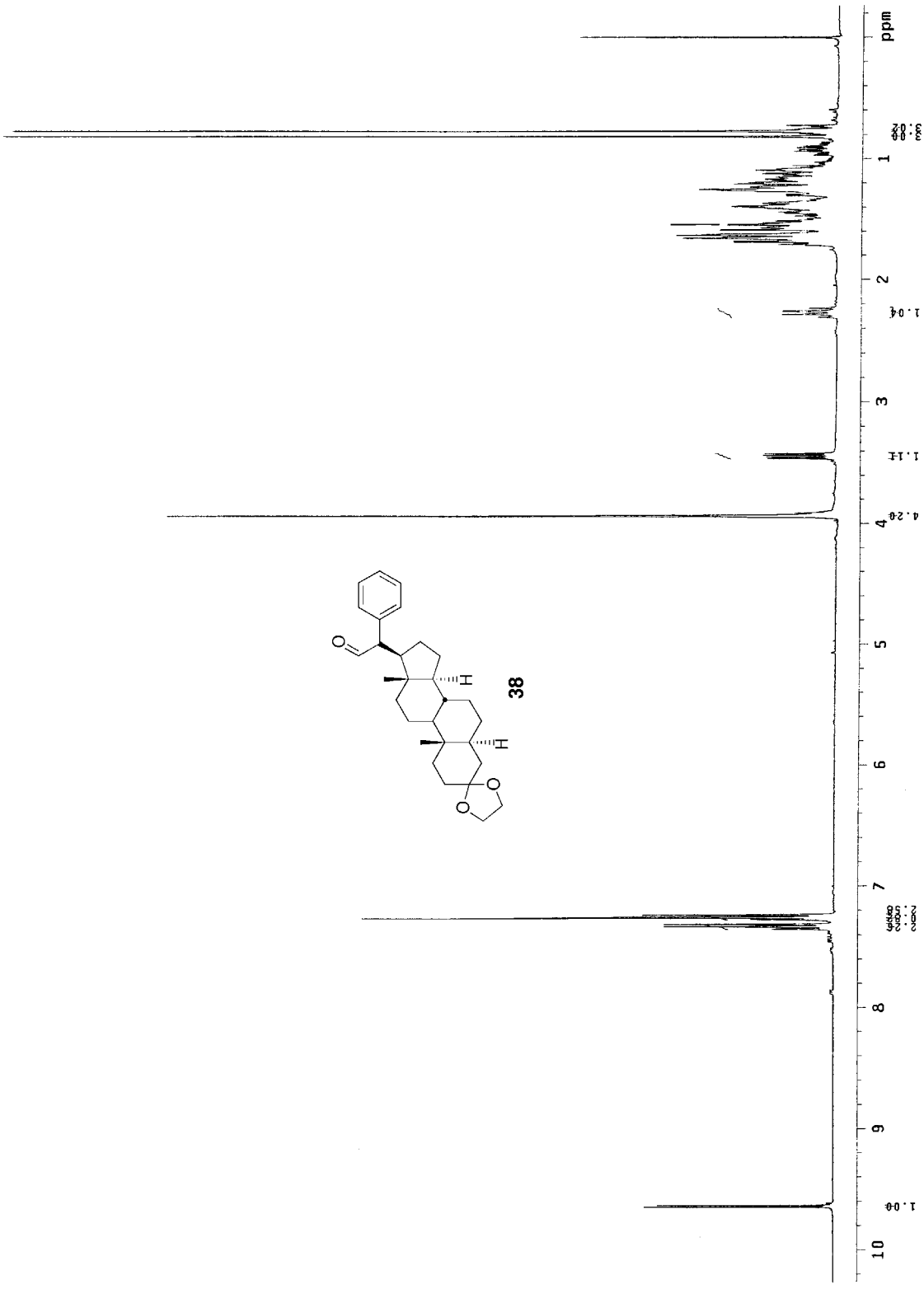
38
O
H
H
O
O
ppm
1
2
3
4
5
6
7
8
9
10

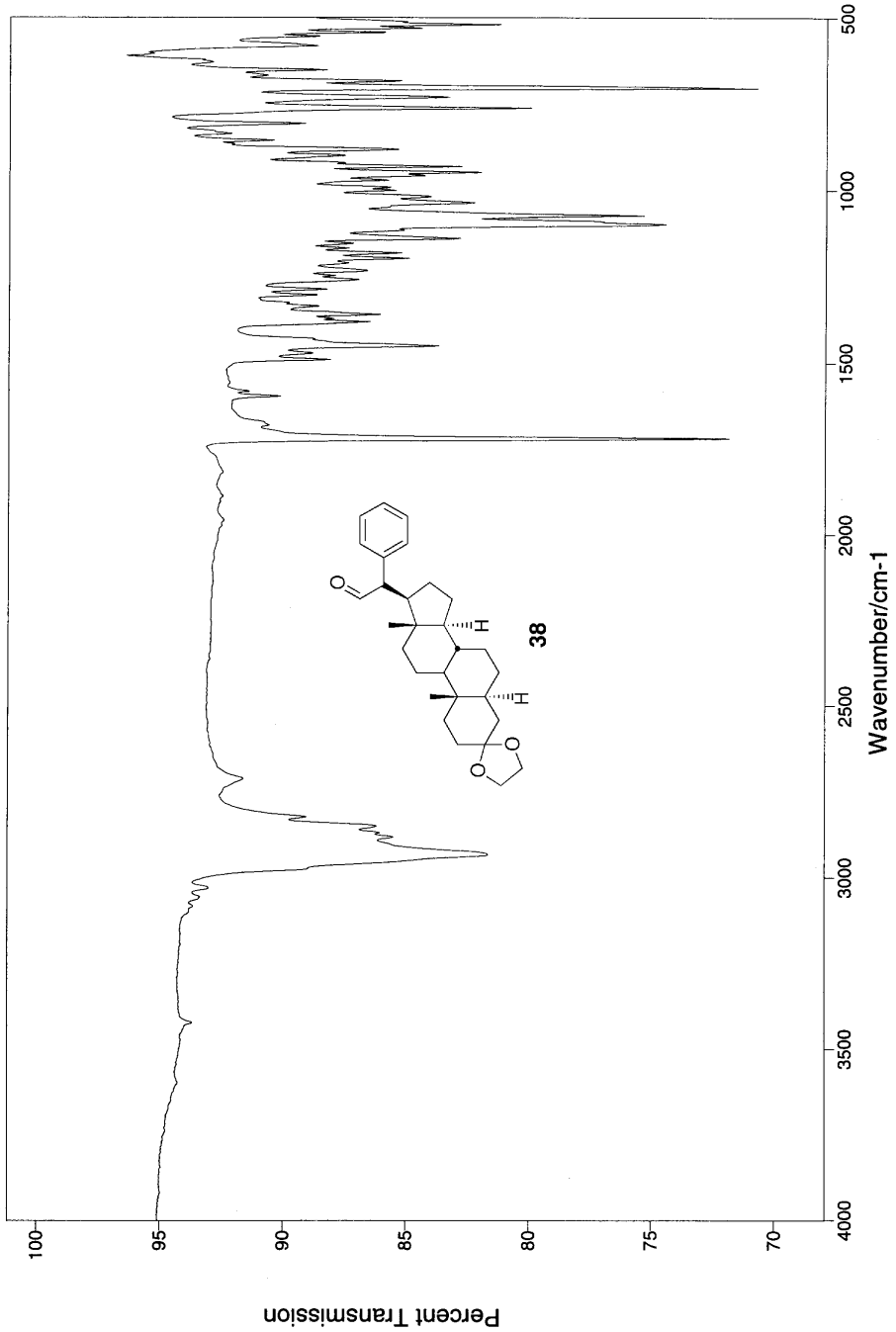
Percent Transmission
100
95
90
85
80
75
70
4000
3500
3000
2500
2000
1500
1000
500
Wavenumber/cm-1
38

Sodium 3-dimethyl acetal-20-phenyl-5α-pregnane-3-one-21-sulfate (40):[94,95]

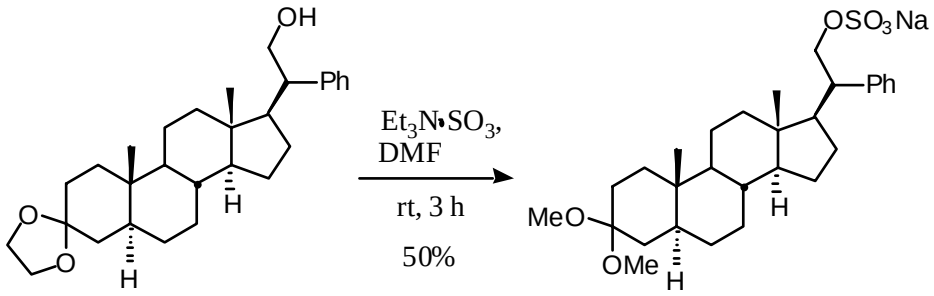

37 **40**

A 5-mL round bottom flask was charged, at room temperature, with compound **37** (10 mg, 0.023 mmol) and DMF (2 mL). To it was added $Et_3N{\cdot}SO_3$ complex (8.3 mg, 0.046 mmol), and the homogeneous reaction mixture was stirred for 3 h at that temperature. The reaction was quenched with H_2O (200 μL), and subjected to reverse phase column chromatography (column bed height 1 inch, dry packed). Initial elution with H_2O returned the unreacted sulfation complex. Subsequent elution with methanol:water (60:40) system afforded the free acid that was dissolved in methanol and passed through Amberlite® CG-120 (sodium form) using methanol as the eluent to give sulfate **40** as a white solid (6 mg, 0.012 mmol, 50%, m.p. 244-248 °C dec.).

^{1}H NMR (C D_3OD) δ 7.28-7.08 (m, 5 H), 4.45 (dd, *J* = 9.6, 4.0, 1H), 4.05 (t, *J* = 9.2, 1H), 3.17 (s, 3H), 3.10 (s, 3H), 2.94-2.86 (m, 1H), 0.84 (s, 3H), 0.82 (s, 3H).

^{13}C NMR δ 215.06, 144.71, 129.70, 129.20, 127.22, 110.58, 71.74, 65.24, 57.95, 55.76, 45.04, 43.81, 40.87, 39.13, 37.31, 37.06, 36.71, 36.71, 33.32, 32.31, 29.85, 29.76, 25.10, 22.51, 12.87, 11.98.

FT-IR (neat) 2920, 1603, 1449, 1362, 1271, 1210, 977, 798, 720, 792, 633.

ESI-MS (*m/z*) calculated ($C_{29}H_{43}NaO_6S$, M^++ Na) 542, observed 542.

OSO3Na
MeO
MeO
H
H
40
ppm
1
2
3
4
5
6
7
8
2.93
3.00
1.24
1.14
1.14
4.48
1.04

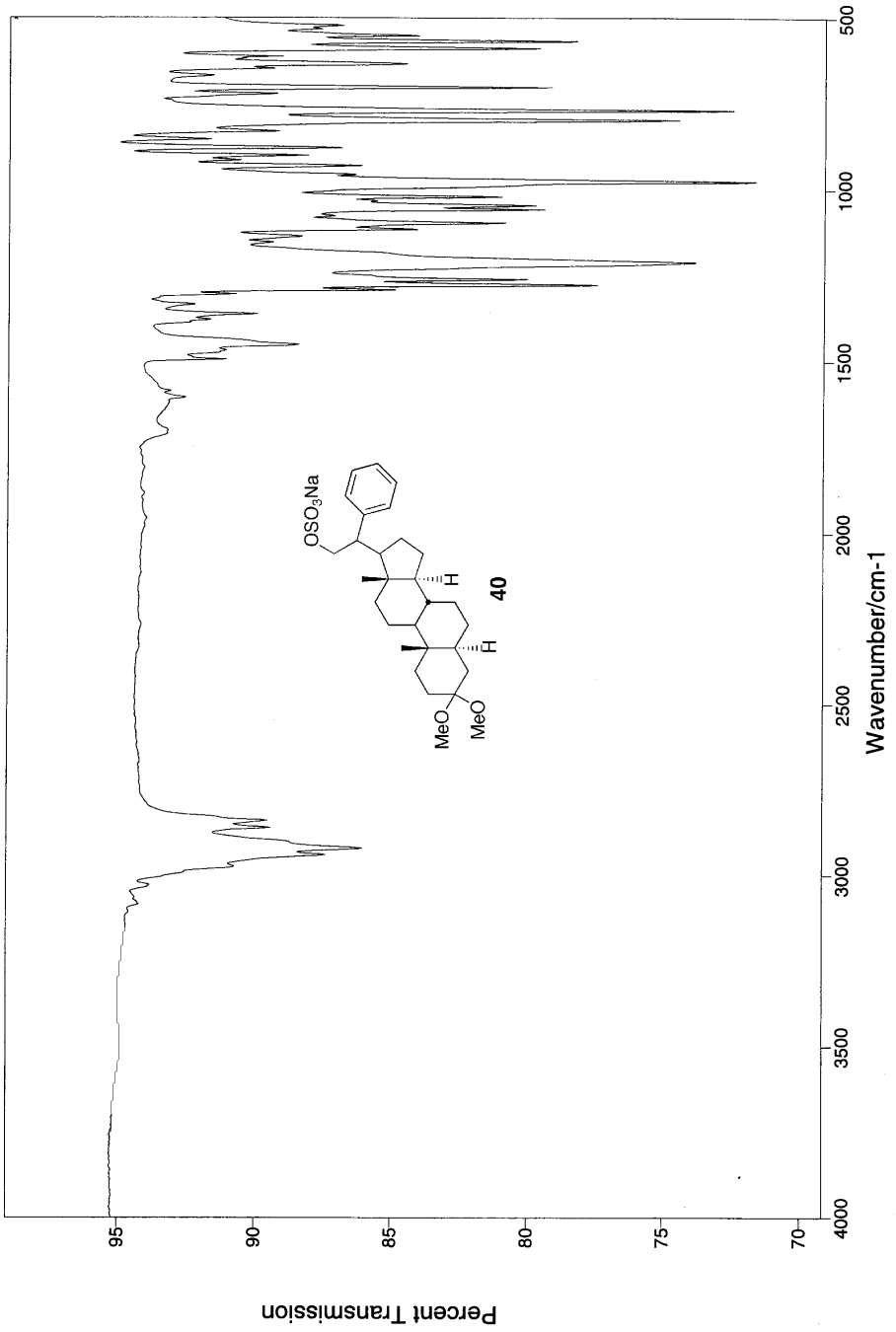
Percent Transmission
95
90
85
80
75
70
4000
3500
3000
2500
2000
1500
1000
500
Wavenumber/cm-1
OSO3Na
H
H
MeO
MeO
40

REFERENCES

1) Hirokawa, N. “Kinesin and Dynein Superfamily Proteins and the Mechanism of Organelle Transport.” *Science* **1998**, *279*, 519-526.

2) Valle, R. B.; Howard, S. S. “Motor Proteins of Cytoplasmic Microtubules.” *Annu. Rev. Biochem.* **1990**, *59*, 909-932.

3) Vale, R. D. “Molecular Motors and Associated Proteins.” In *Guidebook to the Cytoskeletal and Motor Proteins*; Kreis, T. E.; Vale, R. D., Eds. Oxford: Sambrook & Tooze, Oxford, 1999; pp 367-408.

4) Vale, R. D.; Reese, T. S.; Sheetz, M. P. “Identification of a Novel Force-Generating Protein, Kinesin, Involved in Microtubule-Based Motility.” *Cell* **1985**, *42*, 39-50.

5) Bloom, G. S.; Endow, S. A. “Motor Proteins 1: Kinesins.” *Protein Profile* **1995**, *2*, 1109-1171.

6) Endow, S. A. “Determinants of Molecular Motor Directionality.” *Nat. Cell Biol.* **1999**, *1*, E163-E167.

7) Block, S. M. “Leading the Procession: New Insight into Kinesin Motors.” *J. Cell Biol.* **1998**, *140*, 1281-1284.

8) Asbury, C. L.; Fehr, A. N.; Block, S. M. “Kinesin Moves by an Asymmetric Hand-Over-Hand Mechanism.” *Science* **2003**, *302*, 2130-2134.

9) Cross, R. A. “Molecular Motors: Kinesin’s Interesting Limp.” *Current Biol.* **2004**, *14*, R158-R159.

10) Hirokawa, N.; Takemura, R. “Kinesin Superfamily Proteins.” *Encyclopedia of Biological Chemistry*, Publishers Elsevier Ltd., Lennarz, W. J.; Lane, M. D. (Eds.) **2004**, *2*, 508-516.

11) Seog, D.-H; Lee, D.-H; Lee, S.-K. “Molecular Motor Proteins of the Kinesin Superfamily Proteins (KIFs): Structure, Cargo, Disease.” *J. Korean Med. Sci.* **2004**, *19*, 1-7.

12) Vale, R. D. “Microtubule-Based Motor Proteins.” *Current Opin. Cell Biol.* **1990**. *2*, 15-22.

13) Shimizu, T.; Thorn, K. S.; Ruby, A.; Vale, R. D. “ATPase Kinetic Characterization and Single Molecule Behavior of Mutant Human Kinesin Motor Defective in Microtubule-Based Motility.” *Biochemistry*, **2000**, *39*, 5265-5273.

14) Woehlke, G.; Ruby, A. K.; Hart, C. L.; Ly, B.; Hom-Booher, N.; Vale, R. D. “Microtubule Interaction Site of the Kinesin Motor.” *Cell* **1997**, *90*, 207-216.

15) Hirokawa, N.; Takemura, R. “Biochemical and Molecular Characterization of Diseases linked to Motor Proteins.” *Trends Biochem. Sci.* **2003**, *28*, 558-565.

16) Goldstein, L. S. B.; Yang, Z. “Microtubule-Based Transport Systems in Neurons: The Role of Kinesins and Dyneins.” *Annu. Rev. Neurosci.* **2000**, *23*, 39-71.

17) Hirokawa, N.; Takemura, R. “Kinesin Superfamily Proteins and their Various Functions and Dynamics.” *Exper. Cell Res.* **2004**, *301*, 50-59.

18) Setou, M.; Seog, D. H.; Tanaka, Y.; Kanai, Y.; Takei, Y.; Kawagishi, M.; Hirokawa, N. “Glutamate-Receptor-Interacting Protein GRIP1 Directly Steers Kinesin to Dendrites.” *Nature* **2002**, *417*, 83-87.

19) Kanai, Y.; Dohmae, N.; Hirokawa, N. “Kinesin Transports RNA: Isolation and Characterization of an RNA-Transporting Granule.” *Neuron* **2004**, *43*, 513-525.

20) Mandelkow, E.; Mandelkow, E.-M. “Kinesin Motors and Diseases.” *Trends Cell Biol.* **2002**, *12*, 585-590.

21) Holzbaur, E. L. F. “Motor Neurons Rely on Motor Proteins.” *Trends Cell Biol.* **2004**, *14*, 233-240.

22) Hirokawa, N.; Takemura, R. “Molecular Motors in Neuronal Development, Intracellular Transport and Diseases.” *Curr. Opin. Neurobiol.* **2004**, *14*, 564-573.

23) Reid, E. “A Kinesin Heavy Chain (KIF5A) Mutation in Hereditary Spastic Paraplagia (SPG10).” *Amer. J. Hum. Genet.* **2002**, *71*, 1189-1194.

24) Abel, E. D.; Peroni, O.; Kim, J. K.; Kim, Y. B.; Boss, O.; Hadro, E.; Minnemann, T.; Shulman, G. I.; Kahn, B. B. “Adipose-Selective Targeting of the GLUT4 Gene Impairs Insulin Action in Muscle and Liver.” *Nature* **2001**, *409*, 729-733.

25) Hakimi, M.-A.; Speicher, D. W.; Shiekhattar, R. “The Motor Protein Kinesin-1 Links Neurofibromin and Merlin in a Common Cellular Pathway of Neurofibromatosis.” *J. Biol. Chem.* **2002**, *277*, 36909-36912.

26) Efferth, T. etal “Damage of the Kinesin Heavy Chain Gene Contributes to the Antagonism of Cisplatin and Paclitaxel.” *Anticancer Res.* **2000**, *20*, 3211-3219.

27) Sodeik, B. “Mechanisms of Viral Transport in the Cytoplasm.” *Trends Micro Biol.* **2000**, *8*, 465-472.

28) Diefenbach, R. J.; Miranda, S. M.; Diefenbach, E.; Holland, D. J.; Boadle, R. A.; Armati, P. J.; Cunningham, A. L. “Herpes Simplex Virus Tegument Protein US11 Interacts with Conventional Kinesin Heavy Chain.” *J. Virol.* **2002**, *76*, 3282-3291.

29) Rietdorf, J.; Ploubidou, A.; Reckmann, I.; Holmström, A.; Frischknecht, F.; Zettl, M.; Zimmermann, T.; Way, M. “Kinesin-Dependent Movement on Microtubules Precedes Actin-Based Motility of Vaccinia Virus.” *Nature Cell Biol.* **2001**, *3*, 992-1000.

30) Ohira, M. etal “Identification and Characterization of a 500-kb Homozygously Deleted Region at 1p36.2-p36.3 in a Neuroblastoma Cell Line.” *Oncogen* **2000**, *19*, 4302-4307.

31) Kaiser, A.; Brembeck, F. H.; Nicke, B.; Wiedenmann, B.; Riecken, E.-O.; Rosewicz, S. “All-*trans*-Retinoic Acid-Mediated Growth Inhibition Involves Inhibition of Human Kinesin-Related Protein HsEg5.” *J. Biol. Chem.* **1999**, *274*, 18925-18931.

32) Kullmann, F. *et al* “Kinesin-Like Protein CENP-E is Upregulated in Rheumatoid Synovial Fibroblasts.” *Arthritis Res*, **1999**, *1*, 71-80.

33) Hasegawa, T. etal “Interaction Between GADD34 and Kinesin Superfamily, KIF3A.” *Biochem. Biophys. Res. Commun.* **2000**, *267*, 593-596.

34) Zhao, C.; Takita, J.; Tanaka, Y.; Setou, M.; Nakagawa, T.; Takeda, S.; Yang, H. W.; Terada, S.; Nakata, T.; Takei, Y.; Saito, M.; Tsuji, S.; Hayashi, Y.; Hirokawa, N. “Charcot-Marie-Tooth Disease Type 2A Caused by Mutation in a Microtubule Motor KIF1Bβ.” *Cell* **2001**, *105*, 587-597.

35) Setou, M.; Nakagawa, T.; Seog, D. H.; Hirokawa, N. “Kinesin Superfamily Motor Protein KIF17 and mLin-10 in NMDA Receptor-Containing Vesicle Transport.” *Science* **2000**, *288*, 1796-1802.

36) Yamada, K. *et al* “Heterozygous Mutations of the Kinesin KIF21A in Congenital Fibrosis of the Extraoccular Muscle type 1 (CFEOM1).” *Nat. Genet.* **2003**, *35*, 318-321.

37) Rosenbaum, J. L.; Witman, G. B. “intraflagellar transport.” *Nat. Rev. Mol. Cell Biol.* **2002**, *3*, 813-825.

38) Hirokawa, N. “stirring Up Development with the Heterotrimeric Kinesin KIF3.” *Traffic* **2000**, *1*, 29-34.

39) Marszalek, J. R., Liu, X.; Roberts, E. A.; Chui, D.; Marth, J. D.; Williams, D. S.; Goldstein, L. S. B. “Genetic Evidence for Selective Transport of Opsin and Arrestin by Kinesin-II in Mammalian Photoreceptors.” *Cell* **2000**, *102*, 175-187.

40) Bloodgood, R. A. “Directed Movements of Cilliary and Flagellar Membrane Components: a Review.” *Biol. Cell.* **1992**, *76*, 291-301.

41) Sakowicz, R.; Berdelis, M. S.; Ray, K.; Blackburn, C. L.; Hopmann, C.; Faulkner, D. J.; Goldstein, L. S. B. “A Marine Natural Product Inhibitor of Kinesin Motors.” *Science* **1998**, *280*, 292-295.

42) Hopkins, S. C.; Vale, R. D.; Kuntz, I. D. “Inhibitors of Kinesin Activity from Structure-Based Computer Screening.” *Biochemistry* **2000**, *39*, 2805-2814.

43) Wood, K. W.; Cornwell, W. D.; Jackson, J. R. “Past and Future of the Mitotic Spindle as an Oncological Target.” *Cancer* **2001**, *1*, 370-377.

44) Miyamoto, Y.; Muto, E.; Mashimo, T.; Iwane, A. H.; Yoshiya, I. “Direct Inhibition of Microtubule-Based Kinesin Motility by Local Anesthetics.” *Biophys. J.* **2000**, *78*, 940-949.

45) Jordan, M. A.; Wilson, L. “Use of Drugs to Study Role of Microtubule Assembly Dynamics in Living Cells.” *Methods Enzymol.* **1998**, *298*, 252-276.

46) Mayer, T. U.; Kapoor, T. M.; Haggarty, S. J.; King, R. W.; Schreiber, S. L.; Mitchison, T. J. “Small Molecule Inhibitor of Mitotic Spindle Bipolarity Identified in a Phenotype-Based Screen.” *Science* **1999**, *286*, 971-974.

47) Kapoor, T. M.; Mayer, T. U.; Coughlin, M. L.; Mitchison, T. J. “Probing Spindle Assembly Mechanisms with Monastrol, a Small Molecule Inhibitor of the Mitotic Kinesin, Eg5.” *J. Cell Biol.* **2000**, *150*, 975-988.

48) Sakowicz, R.; Finer, J. T.; Beraud, C.; Crompton, A.; Lewis, E.; Fritsch, A.; Lee, Y.; Mak, J.; Moody, R.; Turincio, R.; Chabala, J. C.; Gonzales, P.; Roth, S.; Weitman, S.; Wood, K. W. "Antitumor Activity of a Kinesin Inhibitor." *Cancer Res.* **2004**, *64*, 3276-3280.

49) Bishop, A.; Buzko, O.; Dumas, H. S.; Jung, I.; Kraybill, B.; Liu, Y.; Shah, K.; Ulrich, S.; Witucki, L.; Yang, F.; Zhang, C.; Shokat, K. M. "Unnatural Ligands for Engineered Proteins: New Tools for Chemical Genetics." *Annu. Rev. Biophys. Biomol. Struct.* **2000**, *29*, 577-606.

50) Kapoor, T. M.; Mitchison, T. J. "Allel-Specific Activators and Inhibitors for Kinesin." *Proc. Nat. Acad. Sci.* **1999**, *96*, 9106-9111.

51) Blackburn, C. L.; Hopmann, C.; Sakowicz, R.; Berdelis, M. S.; Goldstein, L. S. B.; Faulkner, D. J. "Adociasulfates 1-6, Inhibitors of Kinesin Motor Proteins from the Sponge *Haliclona* (aka adocia) sp." *J. Org. Chem.* **1999**, *64*, 5565-5570.

52) Bogenstatter, M.; Limberg, A.; Overman, L. E.; Tomasi, A. "Enantioselective Total Synthesis of the Kinesin Motor Protein Inhibitor Adociasulfate 1." *J. Am. Chem. Soc.* **1999**, *121*, 12206-12207.

53) Kull, F. J.; Sablin, E. P.; Lau, R.; Fletterick, R. J.; Vale, R. D. "Crystal Structure of the Kinesin Motor Domain Reveals a Structural Similarity to Myosin. *Nature* **1996**, *380*, 550-555.

54) Sablin, E. P.; Kull, F. J.; Cook, R.; Vale, R. D.; Fletterick, R. J. "Crystal Structure of the Motor Domain of the Kinesin Related Motor ncd." *Nature* **1996**, *380*, 555-559.

55) Sosa, H.; Dias, D. P.; Hoeneger, A.; Whitteker, M.; Wilson-Kubalek, E.; Sablin, E. P.; Fletterick, R. J.; Vale, R. D.; Milligan, R. A. "A Model for the Microtubule-Ncd Motor

Protein Complex Obtained by Cryo-Electron Microscopy and Image Analysis." Cell **1997**, *90*, 217-224.

56) Corey, E. J.; Bakshi, R. K. "A New System for Catalytic Enantioselective Reduction of Achiral Ketones to Chiral Alcohols. Synthesis of Chiral α-Hydroxy Acids." *Tetrahedron Lett*. **1990**, *31*, 611-614**.**

57) Dale, J. A.; Mosher, H. S. "Nuclear Magnetic Resonance Enantiomer Reagents. Configurations *via* Nuclear Magnetic Resonance Chemical Shifts of Diasteriomeric Mandelate, *O*-Methylmandelate, and α-Methoxy-α-trifluoromethylphenylacetate (MTPA) Esters." *J. Am. Chem. Soc*. **1973**, *95*, 512-519.

58) Mori, K.; Puapoomchareon, P. "Preparation of Optically Pure 2,4,4-Trimethyl-2-Cyclohexen-1-ol, a New and Versatile Chiral Building Block in Terpene Synthesis." *Acta Chemica Scand.* **1992**, *46*, 625-629.

59) Laschat, S.; Narjes, F.; Overman, L. E. "Application of Intramolecular Heck Reactions to the Preparation of Steroid and Terpene Intermediates Having cis A-B Ring Fusions. Model Studies for the Total Synthesis of Complex Cardenolides." *Tetrahedron* **1994**, *50*, 347-358.

60) De Jong, J. C.; Wildeman, J.; van Leusen, A. M.; Feringa, B. L. "Improved Synthesis of 2,6,6-trimethyl-1-cyclohexene-1-acetaldehyde, A Key Intermediate for Drimane-Related Sesquiterpens." *Synth. Commun.* **1990**, *20*, 589-596.

61) Julia, p. M.; Julia, S.; Chaffaut, J. A. D. " Synthéses Des α,β et γ-Cyclohomogéraniols." *Bull. Soc. Chim. Fr*. **1960**, *282*, 1732-1734.

62) Corey, E. J.; Cho, H.; Rücker, C.; Hua, D. H. "Studies with Trialkyltriflates: New Synthesis and Applications." *Tetrahedron Lett.* **1981**, *22*, 3455-34.

63) Nicolaou, K. C.; Zhong, Y. –L.; Baran, P. S. “A New Method for One-Step Synthesis of α,β-Unsubstituted Carbonyl System from Saturated Alcohols and Carbonyl Compounds.” *J. Am. Chem. Soc.* **2000**, *122*, 7596-7597.

64) Bélanger, G.; Deslongchamps, P. “Total Asymmetric Synthesis of the Aphidicolin Derivative (11R)-(-)-8-Epi-11-hydroxyaphidicolin Using Tandem Transannular Diels-Alder/Aldol Reactions.” *Organic Lett.* **1999**, *2*, 285-287.

65) Piers, E.; Abeysekera, B. F.; Herbert, D. J.; Suckling, I. D. “ Total Synthesis of the Stemodane-Type Diterpenoids (±)-Stemodin and (±)-Maritimol. Formal Synthesis of (±)-Stemodinone and (±)-Desoxystemodinone.” *Can. J. Chem.* **1985**, *63*, 3418-3432.

66) Mukaiyama, T.; Banno, K.; Narasaka, K. “New Cross-Aldol Reactions. Reactions of Silyl Enol Ethers with Carbonyl Compounds Activated by Titanium Tetrachloride.” *J. Am. Chem. Soc.* **1974**, *96*, 7503-7509.

67) Srikrishna, A.; Krishnan, K. “ Synthesis of (±)-Thaps-7(15)-ene and (±)-Thaps-6-enes.” *J. Chem. Soc. Perkin Trans* **1993**, *1*, 667-673.

68) Atwater, N. W. “4-Substituted Steroids.” *J. Am. Chem. Soc.* **1959**, *82*, 2847-2851.

69) Ling, T.; Poupon, E.; Rueden, E.; Kim, S. H.; Theodorakis, E. A. “Unified Synthesis of Quinone Sesquiterpenes Based on a Radical Decarboxylation and Quinone Addition Reaction.” *J. Am. Chem. Soc.* **2002**, *124*, 12261-12267.

70) Pappas, N.; Nace, H. R. “Norsteroids. II. Application of the Frevorskii Rearrangement to the Preparation of A-Norpregnanes.” *J. Am. Chem. Soc.* **1959**, *81*, 4556-4561.

71) Bruttomesso, A. C.; Doller, D.; Gros, E. G. “Stereospecific Synthesis of Steroidal 20,16-γ-Carbolactones.” *Synth. Commun.*, **1998**, *28*, 4043-4057.

72) Lacomte, V.; Stéphan, E.; Le Bideau, F.; Jaouen, G. “Imroved Addition of Organolithium Reagents to Hindered and/or Enolisable Ketones.” *Tetrahedron* **2003**, *59*, 2169-2176.

73) Solladie′-Cavaiio, A.; Quazzotti, S. “Threo Aryl Trifluoromethyl Chlorohydrins: Synthesis, Reactivity and Structure.” *J. Org. Chem.* **1992**, *57*, 174-178.

74) Rodehorst, R.; Ratcliffe, R. “Improved Procedure for Oxidations with the Chromium Trioxide-Pyridine Complex.” *J. Org. Chem.* **1970**, *35*, 4000-4001.

75) Posner, G. H.; Roskers-Shulman, E. M.; Oh, C. H.; Carry, J.-C.; Green, J. V.; Clark, A. B.; Dai, H.; Anjeh, T. E. N. “$BF_3{\cdot}OEt_2$ Promoted Fast, Mild, Clean and Regioselective Dehydration of Tertiary Alcohols.” *Tetrahedron Lett.* **1991**, *32*, 6489-6492.

76) Ramchandran, P. K.; Cheng, T.; Horton, W. J. “The Synthesis of Euparin and Dehydrotremetone.” *J. Org. Chem.* **1963**, *28*, 2744-2746.

77) Yadav, J. S.; Mysorekar, S. V. “A Facile Conversion of Tertiary Alcohols to Olefins.” *Synth. Commun.* **1989**, *19*, 1057-1060.

78) Czernecki, S.; Georgoulis, C.; Provelenghiou, C. “Nouvelle Methode De Benzylation D′hydroxyles Glucidiques Encombres.” *Tetrahedron Lett.* **1976**, *17*, 3535-3536.

79) Eckenberg, P.; Groth, U.; Huhn, T.; Richter, N.; Schmeck, C. “A Useful Application of Benzyl Trichloroacetimidate for the Benzylation of Alcohols.” *Tetrahedron Lett.* **1993**, *49*, 1619-1624.

80) Lane, C. F. “Organic Synthesis Using Borane-Methyl Sulfide. The Hydroboration-Oxidation of Alkenes.” *J. Org. Chem.* **1974**, *39*, 1437-1438.

81) Chan, T. H.; Brook, M. A.; Chaly, B. T. “A Simple Procedure for the Acetalization of Carbonyl Compounds.” *Synthesis* **1983**, 203-205.

82) Nwaukwa, S. O.; Keehn, P. M. “The Oxidation of Alcohols and Ethers Using Calcium Hypochlorite[$Ca(OCl)_2$].” *Tetrahedron Lett.* **1982**, *23*, 35-38.

83) Luca, L; Giacomelli, G.; Masala, S.; Porcheddu, A. “Trichloroisocyanuric/TEMPO Oxidation of Alcohols Under Mild Conditions: A Close Investigation.” *J. Org. Chem.* **2003**, *68*, 4999-5001.

84) Zhao, M.; Li, J.; Mano, E.; Song, Z.; Tschaen, D. M.; Grabowski, J. J.; Reider, P. J. “Oxidation of Primary Alcohols to Carboxylic Acids with Sodium Chlorite Catalyzed by TEMPO and Bleach.” *J. Org. Chem.* **1999**, *64*, 2564-2566.

85) Parrish, E. J.; Honda, H.; Hileman, D. “Benzotriazole-Chromium Trioxide Complex. A Versatile Oxidant of Organic Compounds.” *Synth. Commun.*, **1990**, *20*, 3359-3366.

86) Corey, E. J.; Gilman, N. W.; Ganem, B. E. “New Methods for the Oxidation of Aldehydes to Carboxylic Acids and Esters.” *J. Am. Chem. Soc.* **1968**, *90*, 5616-5617.

87) Menger, F. M.; Lee, C. “Synthetically Useful Oxidations at Solid Sodium Permanganate Surfaces.” *Tetrahedron Lett.* **1981**, *22*, 1655-1656.

88) Zanka, A. “A Simple and Highly Practical Oxidation of Primary Alcohols to Acids Mediated by 2,2,6,6-Tetramethyl-1-piperidinyloxy (TEMPO).” *Chem. Pharm. Bull.* **2003**, *51*, 888-889.

89) Ji, H.; Mizugaki, T.; Ebitani, K.; Kaneda, K. “Highly Efficient Oxidation of Alcohols to Carbonyl Compounds in the Presence of Molecular Oxygen Using a Novel Heterogeneous Ruthenium Catalyst.” *Tetrahedron Lett.* **2002**, *43*, 7179-7183.

90) Chandrasekaran, S.; Chakraborty, T. K. “Facile Oxidation of Aldehydes to Carboxylic Acids with Chromium (V) Reagents.” *Synth. Commun.* **1980**, *10*, 951-956.

91) Travis, B. R.; Sivakumar, M.; Hollist, G. O.; Borhan, B. “Facile Oxidation of Aldehydes to Acids and Esters with Oxone.” *Organic Lett.* **2003**, *5*, 1031-1034.

92) Corey, E. J.; Schmidt, G. “Useful Procedures for the Oxidations of Alcohols Involving Pyridinium Dichromate in Aprotic Media.” *Tetrahedron Lett.* **1979**, *20*, 399-402.

93) Bowers, A.; Halsall, T. G.; Jones, E. R. H.; Lemin, A. J. “The Chemistry of Triterpenes and Related Compounds. Part XVIII. Elucidation of the structure of Polyporenic Acid C.” *J. Chem. Soc. Chem. Commun.* **1953**, 2548-2561.

94) Comin, M. J.; Maier, M. S.; Roccatagliata, A. J.; Pujol, C. A.; Damonte, E. B. “Evaluation of the Antiviral Activity of Natural Sulfated Polyhydroxysteroids and Their Synthetic Derivatives and Analogs.” *Steroids* **1999**, *64*, 335-340.

95) Bernstein, S.; Nair, V. “A Convenient Procedure for the Preparation of Triethylamine-Sulfur Trioxide.” *Organic Prep. Proc. Int.* **1987**, *19*, 466-467.

96) Sen, S. E.; Roach, S. L.; Boggs, J. K.; Ewing, G. J.; Magrath, J. “Ferric Chloride Hexahydrate: A Mild Hydrolytic Agent for the Deprotection of Acetals.” *J. Org. Chem.* **1997**, *62*, 6684-6686.

97) Geladopoulos, T. P.; Sotiroudis, T. G.; Evangelopoulos, A. E. “A Malachite Green Colorimetric Assay for Protein Phosphatase Activity.” *Anal. Biochem.* **1991**, *192*, 112-116.

98) Tromm, P.; Heimgartner, H. “Hetero-Diels-Alder Reaction with 1,3-Thiazole-5(4H)-Thiones.” *Helv. Chim. Acta* **1988**, *71*, 2071-84.

99) Hegedus, L.; Lipshutz, B.; Nozaki, H.; Reetz, M.; Rittermeyer, P.; Smith, K.; Totter, F.; Yamamoto, H. *Organometallics in Synthesis*, John Wiley and Sons Publishers, **1994**,

100) Stang, P. J.; Treptow, W. “Single-Step Improved Synthesis of Primary and Other Vinyl Trifluoromethanesulfonates.” *Synthesis* **1980**, 283-284.

101) Cacchi, S.; Morera, E.; Ortar, G. “Palladium-Catalyzed Carbonylation of Vinyl Triflates: A Novel Method for One-Pot Homologation of Ketones to Unsaturated Carboxylic Acid Derivatives.” *Tetrahedron Lett.* **1985**, *26*, 1109-1112.

102) Fernandez-Gacio, A.; Vitale, C.; Mounrino, A.; “Synthesis of New Aromatic (C17-C20)-Locked Side-Chain Analogues of Calcitriol (1α, 25-Dihydroxyvitamin D_3).” *J. Org. Chem.* **2000**, *65*, 6978-6983.

103) Frigerio, M.; Santagostino, M.; Sputore, S. “A User-Friendly Entry to 2-Iodoxybenzoic Acid (IBX).” *J. Org. Chem.* **1999**, *64*, 4537-4538.

104) Pilcher, A. S.; Ammon, H. L.; DeShong, P. “Utilization of Tetrabutylammonium (Triphenylsilyl) Difluorosilicate as a Fluoride Source for Nucleophilic Fluorination.” *J. Am. Chem. Soc.* **1995**, *117*, 5166-5167.

105) Armarego, W. L. F.; Perrin, D. D. “Purification of Laboratory Chemicals.” Butterworth Heinmann Publishers, Oxford, 2000, 4th Ed.

106) Still, W. C.; Kahn, M.; Mitra, A. “Rapid Chromatographic Technique for Preparative Separation with Moderate Resolution.” *J. Org. Chem.* **1978**, *43*, 2923-2925.